Final Report

Demonstration of an Enhanced Vertical Magnetic Gradient System for UXO

ESTCP Project MM-0633

APRIL 2008

Dr. William Doll
Battelle

Environmental Security Technology Certification Program

Report Documentation Page

Form Approved
OMB No. 0704-0188

1. REPORT DATE	2. REPORT TYPE	3. DATES COVERED
MAY 2008	**N/A**	**-**

4. TITLE AND SUBTITLE	5a. CONTRACT NUMBER
Demonstration of an Enhanced Vertical Magnetic Gradient System for UXO	5b. GRANT NUMBER
	5c. PROGRAM ELEMENT NUMBER
6. AUTHOR(S)	5d. PROJECT NUMBER
	5e. TASK NUMBER
	5f. WORK UNIT NUMBER
7. PERFORMING ORGANIZATION NAME(S) AND ADDRESS(ES) **Battelle**	8. PERFORMING ORGANIZATION REPORT NUMBER
9. SPONSORING/MONITORING AGENCY NAME(S) AND ADDRESS(ES)	10. SPONSOR/MONITOR'S ACRONYM(S)
	11. SPONSOR/MONITOR'S REPORT NUMBER(S)

12. DISTRIBUTION/AVAILABILITY STATEMENT
Approved for public release, distribution unlimited

13. SUPPLEMENTARY NOTES
The original document contains color images.

14. ABSTRACT

15. SUBJECT TERMS

16. SECURITY CLASSIFICATION OF:			17. LIMITATION OF ABSTRACT	18. NUMBER OF PAGES	19a. NAME OF RESPONSIBLE PERSON
a. REPORT	b. ABSTRACT	c. THIS PAGE			
unclassified	**unclassified**	**unclassified**	**UU**	**111**	

Standard Form 298 (Rev. 8-98)
Prescribed by ANSI Std Z39-18

Table of Contents

Acronym List

AGL	Above ground level
AS	Analytic signal
ASCII	American Standard Code for Information Interchange
ADU	Attitude determination unit
CERCLA	Comprehensive Environmental Response, Compensation, and Liability Act
DAS	Data analysis system
DoD	Department of Defense
DQO	Data Quality Objective
ESTCP	Environmental Security Technology Certification Program
FAA	Federal Aviation Administration
FKPBR	Former Kirtland Precision Bombing Range
FOM	Figure of Merit
FUDS	Formerly Used Defense Sites
GIS	Geographic Information System
GPS, DGPS	(Differential) Global Positioning System
HAZWOPR	Hazardous Waste Operations and Emergency Response
INS	U.S. Immigration and Naturalization Service
IR	Improvement Ratio
NAD	North American Datum
ORAGS	Oak Ridge Airborne Geophysical System
ORNL	Oak Ridge National Laboratory
SERDP	Strategic Environmental Research & Development Program
STC	Supplemental Type Certificate
TIF, GeoTIF	(Geographically referenced) Tagged Information File
TF	Total (magnetic) field
USAESCH	U.S. Army Engineering and Support Center, Huntsville
UTM	Universal Transverse Mercator
UXO	Unexploded Ordnance
VG	Vertical (magnetic) gradient
VSEMS	Vehicular Simultaneous Electromagnetic Induction and Magnetometer System

List of Figures

List of Tables

Acknowledgements

This work was funded by the Environmental Security Technology Certification Program under the direction of Dr. Jeffrey Marqusee and Dr. Anne Andrews, and supported by Mr. Scott Millhouse at the U.S. Army Corps of Engineers Mandatory Center of Excellence for Ordnance and Explosives, Huntsville, Alabama. The report was written by employees of Battelle – Oak Ridge Operations.

Abstract

In September 2006, Battelle unveiled two new airborne vertical magnetic gradient systems for mapping and detection of unexploded ordnance (UXO). These systems, dubbed VG-16 and VG-22, were developed with corporate funds on the basis of successful evaluation of a vertical magnetic gradient prototype under ESTCP Project 200038.

The VG-16 system utilizes sixteen cesium vapor magnetometers configured as eight vertical gradiometers with 0.5m vertical separation of magnetometers forming each gradiometer "pod" and 1.7m horizontal separation between gradiometers. This system is designed for wide-area assessment where it is not essential that a high percentage of small ordnance items be detected. Swath width of the VG-16 system is 12m, with four gradiometer pods on the foreboom and two on each of the sidebooms. This arrangement is essentially an adaptation of the predecessor Arrowhead system, wherein each single magnetometer on the Arrowhead is replaced by a gradiometer pod on the VG-16 system.

The VG-22 system was designed to enhance sensitivity to small ordnance items by concentrating more gradiometer pods in the foreboom structure and operating with those pods closer to the ground surface. This system has 7 gradiometer pods in the foreboom at 1m horizontal separation for a swath width of 6m. There are also two pods at 1.7m separation in each of the sidebooms. These sensors acquire ancillary data at higher altitude than the sensors in the foreboom to provide a more volumetric data set for more robust inversion.

Both systems were flown at two locations as part of this study. First, data were acquired at Battelle's UXO test site in West Jefferson Ohio, to allow performance assessment for a wide range of known ordnance types at representative depths and orientations. The systems were then flown over two areas at the Former Kirtland Precision Bombing Range (FKPBR), New Mexico, used previously for Wide Area Assessment research. The 500-acre southern study area at Kirtland was seeded with ordnance items ranging from 40mm to 155mm. Two 500-acre plots were chosen for surveying in the north and were expected from previous data to contain historic ordnance, primarily M38 practice bombs and larger items, as well as ordnance fragments.

The VG-16 system had a Pd of 77% for 77 metallic items at 1.5m flight altitude at Battelle's Ohio test site. The VG-22 system yielded a Pd of 100% for the same altitude and test items. Locational accuracy, based on dipole inversion of anomalies for the VG-22 system at 1.5m altitude, had a mean of 0.3m and a standard deviation of 0.2m

At FKPBR, the VG-22 had an overall Pd of 86% for 88 blind-seeded items, including 100% detection of 81mm mortars and 40mm projectiles, and 80% detection of 57mm projectiles. Subsequent assessment of missed items determined that an overall Pd of 98% could have been achieved for VG-22 if we had selected a lower detection threshold (2.0nT/m vs. 2.5nT/m), at a cost of raising the number of picks from 12 picks per acre to 20 picks per acre. The VG-16 had an overall Pd of 55% in the seeded South Area. Validation results from the North Area at FKPBR, where M-38 practice bombs are the predominant ordnance type, were largely inconclusive because there were few if any UXO-like objects recovered from 260 excavations. Results are presented as pseudo-ROC curves with Pd as the fraction of point-like targets and Pfp presented as the fraction of non-point-like targets.

1 Introduction

1.1 Background

It is estimated that UXO may contaminate 15 million acres or more within the United States alone. A need for improved technologies for mapping and detection of UXO has led to development of a sequence of airborne reconnaissance systems, using electromagnetic (Beard et al., 2004; Doll et al., 2005; Holladay et al., 2006) and magnetic (Gamey et al., 2004) sensors. The benefits of vertical gradient configurations in magnetometer systems are common knowledge, and these configurations are routinely used in ground-based UXO investigations. Overall, airborne systems provide a tool for wide-area assessment to support evaluation and footprint reduction over large DoD sites where only a portion of the site is contaminated with ordnance.

In 2002, Battelle staff (then at Oak Ridge National Laboratory) evaluated a prototype airborne vertical magnetic gradient system for mapping and detection of unexploded ordnance (Oak Ridge National Laboratory, 2005). This study demonstrated clear advantages for vertical gradient over total field configurations.

At least two categories of magnetic noise influence the effectiveness of airborne systems for UXO mapping and detection (Gamey et al., 2004). These are rotor noise and maneuver noise. Rotor noise is a type of interference, where a lightly magnetized rotor induces an oscillatory overprint on the sensor data. Maneuver noise, also known as compensation error, is caused by the magnetic properties of the helicopter airframe. This noise could be eliminated by a "perfect" compensation correction, but real corrections always fall short of perfection leaving an uncorrected (or residual) compensation error. Regardless of their sources, the deleterious effects are largely coherent between two closely spaced sensors in a vertical gradient configuration. As such they are amenable to reduction by subtraction, and reduction by design is preferable to reduction by filtering.

Based on the success of the 2002 tests, Battelle committed corporate funds to design and construct two new systems, both employing the vertical gradient concept. The VG-16 system (Figure 1-1) was designed to maximize sensitivity in wide-area assessment surveys, where data might be acquired at about 3m altitude or higher. By comparison, the VG-22 system (Figure 1) was designed to address the detection of small ordnance items, 81mm and smaller, which typically have detection rates of less than 50% in airborne total field system performance assessments (Table 1-1).

Table 1-1: Results of Airborne Total Field System Detection Assessment, Pueblo of Isleta, NM, 2002*

Type	Total Emplaced	ORAGS. Detects	Air MTADS Detects
2.75-in	12	7	11
60mm	20	5	4
81mm	40	15	19
105mm	40	15	29

* from Tuley and Dieguez, 2005

The VG-16 and VG-22 systems differ in the number of magnetometers as well as the horizontal separation between magnetometer pods (where a pod houses two vertically-separated magnetometers) and in their swath width. A rack-mount is used to house the on-board electronics for both systems. The VG-16 system employs 16 cesium-vapor airborne-quality magnetometers, and has 1.7m horizontal separation between magnetometer pods rendering a 12m swath width. In contrast, the VG-22 employs 22 cesium-vapor airborne-quality magnetometers in a similar vertical magnetic gradient configuration with 1.0m horizontal separation between seven magnetometer pods in the fore-boom structure rendering a 6m swath width. The swath width ultimately determines the number of survey passes, and thus the flight time required to survey a site of specified size. The VG-22 also was designed to be flown with sensors closer to the earth's surface. At sites where the minimum flight altitude is 3m or higher, where large items are of primary concern, or where the purpose of the survey is to identify concentrations of metal (as opposed to detection of individual items), the VG-16 would be a more technically appropriate and cost-effective system choice that would outperform total field systems. On the other hand, if detection of smaller individual items is the primary survey objective, or where it is more critical to attain the highest detection rates, the VG-22 system is a more appropriate choice.

Two sites were surveyed as part of this project. First, data were acquired with both systems at an airborne UXO system test grid which was developed by Battelle in West Jefferson, Ohio. This site is seeded with common ordnance items ranging in size from 60mm to 155mm at the three principal orientations and at depths appropriate to each ordnance type. In addition, data were acquired at the Kirtland Precision Bombing Range (KPBR) in New Mexico, at a site established by ESTCP for development and evaluation of Wide Area Assessment (WAA) technologies. VG-16 and VG-22 were deployed at two areas of the KPBR: A 500-acre site located between the runways at Double Eagle Airport (within the KPBR) was selected as a blind test grid. Approximately 100 seed items were emplaced by ESTCP contractors. Detection of those items was assessed by Institute for Defense Analysis staff based on dig lists provided by Battelle for both systems. Data were also acquired by both systems in an area north of the Double Eagle airport (referred to as the "North Area"). For the VG-16, surveys within the North Area were conducted within two 500-acre plots, and for the VG-22, data were acquired within two 250-acre plots located within the 500-acre VG-16 plots.

1.2 Objectives of the Demonstration

There were two distinct objectives for this demonstration. First and foremost, it provided a means of assessing the effectiveness of two vertical gradient configurations in comparison with total field airborne configurations for mapping and detection of small ordnance items. Previous assessments of the airborne technologies by IDA for the ESTCP Program Office determined that detection of small ordnance with total field airborne systems was unreliable, with less than 50% detection of 60mm and 81mm in a New Mexico test.

A second objective of the demonstration was to assess the effectiveness of the vertical magnetic gradient configurations for Wide Area Assessment (WAA) applications. The Demonstration Site for this project has been used for previous WAA demonstrations, and therefore provides a basis for achieving this second objective.

1.3 Regulatory Drivers

No specific regulatory drivers influenced this technology demonstration. UXO-related activity is generally conducted under CERCLA authority. Regardless of a lack of specific regulatory drivers, many DoD sites and installations are aggressively pursuing innovative technologies to address a variety of issues associated with ordnance and ordnance-related artifacts (e.g. burial sites) that resulted from weapons testing and/or training activities. These issues include footprint reduction and site characterization, areas of particular focus for this technology demonstration. In many cases, the prevailing concerns at these sites can lead to airborne surveying and other remediation activities despite the absence of relevant regulatory drivers and mandates.

1.4 Stakeholder / End-user Issues

Issues related to this demonstration project center on the appropriate use of the technology. Clearly, the improved airborne system is unable to detect all UXO items of potential interest. This may not be critical for WAA surveys, where detection of a portion of the target ordnance items, or of concentrations of small ordnance items is acceptable. Airborne geophysical systems continue to be constrained by the presence of tall vegetation and rough terrain that increases the distance between the system and the UXO items of interest, thereby limiting detection ability. This has been shown to be less problematic for vertical gradient systems than for total field systems. It remains apparent that application of the technology to small survey areas will not be cost-effective due to the large cost associated with mobilization/ demobilization and considerable helicopter costs. Users should consider both the intended UXO targets and survey area (both size, terrain, and vegetation) before considering the use of airborne systems for UXO detection, mapping, and/or WAA.

2. Technology Description

2.1 Technology Development and Application

The VG-16 system was designed to maximize sensitivity in wide-area assessment surveys, where data are to be acquired at about 3m altitude or higher. By comparison, the VG-22 system was designed to address the concerns raised in the IDA report with regard to airborne magnetometer systems, where it is critical to detect and assess ordnance 81mm and smaller. The VG-16 and VG-22 systems differ in the number of magnetometers as well as the separation between magnetometer pods (where a pod houses two magnetometers) and in their swath width. A rack-mount configuration is used to house the electronics for both systems (Figure 1-1). Sensor positioning is provided by post-processed GPS/IMU data with 100Hz update rate and 2cm/0.01degree accuracy.

The VG-16 system (Figure 1-2) employs 16 cesium-vapor airborne-quality magnetometers, and has 1.7m horizontal separation between magnetometer pods rendering a 12m swath width. In contrast, the VG-22 (Figure 1-3) employs 22 cesium-vapor airborne-quality magnetometers in a similar vertical magnetic gradient configuration with 1.0m horizontal separation between seven magnetometer pods in the foreboom structure rendering a 6m swath width. The swath width ultimately determines the number of survey passes, and thus the flight time required to survey a site of specified size. The VG-22 also was designed to be flown with sensors closer to the earth's surface. At sites where the minimum flight altitude is 3m or higher, where large ordnance is of primary concern, or where the purpose of the survey is to identify concentrations of ordnance (as opposed to detection of individual ordnance items, i.e. a lower P_d is acceptable), the VG-16 would be a more technically appropriate and cost-effective system choice that would outperform total field systems. On the other hand, if detection of smaller individual ordnance is the primary survey objective, or where it is more critical to attain the highest possible P_d, the VG-22 system is a more appropriate choice.

Figure 2-1. Recording equipment rack-mounted in the helicopter for both systems.

Figure 2-2. Battelle's VG-16 airborne vertical magnetic gradient system.

Figure 2-3. VG-22 airborne vertical magnetic gradient system.

2.2 Previous Testing of the Technology

In addition to the surveys at the Battelle Airborne UXO Test Grid in Ohio, and the Former Kirtland Precision Bombing Range (FKPBR) in New Mexico (this report), the VG-16 system was deployed in Wisconsin and Florida during fiscal year 2007. At Fort McCoy, Wisconsin, it was used for a wide-area assessment survey of the 570-acre Badger Drop Zone. At the Rodman Training Range on the Pinecastle Range Complex, Florida it was used for a 2800 acre survey at higher altitudes. The VG-22 system was deployed at Marine Corps Base Camp Lejeune, North Carolina over a 910 acre survey for UXO in a salt marsh environment.

The vertical magnetic gradient technology was previously demonstrated for ESTCP as a prototype system with data acquired at the Aberdeen Test Center, Maryland, Pueblo of Laguna, New Mexico and the Badlands Bombing Range, South Dakota. Results of these tests were submitted to ESTCP in 2005 (Oak Ridge National Laboratory, 2005).

At Fort McCoy in western Wisconsin, the 570-acre Badger Drop Zone (BDZ) was surveyed with the VG-16 system in October 2006 for WAA applications. The resulting analytic signal map (Figure 2-4) was used to generate an anomaly density map (Figure 2-5). Anomaly density was calculated as the product of three terms: the number of picked anomalies per 25m X 25m block, the percentage grid cells in each block that contain measurements, and a scaling term, sixteen blocks per hectare. The information collected from this survey will be used to assess the level of UXO contamination and identify selected areas for future removal operations thus insuring long-term sustainability of the BDZ as a training facility and maneuver area.

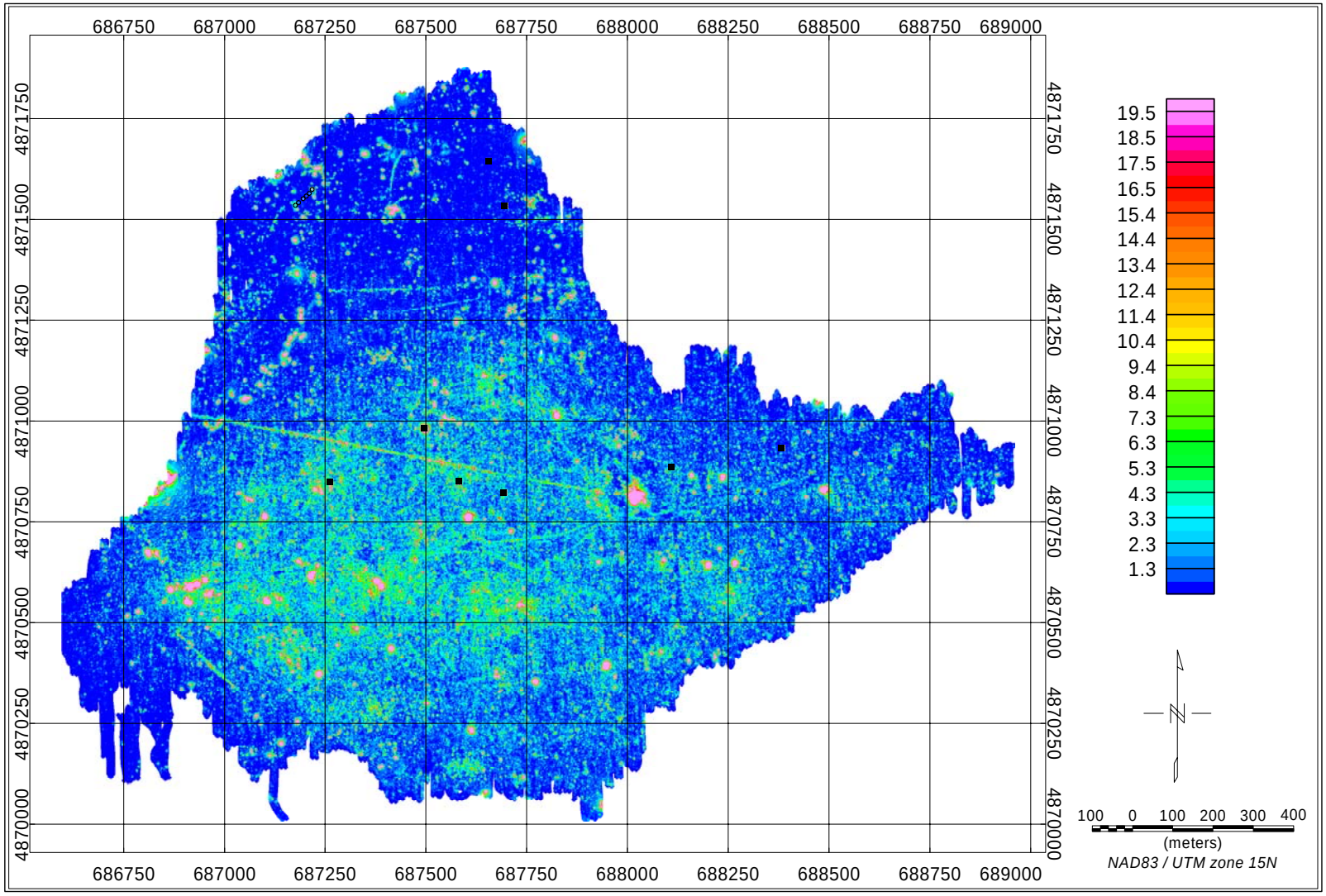

Figure 2-4. Analytic signal map of the Badger Drop Zone at Fort McCoy, WI. The color bar represents analytic signal values in nT/m, with coordinates in NAD83 / UTM Zone 15N.

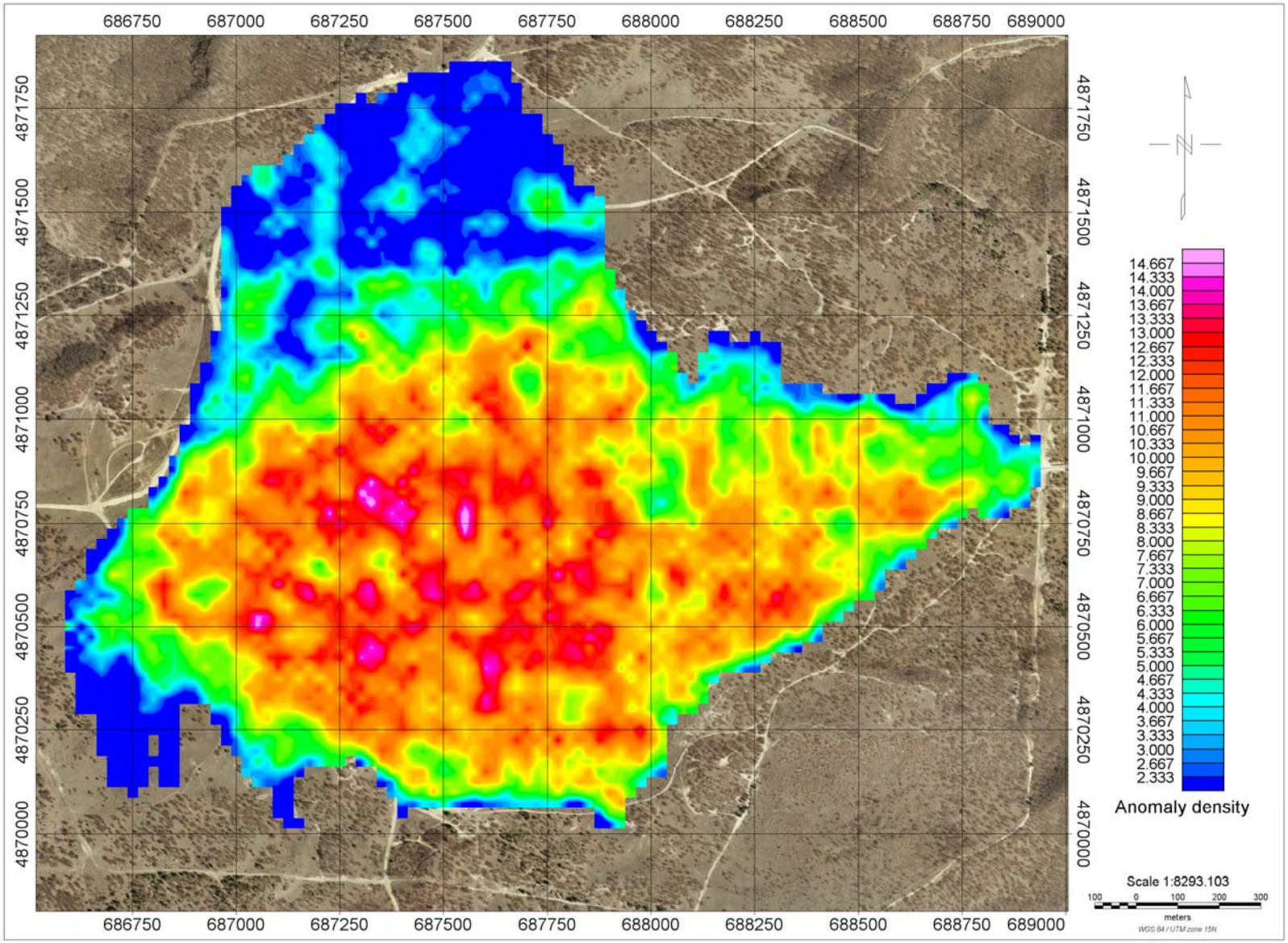

Figure 2-5. Anomaly density map (anomalies per hectare) of the Badger Drop Zone, Fort McCoy

2.3 Factors Affecting Cost and Performance

The cost of an airborne survey depends on many factors, including:

- Helicopter service costs, which depend on the cost of ferrying the aircraft to the site fuel costs, terrain and vegetation conditions impacting flight line configuration and turn-around, etc.,
- Total size of the blocks to be surveyed,
- Length of flight lines,
- Extent of topographic irregularities or vegetation that can influence flight variations and performance
- Ordnance objectives which dictate survey altitude and number of flight lines
- Temperature and season, which control the number of hours that can be flown each day
- Location of the site, which can influence the cost of logistics
- Survey objectives and density of coverage, specifically high density for individual ordnance detection versus transects for target/impact area delineation and footprint reduction.

The difference in cost for the VG-16 and VG-22 systems lies largely in their swath width. The VG-16 system acquires data along an entire 12m swath with each pass, while the swath of the VG-22 system is only 6m. The user must consider whether the added value of the VG-22 system compensates for the additional cost, and this is dependent on the purpose of the survey, geologic conditions, and ordnance types anticipated at the site, as well as the other factors cited above.

2.4 Advantages and Limitations of the Technology

Airborne surveys for UXO are capable of providing data for characterizing potential UXO contamination at a site at considerably lower cost per acre than ground-based systems. Furthermore, the data may be acquired in a shorter period of time. Airborne systems are particularly effective at sites having low-growth vegetation and minimal topographic relief. They can also be used where heavy brush or mud makes it difficult to conduct ground-based surveys. Detection performance of airborne systems is lower than that of ground surveys (e.g. towed array surveys using the Vehicular Simultaneous Electromagnetic Induction and Magnetometer System, VSEMS), which can operate with sensors at less than 0.5 m AGL.

Both airborne and ground magnetometer systems are susceptible to interference from magnetic rocks and magnetic soils. Rugged topography or tall vegetation limits the utility of helicopter systems, necessitating survey heights too high to resolve individual UXO items. The performance of the vertical gradient configurations demonstrated in this project is superior to that of total field systems, and should allow effective operation where topography or vegetation requires a few meters of increase in the functional altitude of operation.

The primary advantage of the airborne technology is the capability to cover large areas more quickly and cheaply than conventional ground-based surveys. Where large UXO items are involved, the wider sensor spacing and higher altitudes of airborne arrays result in very little reduction in detection capability. Large UXO such as bombs or large caliber shells have been demonstrated to have spatially large magnetic anomalies with amplitudes easily detectable from typical survey heights. Detection of smaller items, however, is more limited as a result of wider sensor spacing and higher altitudes. Again, the vertical magnetic gradient systems are designed to improve on total field system performance in this regard. Airborne systems also have an advantage in areas where ground access is limited or difficult due to surface conditions (swamp or marsh) or inherent danger (exposure to UXO or other contaminants). Areas with a sensitive ecological environment may also benefit from the less intrusive airborne technologies.

3. Demonstration Design

3.1 Performance Objectives

All quantitative objectives are based on comparison of the vertical gradient response relative to the total field data from the lower sensor of the gradient pair. In particular, the reduction of rotor and maneuver noise can be examined.

Table 3-1: Performance objectives of vertical gradient system.

Type of Performance Objective	Primary Performance Criteria	Expected Performance (Metric)	Actual Performance Objective Met?
Qualitative	Ease of Use	Pilot approval	Yes
	Terrain/vegetation restrictions	Acceptable for targets of interest	Yes
	Aerodynamic stability	Safety, certification, no restrictions	Yes
	Detection capabilities	Better delineation of clustered targets,	Yes
Quantitative	Signal-noise (compared to TF)	>4x SNR improvement in rotor noise over TF system	Yes (4.3x)
	Probability of Detection	per Table 4-2	Yes, except for 40mm (VG-16) and 60mm (both systems)
	False Alarm Rate	<10% FP /(UXO + FP count) (VG16)* <10% FP /(UXO + FP count) (VG22)*	Unresolved. Only one UXO-like object was uncovered in the North Area validation.
	Location Accuracy	<0.5m mean, <0.4m s.d. northing and easting (after inversion) <0.4m mean and <0.3 s.d. northing and easting (after inversion)	Yes
	Survey Rate	100 hectare/day for VG-16; 50 hectare/day for VG-22	Yes
	Percent Site Coverage	100% of the accessible area	Yes

* We define FP (false positives) as non-ferrous sources.

3.2 Selecting Test Sites

Battelle's Airborne UXO Test Grid in Ohio was chosen because it contains ordnance items of a size and at separations that were chosen specifically for airborne system assessment, as well as lower mobilization costs for the helicopter and geophysical crews. In addition, the ESTCP Program Office requested that a demonstration be conducted at the FKPBR in New Mexico, where previous WAA surveys were conducted. It is thought that this could provide valuable comparisons with other WAA survey tools while reducing overall cost of the demonstration to ESTCP.

3.3 Test Site History / Characteristics

3.3.1 West Jefferson Test Grid

The geology at the West Jefferson Airborne UXO Test Grid consists of a glacial till layer, typically 50-200 ft thick, overlying carbonate bedrock. The glacial till layer contains rocks with a wide variety of compositions and sizes, some of which can generate significant magnetic anomalies.

A 2-hectare area (100m x 200m) was selected in June 2006, and preliminary ground-based vertical magnetic gradient data were acquired in the summer of 2006. Anomalies exceeding a 25nT/m threshold were investigated. Of these, 37 were determined to be associated with manmade metallic debris, and 31 were determined to be associated with magnetic rocks. These items were removed from the site. In addition, it was found that there were areas where the density of anomalies was too great to be suitable for a test grid. Many of these were contained in a band trending NE to SW, north of the center of the map area. In order to have an area of adequate size for airborne testing, the site was expanded by about 25%. A pre-seed analytic signal map of the site is shown in Figure 3-1.

A total of 79 individual test items were emplaced at the site, consisting of fourteen different types of ordnance, generally emplaced at three distinct orientations (north-south east-west, and vertical) and three representative depths (ranging from 0.0 to 1.5m). These are summarized in Table 3-2. Three of the 79 items (the MK-118s) were nonmagnetic, to be used in subsequent evaluation of other sensor systems. In addition, four groups of closely-spaced targets were emplaced, each consisting of 20-80 small ordnance items or surrogates, to evaluate sensitivity to concentrations of small metal items.

Table 3-2: Individual Test Items Emplaced

Ordnance Type	Number Emplaced	Mass (kg)
155 artillery	12	24.1-26.5
105 M60 artillery	9	9.5-12.7
MK76	3	11.2
60mm mortar	18	1.0-1.1
81mm mortar	18	3.2
M12 AT mines	2	3.7
M20 AT mines	2	4.1
BDU-33 bombs	3	0.77
3-in Stokes mortar	3	3.0-3.7
BDU-28 submunitions	3	0.77
MK-118 submunitions	3	0.6
3 lb practice bombs	3	1.4

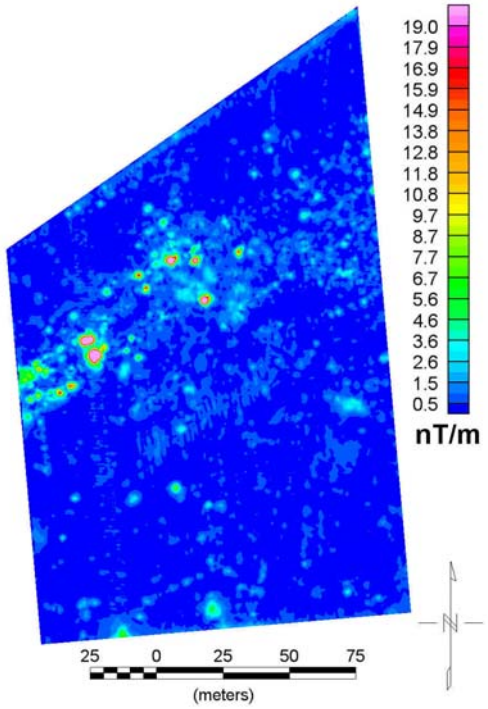

Figure 3-1. Pre-seed ground-based analytic signal map of the test site.

Figure 3-2. West Jefferson test site with selected ordnance items before emplacement.

Items were emplaced at intervals of 10-15m, depending on the size of the emplaced object. This allows magnetometer data to be acquired to altitudes of at least 5m AGL without significant overlap of anomalies. Care was taken to avoid anomalous areas and boundaries where items outside of the survey grid could cause interference. All item locations were documented by a civil surveyor. A post-seed ground-based survey was conducted to support subsequent airborne acquisitions.

3.3.2 Former Kirtland Precision Bombing Range

The FKPBR (Figure 3-3) is a 38,000 acre area that was used in World War II as a training area for Kirtland Air Force Base. The ESTCP WAA pilot study area consists of 5000-6500 acres adjacent to Double Eagle Airport, near Albuquerque NM. Within this study area are at least three bombing targets, and a Simulated Oil Refinery Target (SORT). Known or suspected ordnance types at the site are M-38 practice bombs and 250-lb high explosive bombs. The runways of Double Eagle Airport encompass the South Area and several power lines, fences and outbuildings are located adjacent to, or within the survey areas. Most prominent are a building along the SE side of the South Area, and a power line that crosses the southern portion of the eastern North Area.

Figure 3-3. FKPBR showing helicopter in the North Area.

3.4 Present Operations

The West Jefferson Ohio Test grid is located on Battelle-owned property adjacent to other corporate facilities that are used primarily for defense contracting tasks. The test grid is monitored by video cameras from the adjacent site.

The FKPBR site is a formerly used defense site (FUDS). It has been subject to previous geophysical surveys and partial excavation, primarily under the guidance of the ESTCP Program Office. It is currently undeveloped, but immediately adjacent to the Double Eagle Airport, waste treatment facilities, and a shooting range.

3.5 Pre-demonstration Testing and Analysis

Shakedown testing of the assembled airborne systems and associated components was conducted in Bolton, Ontario, Canada during September 2006. Both systems were test flown by an aeronautical

engineer and determined to be completely flight-worthy. Federal Aviation Administration / Transport Canada installation certification was subsequently issued.

3.6 Testing and Evaluation Plan

3.6.1 Demonstration Set-up and Start-up

Mobilization involved packing and transporting all system components by trailer to the appropriate site and installing them on a Bell 206L Long Ranger helicopter. Calibration and compensation flights were conducted and results evaluated. The cesium magnetometers, GPS systems (positioning and attitude), fluxgate magnetometers, data recording console, laser altimeter and acoustic altimeters were tested to ensure proper operation and performance.

3.6.2 Period of Operations

Data were acquired at the West Jefferson Test Site from October 20-25, 2006, with one partial day of travel at either end for mobilization.

The period of operations at Kirtland extended from April 16 through May 10, 2007. The crew travelled to New Mexico between April 16 and April 18. Weather delayed the helicopter arrival until April 20. Installation was completed on April 21, but high winds caused data acquisition to be delayed until April 22. Data acquisition with the VG-22 system extended through April 29. This constitutes an overall average daily acquisition rate of 125 acres/day inclusive of weather days, site availability limitations, and other constraints. The VG-22 system was replaced with the VG-16 system on April 29. Acquisition with the VG-16 system was conducted between April 30 and May 8, with de-installation and demobilization beginning on May 9. The average daily acquisition rate for the VG-16 system was 222 acres/day inclusive of weather and constraints. The daily acquisition rate for the VG-22 system is estimated at half that of the VG-16 system due to the narrower swath width of the VG-22.

3.6.3 Area Characterized

The West Jefferson Airborne UXO Test Grid was surveyed in its entirety at altitudes of 1.5, 3, 5, and 10m AGL.

The FKPBR demonstration was conducted over portions of the two (North and South) areas previously surveyed for WAA purposes at Kirtland (Figure 3-4). Given the two distinct purposes of the demonstration (Section 1.2), we used the breakdown shown in Table 3-3 for the 2000 acres of VG-16 and 1000 acres of VG-22 data acquired at Kirtland. This involved acquisition within three areas: Area 1) 1000-acres in the North Area including portions of the N2 and SORT targets, and areas previously surveyed with ground-based VSEMS; Area 2) 500 acres within the 1000 acre area, and consisting of two contiguous areas (250 acres each) where ordnance is known to exist in association with targets; and Area 3) a 500-acre portion of the South Area which is known to be largely void of ordnance, and in which ESTCP arranged for blind-seeded items to be emplaced in advance of the survey. Thus, we acquired data with the VG-16 system at Area 1 (1000 acres) and Area 2 (500 acres) at the minimum safe altitude, and at Area 3 (500 acres) at 5m altitude, for a total of 2000 acres. We flew the VG-22 system at Area 2 (500 acres) and Area 3 (500 acres) at the minimum safe altitude, for a total of 1000 acres.

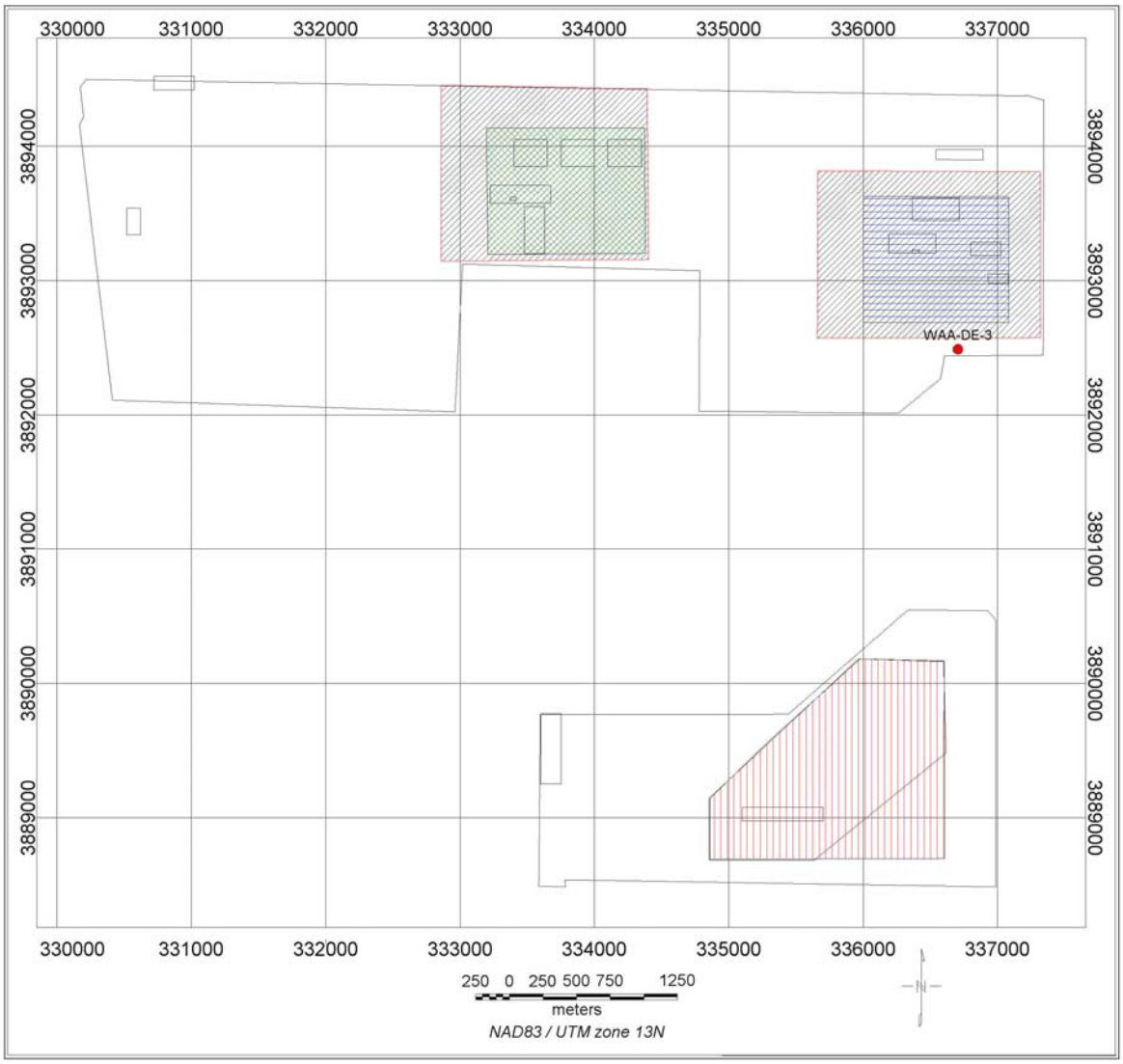

Figure 3-4. Map of the FKPBR WAA sites, showing the north and south areas adjacent to Double Eagle Airport from previous ESTCP WAA projects. Area 1 (the grey area) consists of 2000 acres; Area 2 (the green and blue areas) totals 500 acres, and Area 3(shaded red) consists of 500 acres. Locations of previous ground surveys (provided by M. May, IDA) are included as smaller rectangles. Perimeter polygon for the north and south areas provided by H. Nelson, Naval Research Laboratory.

Table 3-3: Breakdown of survey blocks for Battelle VG systems at FKPBR.

System	Area	Altitude	Purpose
VG-16	Area 1	ALASA*	To assess performance for WAA applications at targets
VG-16	Area 2	5m	To assess VG performance at higher altitudes for WAA applications
VG-16	Area 3	ALASA	To assess VG-16 performance for small ordnance targets
VG-22	Area 2	ALASA	To assess improved performance of VG-22 in separating closely-spaced anomalies
VG-22	Area 3	ALASA	To assess VG-22 performance for small ordnance targets

* ALASA – As Low As Safely Achievable

3.6.4 Residuals Handling

This section does not apply to this report.

3.6.5 Operating Parameters for the Technology

The VG-16 and VG-22 systems are designed for daylight operations only. Parallel lines are flown across the area in a direction dependent upon local logistics and weather conditions. The binary data are recorded on the console at a rate of 1200 samples per second, and down-sampled to 120 samples per second.

Labor requirements included a geophysical project manager, data processor, pilot, mechanic, and system operator. Operations are monitored in real time by the system operator from the in-flight display. Data Quality Control (QC) functions are performed post-flight by the data processor and/or project manager. QC checks cover GPS quality, diurnal activity, area coverage, magnetic data quality and supplemental data quality (laser altimeter, fluxgate, orientation). Re-flights were assigned on a daily basis. Quality Assurance (QA) functions include verification of calibration grid data using ground survey techniques.

3.6.6 Demobilization

De-installation was carried out by dismounting the booms from the helicopter frame and then packing the sensors and instruments in shipping containers. The containers were placed in a trailer and transported back to Oak Ridge, Tennessee.

4. Performance Assessment

4.1 Performance Criteria

Effectiveness of the demonstration is determined from comparisons of the processed/analyzed results from the demonstration survey and the established ground-truth. Some qualitative parameters may be judged against results of previous airborne and ground-based surveys at FKPBR and elsewhere. Evaluation of seeded items provides a basis for assessing detection of small ordnance items. These comparisons include both the quantitative and qualitative items described in this section, which are documented fully in project reports available from ESTCP. Demonstration success is defined as the successful acquisition of airborne geophysical data (without any aviation incident or airborne system failure) and meeting the baseline requirements for system performance as established previously in Section 3.1. Methods utilized by Battelle on both current and past airborne acquisitions to ensure airborne survey success include daily QA/QC checks on all system parameters (e.g. GPS, magnetometer operation, data recording, system compensation measurements, etc.) in the acquired data sets, a series of compensation flights at the beginning of each survey, continual inspection of all system hardware and software ensuring optimal performance during the data acquisition phase, and review of data upon completion of each processing phase.

Several factors associated with data acquisition cannot be strictly controlled, such as aircraft altitude and attitude. Altitude is recorded and entered into the data analysis and comparisons with previous results. The aircraft attitude measuring system provides a documented database that cannot be directly compared with previous surveys when this system was not available. The consistent and scientific evaluation of performance is accomplished by using identical or parallel (where parameters are dataset dependent) processing methods with identical software to produce a final map, and following consistent procedures in interpretation when comparing new and existing datasets from the respective test sites.

Data processing involves several steps, including GPS post-processing, compensation, spike removal, time lag correction, heading correction, filtering, gradient calculations, and gridding. Each step can be performed in the same manner on the total field data to provide a basis for comparing the performance of the vertical gradient to total field systems. The processing procedures have been selected and developed from experience with similar data over several years for optimal sensitivity to UXO.

Data collection occurred at the specified flight altitudes over the various test areas. Table 4-1 identifies the expected performance criteria for this project, complete with expected/desired values (quantitative) and/or definitions and descriptions (qualitative).

Table 4-1: Performance Criteria and Results for the Battelle airborne gradiometer systems

Performance Criteria	Expected Performance Metric (Pre-demo)	Performance Confirmation Method	Actual Performance (Post-demo)
Primary Criteria (Performance Objectives) – Quantitative			
System Performance	Ordnance detection (VG16) >90% detection of M38 on North Area	Comparison to excavation data. Number of detections / number of excavated military munitions and munitions debris.	Unresolved. Only one UXO-like object was uncovered during the validation of the North Area.
	Ordnance detection (VG22) >90% detection of M38 on North Area	Comparison to excavation data. Number of detections / number of excavated military munitions and munitions debris	Unresolved. Only one UXO-like object was uncovered during the validation of the North Area.
	Ordnance detection on blind seed grid per Table 4-2.	Comparison to blind seed data. Number of detections / number of seed items.	Yes, except for 40mm (VG-16) and 60mm (both systems)
	False positives (VG16 and VG22) <10% in North Area (2)	Comparison to excavation data. Number of bad picks / total number of picks.	Unresolved. Only one UXO-like object was uncovered during the validation of the North Area.
	Rotor noise performance improved over TF system (SNR improved by 4x)	SNR calculated from VG and TF over common targets (Section 4.5.1.7)	Yes, Achieved 4.3x noise reduction
	Low frequency noise improvement over TF system (FOM & IR improved by 4x)	FOM & IR calculated from VG and TF during compensation flight (Section 4.5.1.6)	Yes, Achieved 6.6x noise reduction
	Anomaly positional accuracy <0.5m mean, <0.4m s.d. northing and easting(after inversion, VG-16) <0.4m mean and <0.3 s.d. northing and easting (after inversion, VG-22)	Comparison to excavation and seed item locations.	Yes VG-16: 0.44m mean, s.d. northing and easting: 0.33m and 0.29m VG-22: 0.02 mean; s.d. northing and easting: 0.21m, 0.22m

Primary Criteria (Performance Objectives) – Qualitative			
Process Waste	None	Observations	
System Performance	Delineation of clustered targets	Comparison of results for seeded pairs of closely-spaced targets with results of Gamey et al., 2007.	Unresolved. Pairs of targets were generally too far apart to register as clusters. Results match detection of single targets.
	Altitude effects on sensitivity	Comparison of low level data with data acquired at 5m altitude	5m results are suitable for WAA surveys. See Section 4.5.11.

Secondary Criteria (Performance Objectives) – Quantitative			
Hazardous Materials	None expected	Observations and documentation during excavations	No hazardous materials encountered.

Secondary Criteria (Performance Objectives) – Qualitative			
Reliability	No system or component failures	Observations and documentation	No system components failed during the surveys
Ease of Use	Pilot "comfort" when flying with the system installed	Observations and documentation	Pilot finds performance is comfortable under normal weather conditions.
Safety	Conformance with all FAA requirements and requirements documented in the Mission Plan	Observations and documentation	Systems met all FAA flightworthiness requirements.
	Aerodynamic stability	Performance as assessed by pilot and aeronautical engineer, comparison with predecessor systems	Both systems are very stable; VG-22 is a little more difficult to fly than VG-16.
	Certification	FAA/STC certification awarded	FAA STC certificate awarded for both configurations.
Maintenance	System mount points, hardware, and component inspection	Observations and documentation	Minimal wear and tear.

(1) We define the term "ordnance detection" to mean the percentage of ordnance items that produced magnetic anomalies discernable above the noise floor and within a defined search radius. The term does not imply that the anomalies were or were not correctly classified.

(2) By the term "false positive" we refer to non-ferrous sources. Thus all ferrous items (ordnance and non-ordnance) are considered true positives, and reported anomalies associated with rocks or non-ferrous manmade items are considered false positives. Assume that all picked anomalies are

excavated.
(3) By the term "anomaly positional accuracy" we mean the distance between the documented UXO or clutter item location and the location predicted by the geophysical anomaly or its inversion.

The Vertical Gradient Systems outperformed the total field systems as assessed by Tuley (2005), to the extent that background conditions at these two proximal sites can be considered equivalent. Table 4-2 provides a summary of the calculated performance of these systems and the target detection for each type of ordnance to be emplaced in the test grid at FKPBR. For each ordnance type, we report only the best performing airborne system result from Pueblo of Isleta. False alarm rates (FAR) are strongly influenced by site conditions and could not be predicted.

Table 4-2: Observed and anticipated detection rates for VG-16 and VG-22 at FKPBR seeded grid vs. detection rates from Isleta as reported by Tuley et al., 2005

Ordnance type	Isleta Detection	VG-16 Expected	VG-16 Observed	VG-22 Expected	VG-22 Observed
40mm	NA	5%	0%	10%	100%
57mm	NA	25%	40%	30%	80%
60mm	25%	50%	11%	60%	56%
81mm	47%	60%	72%	70%	100%
105mm Proj	73%	85%	86%	90%	100%
105mm HEAT	NA	85%	100%	90%	100%
155mm	NA	90%	100%	95%	100%

4.2 Performance Confirmation Methods

Assessment of performance of the VG systems to anticipated performance (e.g. Table 4-2 and quantitative elements in Tables 3-1 and 3-2) are straightforward, and were accomplished through controlled information exchange between Battelle and ESTCP and their contractor, IDA, using the survey from FKPBR. Numbers and locations of seeded items in the FKPBR were not specified to Battelle in advance of an IDA assessment of performance. Battelle provided dig lists for the FKPBR South Area for both VG-16 and VG-22. IDA analyzed the dig lists and initially provided Pd and positional accuracy statistics for both systems, and for each ordnance type. Subsequently, IDA divulged all burial parameters for the seeded items.

In the FKPBR North Area, ESTCP conducted 261 validation digs based on VG-16 and VG-22 dig lists provided by Battelle, as well as dig lists derived from VSEMS ground-based measurements which were conducted several months earlier, during a previous phase of the ESTCP WAA Program.

Direct comparison of the VG-16 and VG-22 vertical gradient data to previous total field results (e.g. Isleta 2003) has many constraints. For example, the actual survey height will not be the same for both systems at any given point. This will have the effect of differentially improving anomalous responses. These factors serve to alter the "signal" in the signal-noise ratio comparisons.

For high frequency rotor noise, the standard deviation of the total field or vertical gradient data over a representative section of flat background readings will be used to determine standardized

"noise". For low frequency compensation noise, the Figure of Merit (FOM) and Improvement Ratio (IR) will be used. The FOM is a measure of the residual aircraft signature after compensation. It consists of the sum of the peak-peak noise in each of the twelve separate parts of the compensation maneuver.

$$FOM = \sum noise_{ij}$$

where noise = average residual peak-peak deflection,
and i = cardinal direction (N, S, E, W)
and j = maneuver (pitch, roll, yaw).

The Improvement Ratio is the ratio of the standard deviation of the raw/residual peak-peak deflections. These two metrics are a measure of the effectiveness of the compensation algorithm in reducing airframe signature in the bandwidth of the helicopter maneuvering parameters. These are typically below 1Hz in frequency. The FOM is an absolute measure of remaining noise after correction, whereas the IR shows the relative change in a before/after sense. The effects of uncorrected airframe noise can only be seen in gridded survey data where they appear as long wavelength features parallel to the flight lines. This correction can be simulated by high-pass filters, but this process loses its effectiveness at higher altitudes where ordnance anomalies drop into the reject band of the filter.

4.3 Data Analysis, Interpretation and Evaluation

Airborne magnetometer systems do not distinguish between UXO and ferrous scrap for the many anomalies mapped without interpretation. The vertical gradient and analytic signal maps that will be provided will depict bombing targets (areas of high ordnance density), infrastructure (fences or larger items or areas of ferrous debris associated with human activity), and potential UXO items (discrete sources). Those responses interpreted as potential UXO, likely also include smaller pieces of ferrous debris.

4.4 West Jefferson Field Results

Measured vertical gradient and resulting analytic signal maps from altitudes of 1.5, 3, 5, and 10m altitude data acquired with the VG-16 system, are shown in Figures 4-1 through 4-4. The corresponding 1.5m maps for theVG-22 system are shown in Figure 4-5.

Figure 4-6 shows total field and analytic signal maps that would be derived for a total field system at the test site. To develop these maps, we have taken the lower magnetometers for each gradiometer pair and processed those data using the processing approach previously used with Battelle's Arrowhead system. By using the lower magnetometers, the total field surrogate has an altitude advantage of 0.25m compared to the center point of the gradiometer pods.

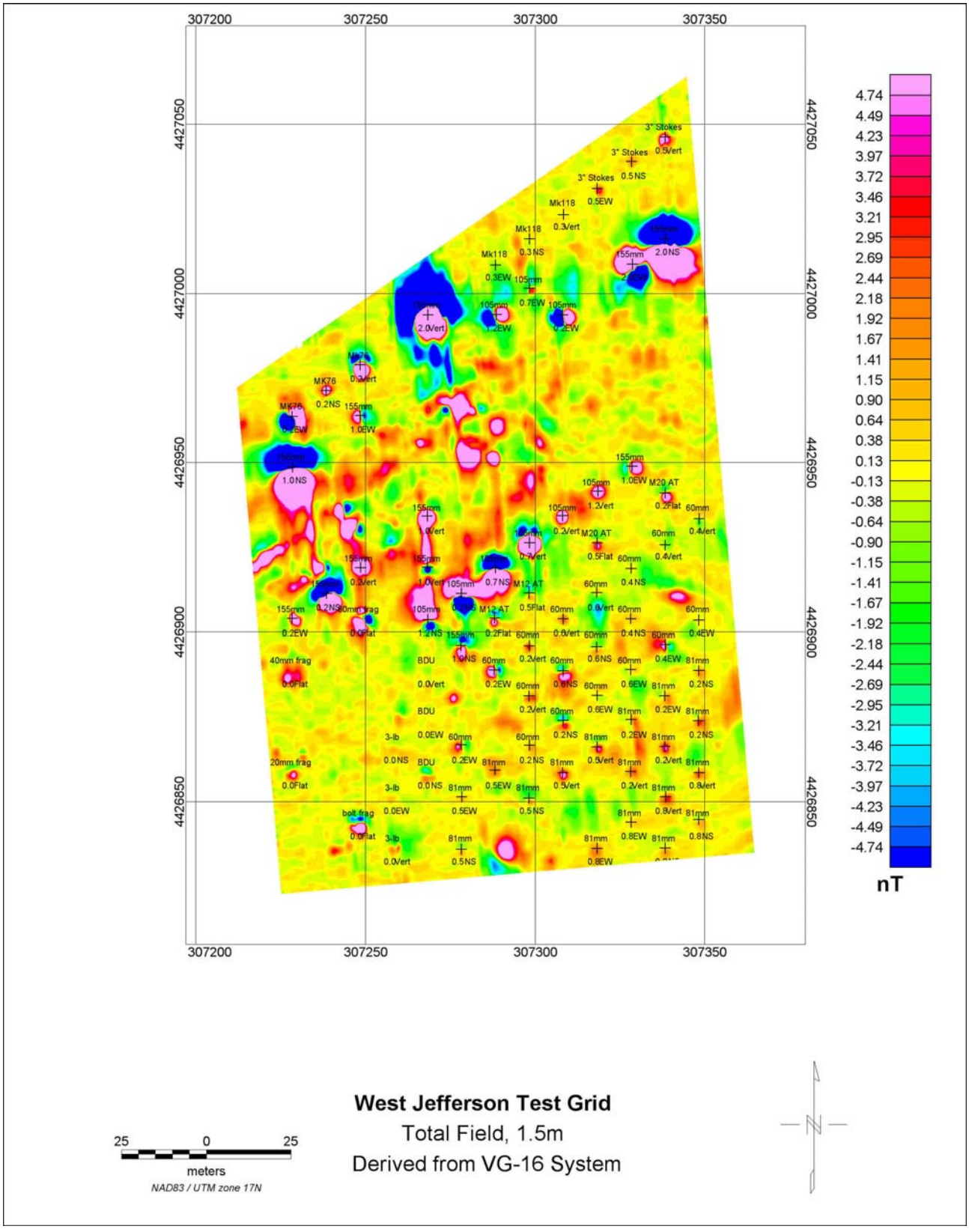

Figure 4-1a. VG-16 airborne vertical magnetic gradient results for 1.5m altitude from the West Jefferson Test Site.

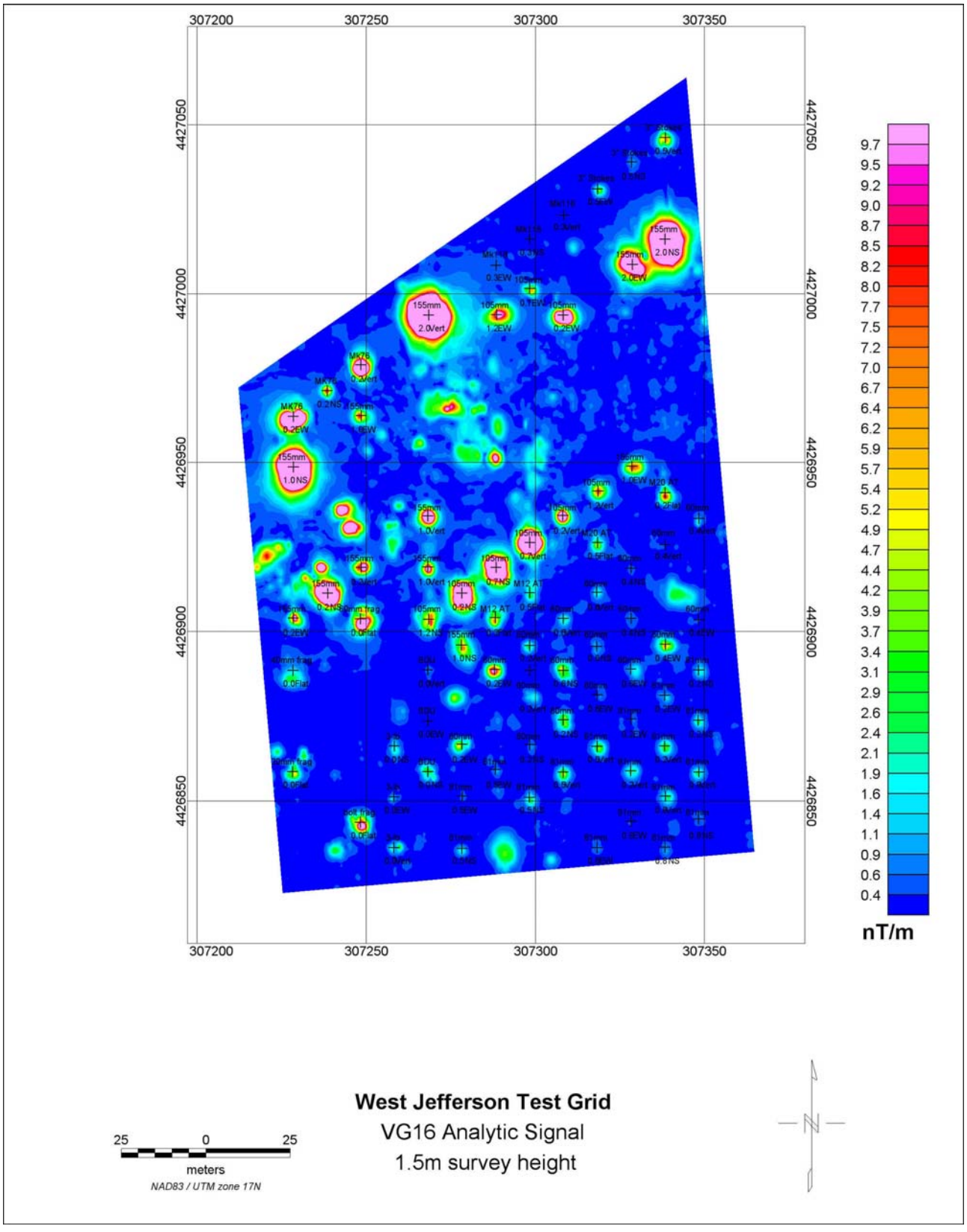

Figure 4-1b. VG-16 airborne analytic signal results for 1.5m altitude from the West Jefferson Test Site.

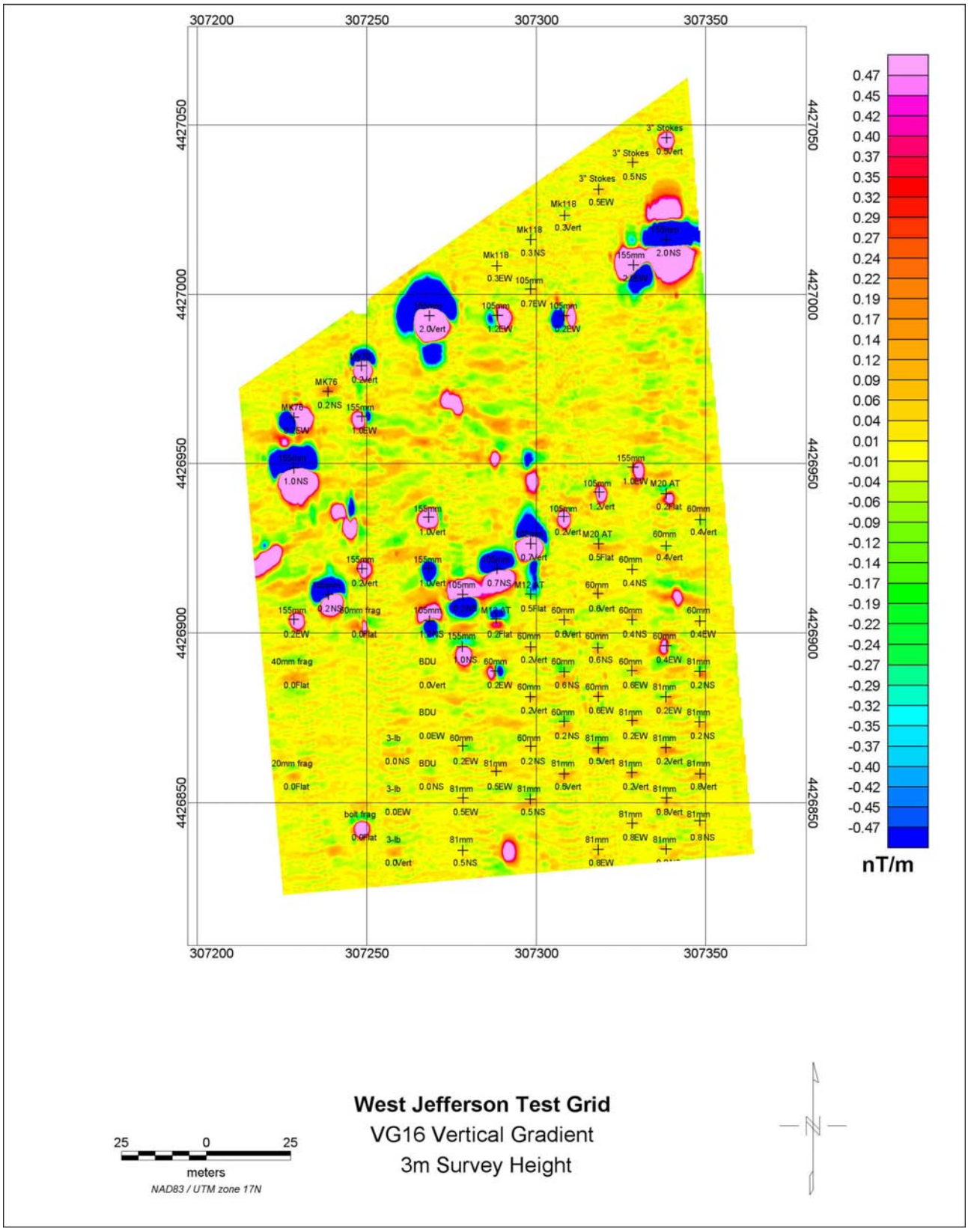

Figure 4-2a. VG-16 airborne vertical magnetic gradient results for 3m altitude from the West Jefferson Test Site. Note that the color bar is different from Figure 4.1a because of the weaker signal at increased altitude.

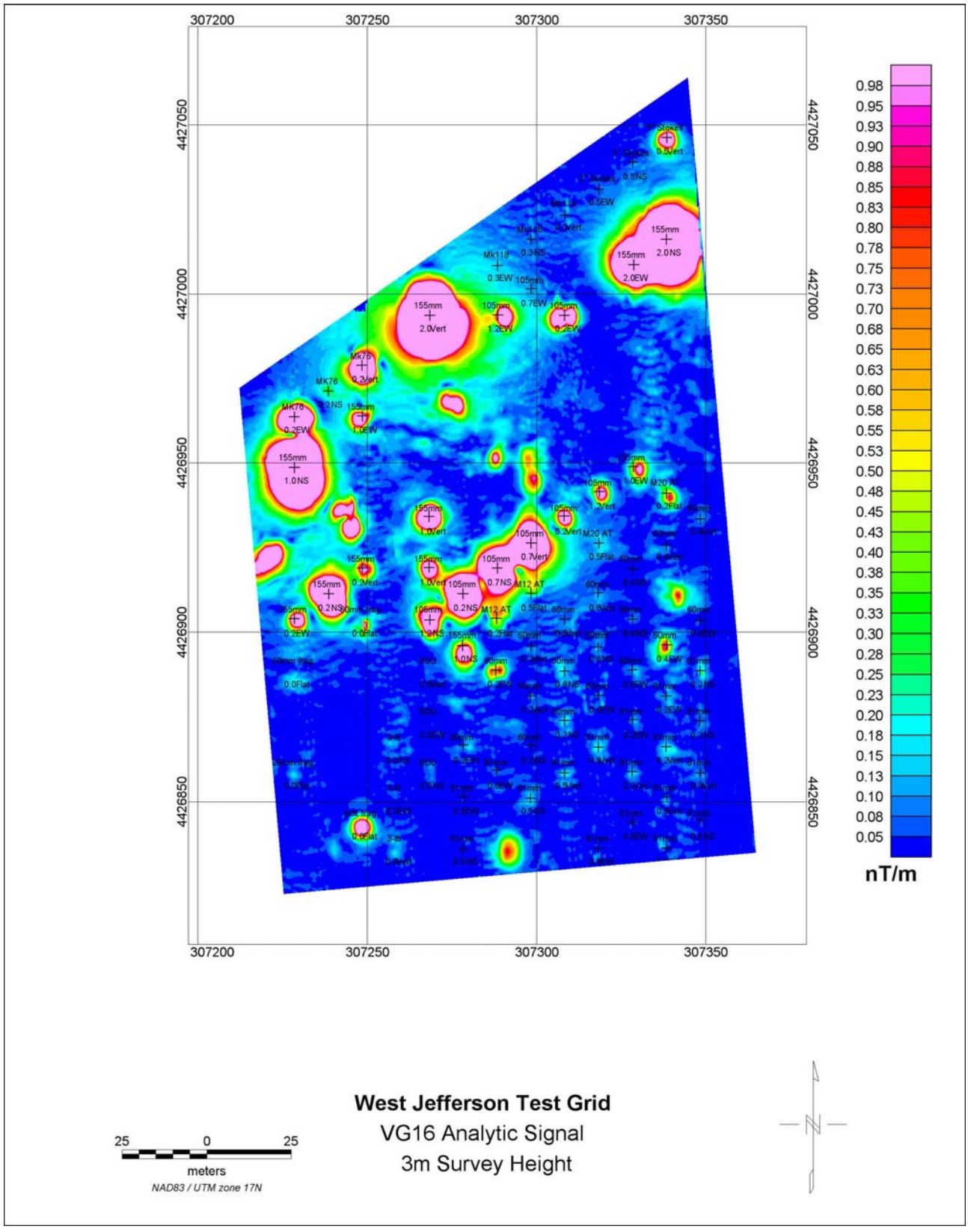

Figure 4-2b. VG-16 airborne analytic signal results for 3m altitude from the West Jefferson Test Site. Note that the color bar is different from Figure 4.1b because of the weaker signal at increased altitude.

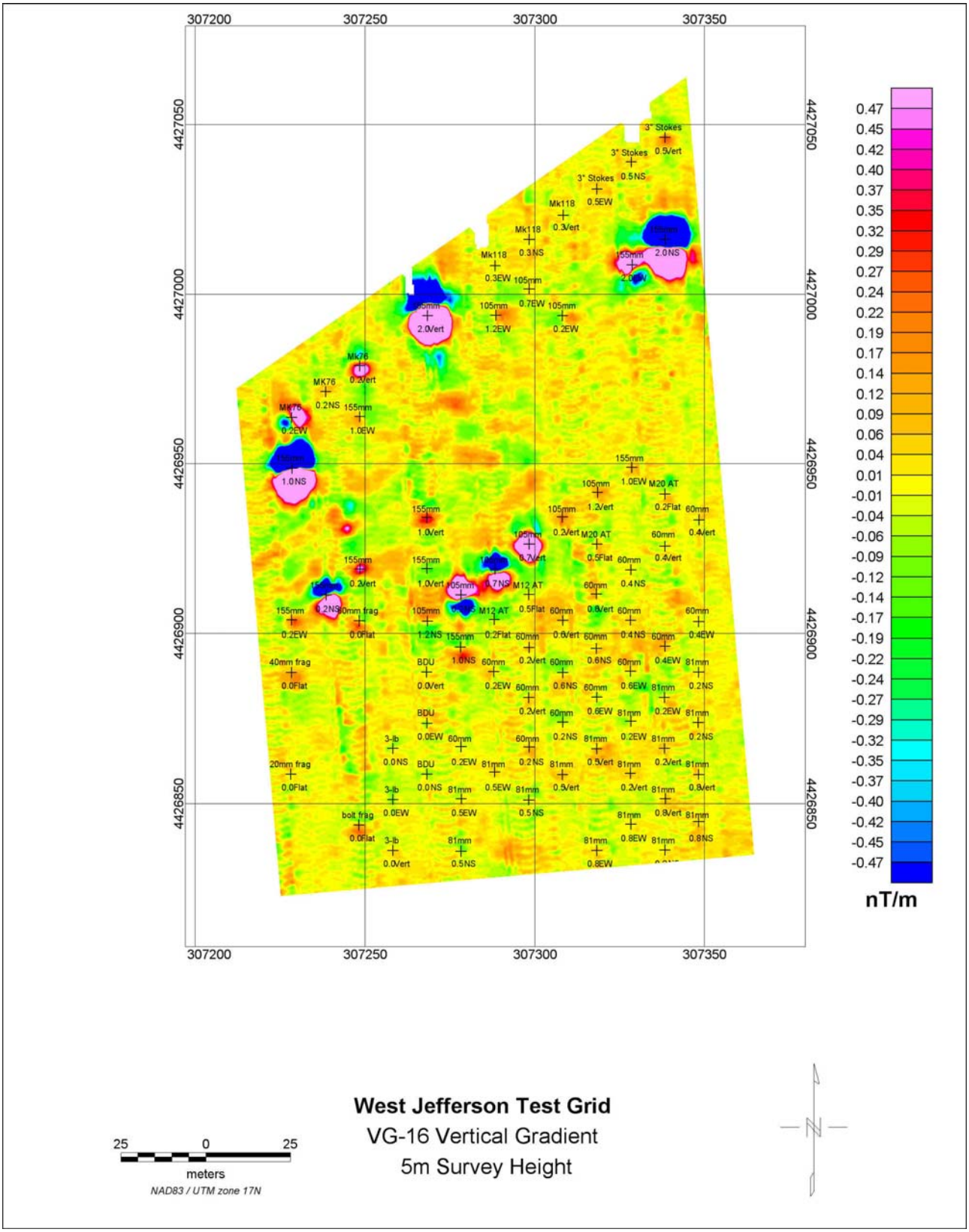

Figure 4-3a. VG-16 airborne vertical magnetic gradient results for 5m altitude from the West Jefferson Test Site. Note that the color bar is different from Figures 4.1a, because of the weaker signal at increased altitude.

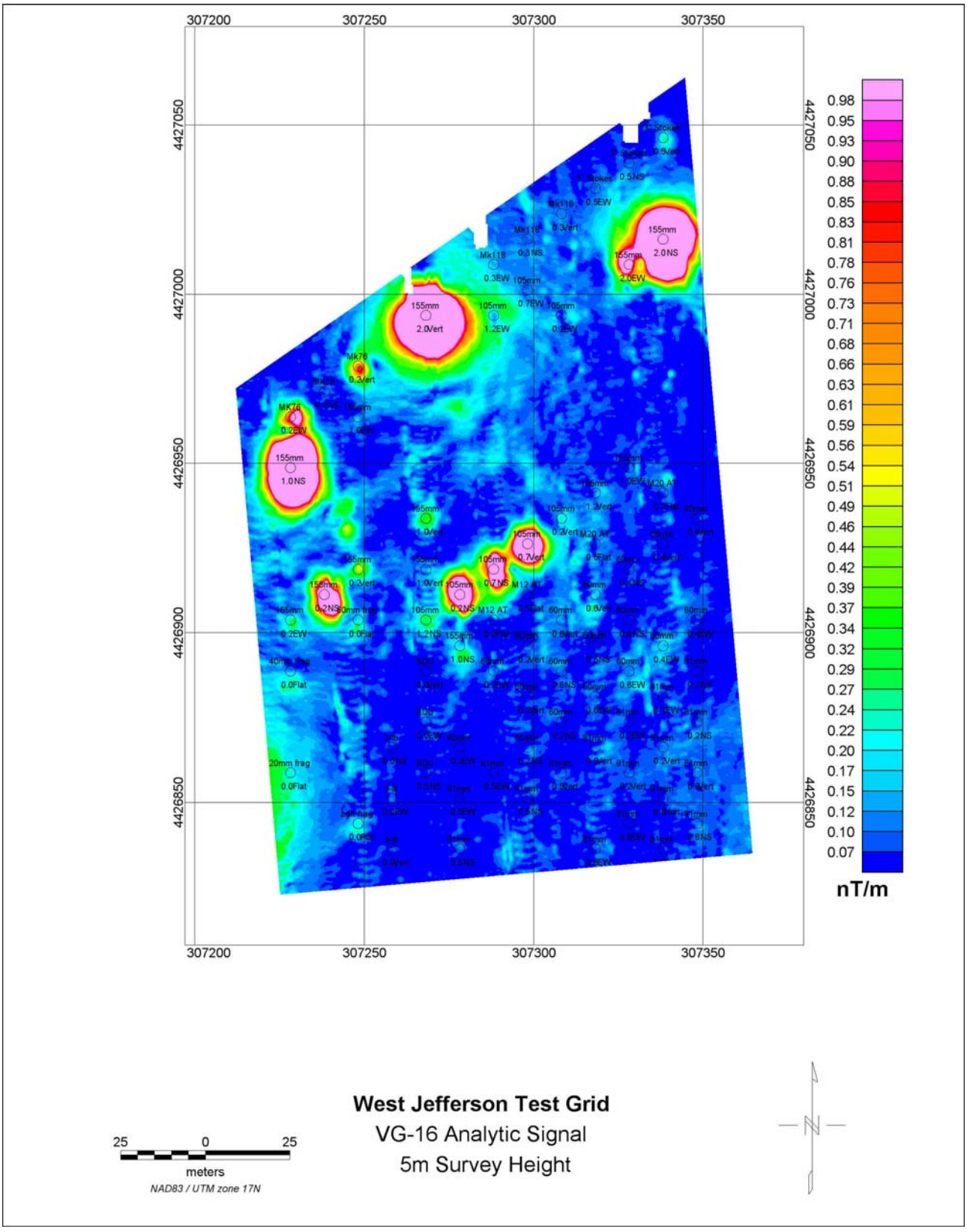

Figure 4-3b. VG-16 airborne analytic signal results for 5m altitude from the West Jefferson Test Site. Note that the color bar is different from Figures 4.1b, because of the weaker signal at increased altitude.

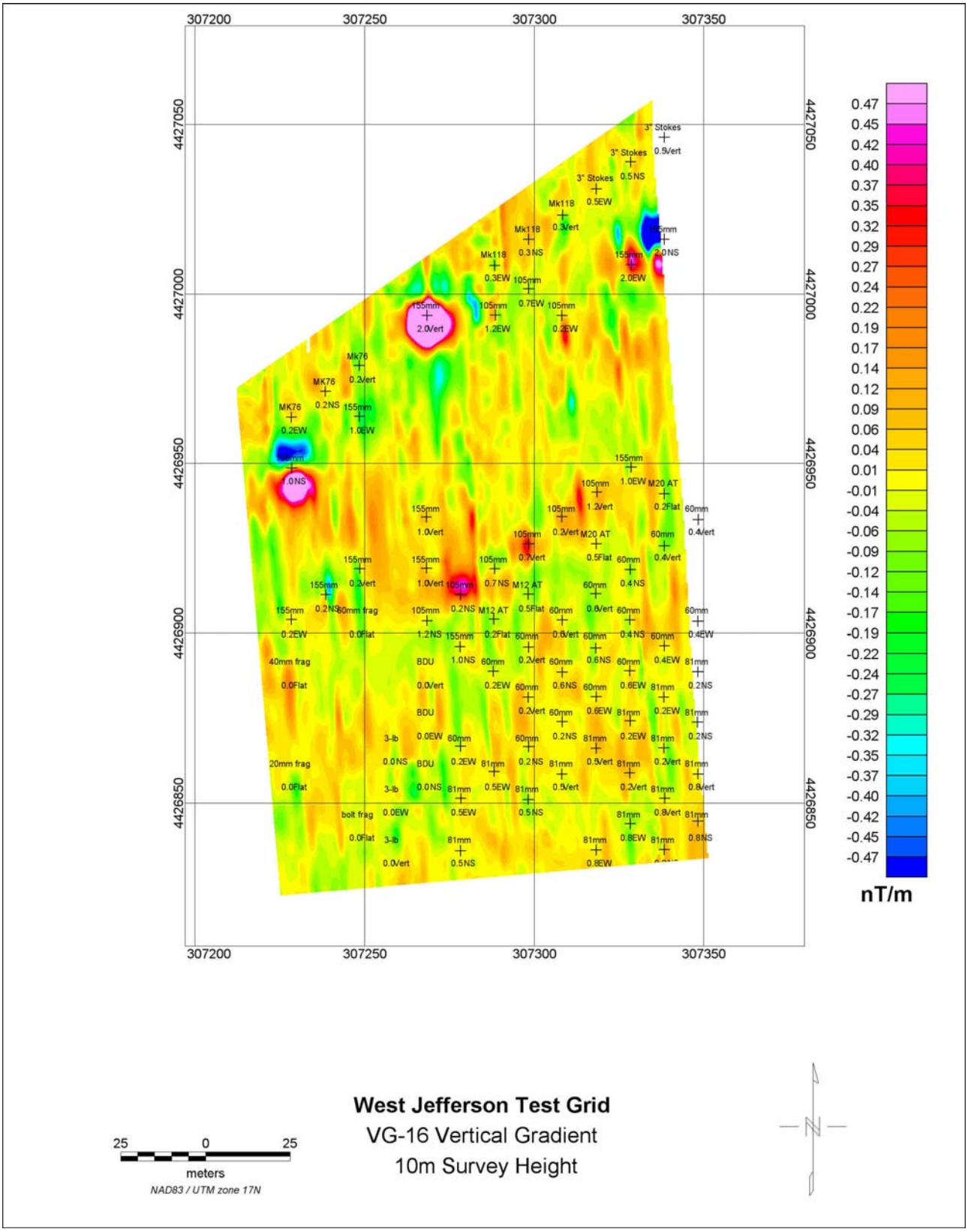

Figure 4-4a. VG-16 airborne vertical magnetic gradient results for 10m altitude from the West Jefferson Test Site.

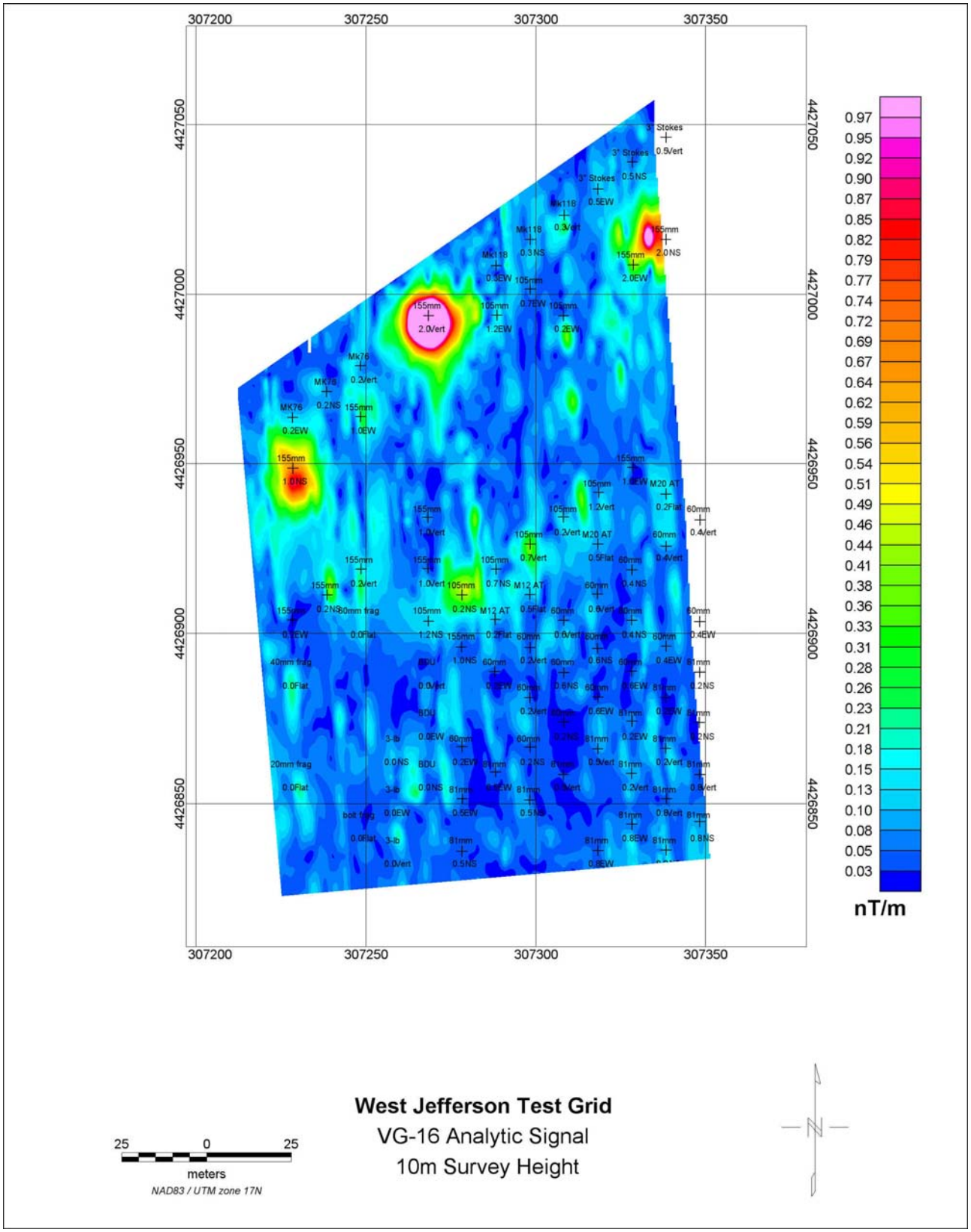

Figure 4-4b. VG-16 airborne analytic signal results for 10m altitude from the West Jefferson Test Site.

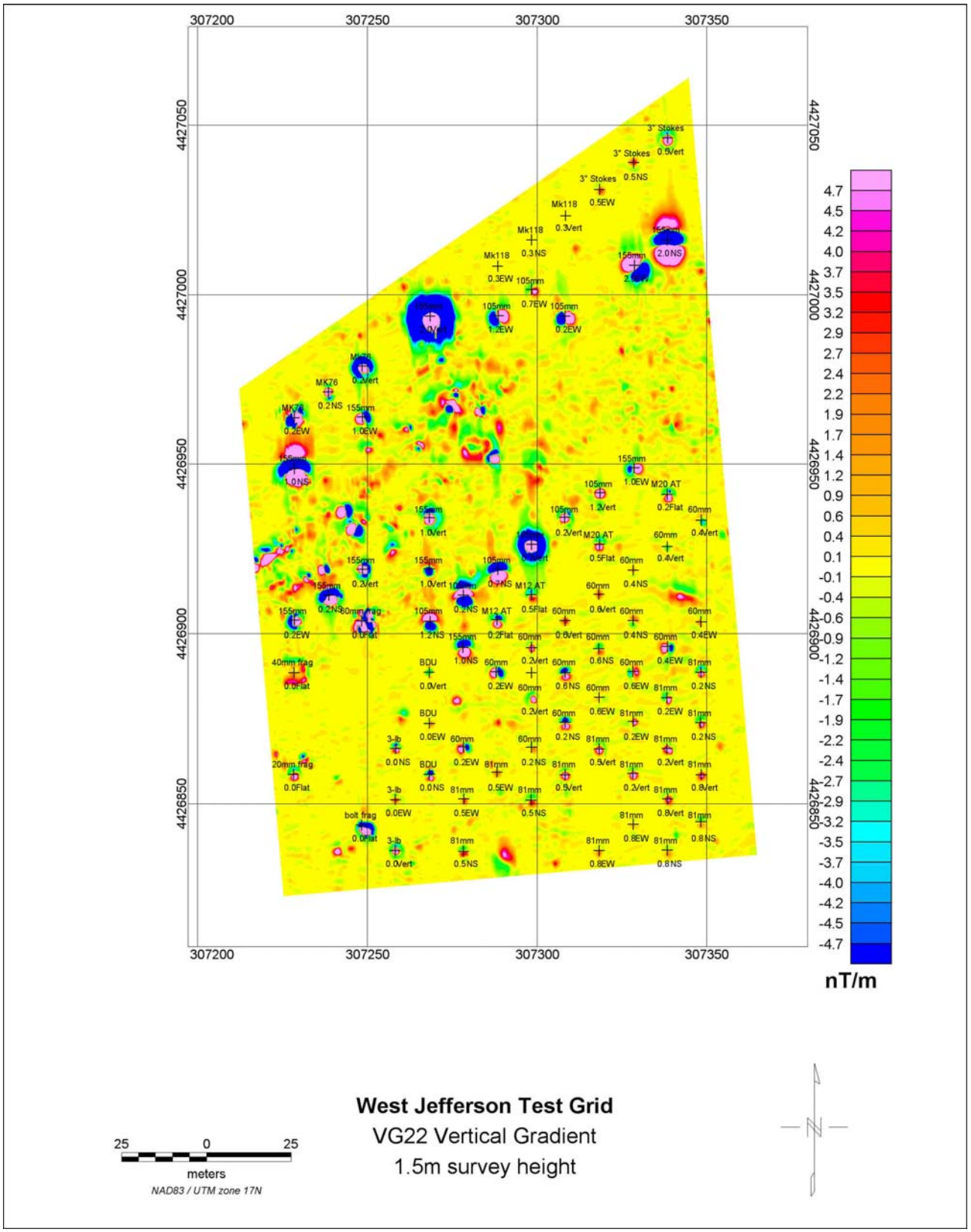

Figure 4-5a. VG-22 airborne vertical magnetic gradient results for 1.5m altitude from the West Jefferson Test Site. The color bar used here is the same as in Figure4.1a, as both data sets were acquired at similar altitude.

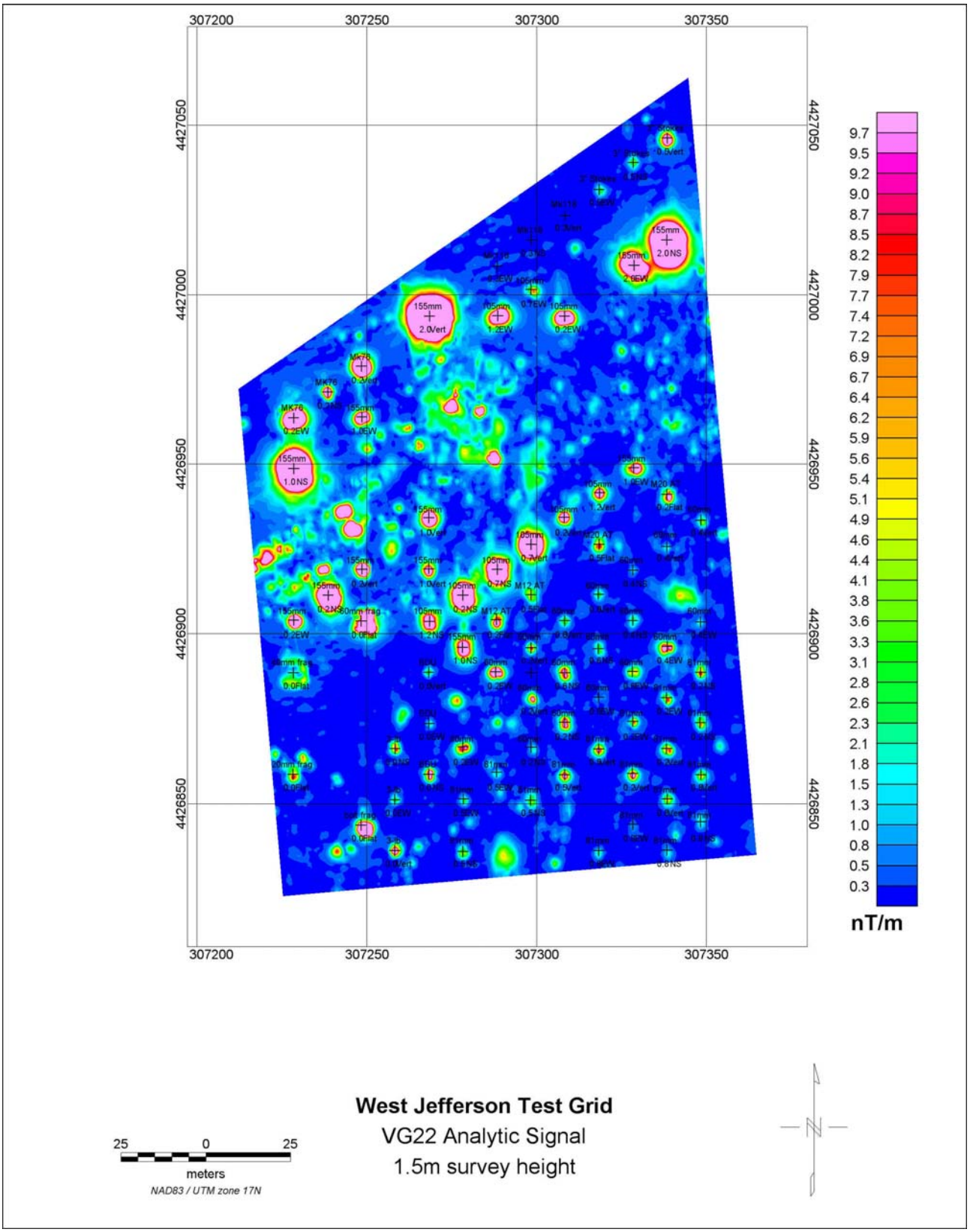

Figure 4-5b. VG-22 airborne analytic signal results for 1.5m altitude from the West Jefferson Test Site. The color bar used here is the same as in Figure4.1b, as both data sets were acquired at similar altitude.

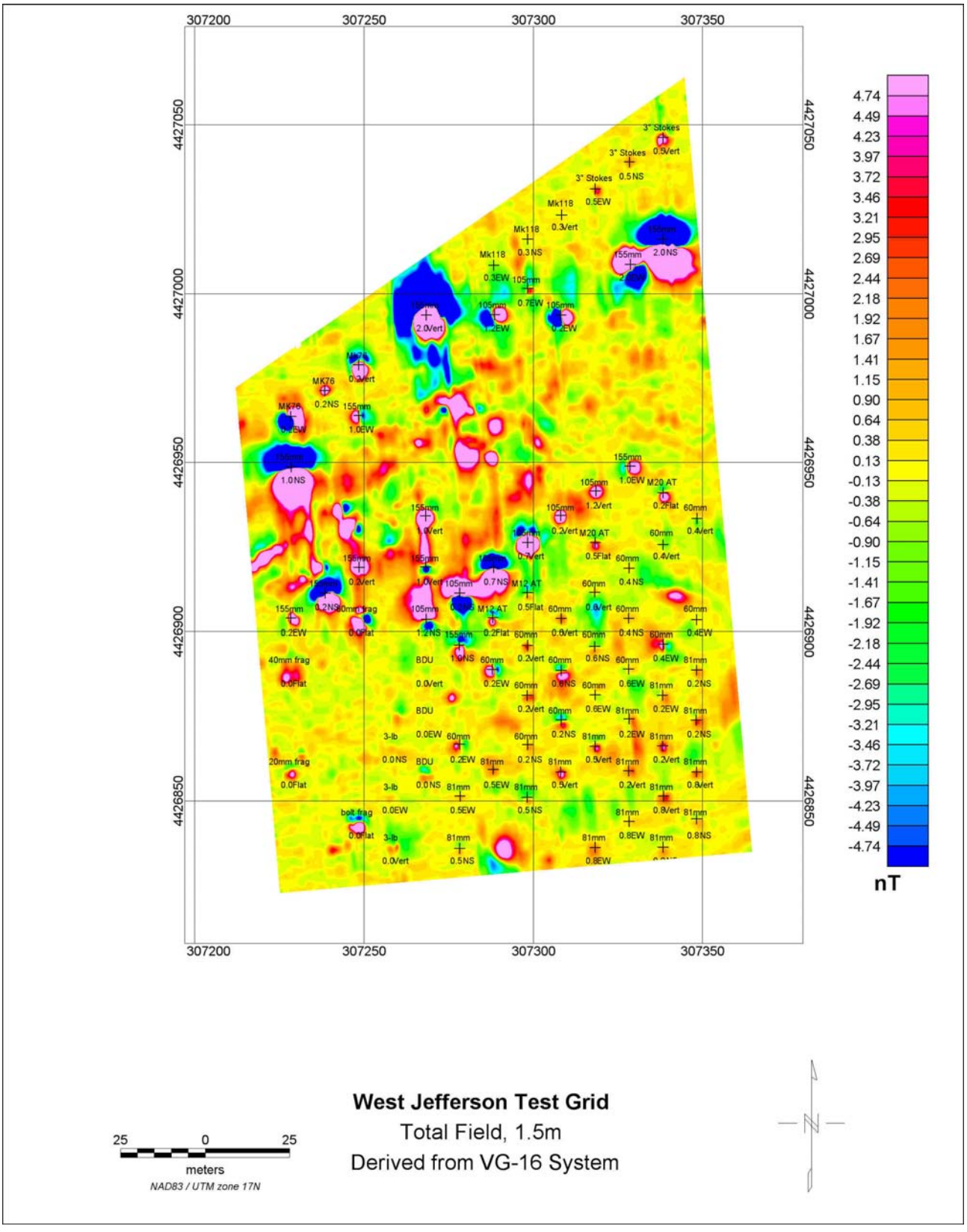

Figure 4-6a. Total field map, using the lower sensors of the gradiometer pods, to represent what could be expected for a total field system at the test grid.

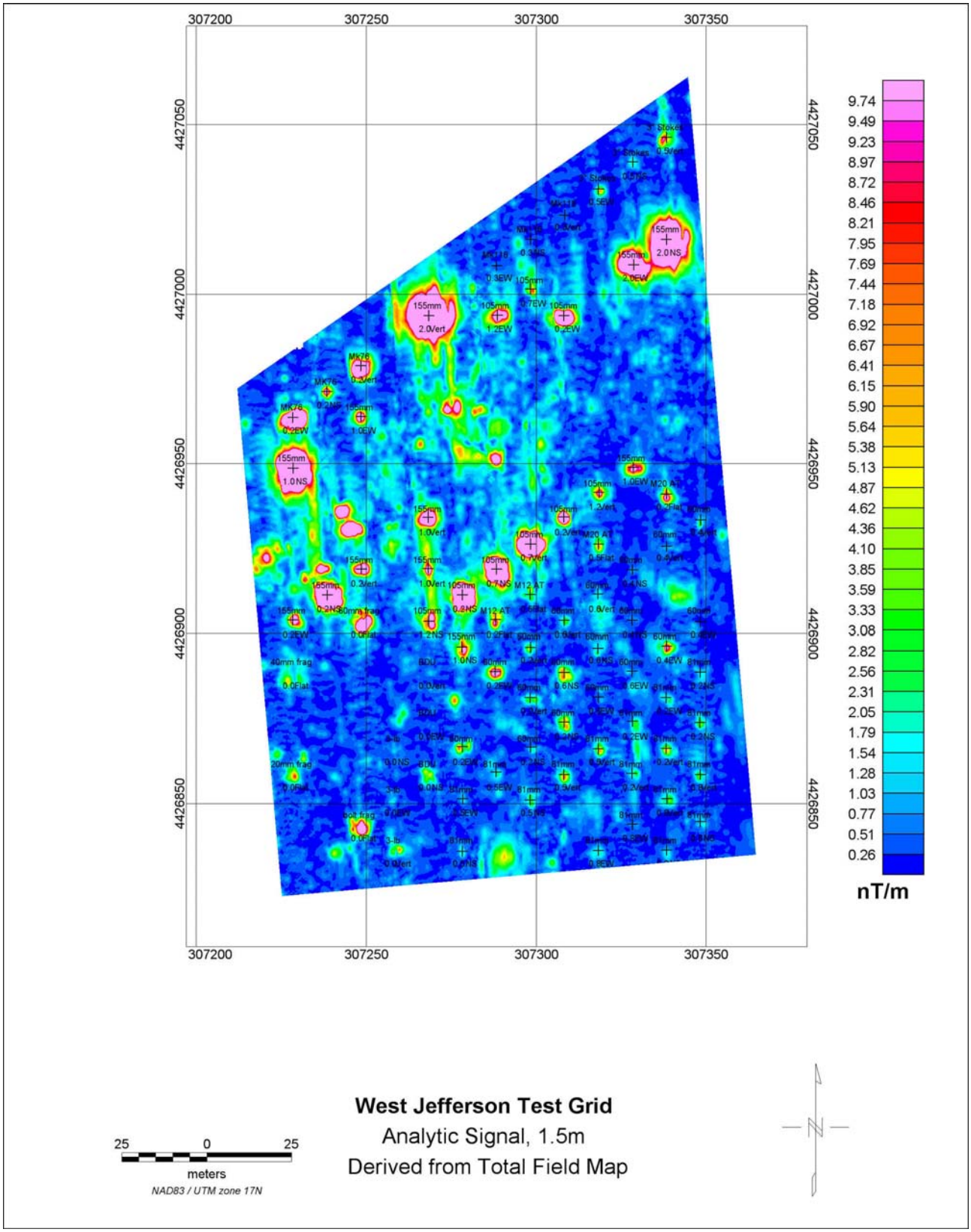

Figure 4-6b. Analytic Signal map derived from Total Field, using the lower sensors of the gradiometer pods, to represent what could be expected for a total field system at the test grid.

Scales for Figures 4-1 through 4-4 were selected in order to emphasize the smallest detectable items. Figures 4-5 and 4-6 have identical scales, chosen to concur with the noise threshold of the system at this site. Actual altitudes differed somewhat from the planned altitudes, as shown in Table 4-3.

Table 4-3: Altitude Statistics for Test Flights

Nominal Altitude	Minimum Altitude	Mean Altitude	Max Altitude	σ
VG-16				
1.5m	1.21	1.62	2.02	0.17
3m	3.38	3.78	5.56	0.42
5m	5.37	5.74	6.09	0.19
10m	9.19	10.05	12.26	0.64
VG-22				
1.5m	1.14	1.52	1.84	0.20
3m	2.97	3.47	5.23	0.46
5m	5.09	5.97	5.57	0.21
10m	9.03	9.66	10.86	0.34

4.4.1 Detection Results

ROC curves for the VG22 are shown in Figures 4-7 through 4-8. All analytic signal anomaly peaks were automatically picked using a 1.0 nT/m threshold. Further discussion of the detection threshold is provided later in this document. The 1.0nT/m threshold resulted in a selection of 198 anomalies. Of these, 77 were associated with emplaced targets (including surface items). All of the emplaced items were detected except for the Mk-118 Rockeyes, which were almost completely non-ferrous and are excluded from this analysis.

An automated dipole inversion routine was applied to the data to calculate the location, moment, dipole inclination/declination and RMS fit error. The angle between the Earth's field and the dipole vector was also calculated, as was the final forward model and residual after removal of the forward model. For discrimination purposes, the results were sorted based on RMS error normalized to analytic signal anomaly amplitude. The resulting ROC curve is shown in Figure 4-7. If items smaller than 81mm mortars are removed from consideration and treated as false positives the ROC curve improves as shown in Figure 4-7. This illustrates how the discrimination process suffers from low signal amplitude even if the overall detection rate does not.

The inversion results were sorted by each of the other parameters as well, but no other single parameter showed a positive correlation with the ground truth. In particular, the deviation between the Earth's field vector and the inversion dipole vector showed a negative correlation implying that the UXO has a strong remanent component, whereas the ground clutter does not (Figure 4-8). This can be explained by two facts. None of the ordnance used here have been degaussed nor have they undergone shock demagnetization. The items from Twentynine Palms and USAESCH were retrieved from site clearing, while the items from APG have never been fired. The site has been cleared of the larger ground clutter which would have the highest probability of remanence.

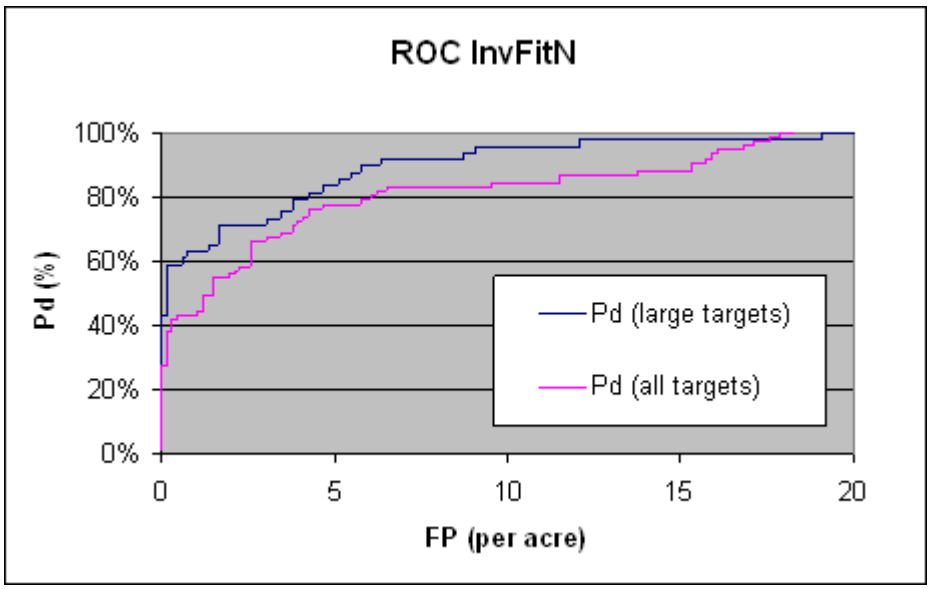

Figure 4-7. ROC curve for VG22 at 1.5m altitude for anomalies sorted based on normalized inversion fit.

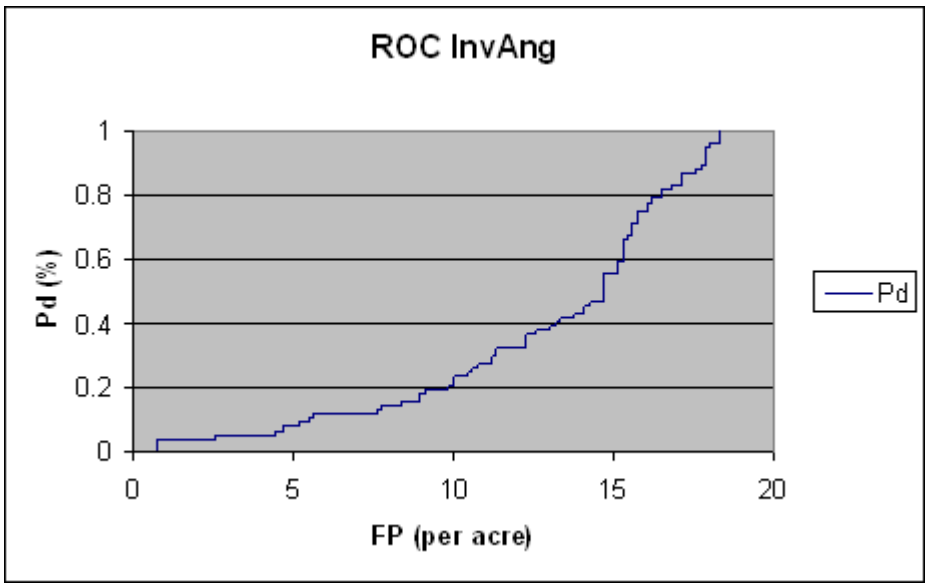

Figure 4-8**.** ROC curve for VG22 at 1.5m altitude for anomalies sorted based on deviation of dipole vector from Earth's field vector (surrogate for remanence).

In Figure 4-9and Table 4-4, we compare the number of test items detected with the Geosoft automatic picking routine as a function of the approximate flight altitude. For each grid, a threshold was selected by visual inspection of anomalies that were apparent in the analytic signal map. The greater sensitivity of the VG-22 system over the VG-16 system is apparent, as is the improved sensitivity of both VG systems over a TF system.

Table 4-4: Numbers of targets detected and total number of picks for three grids

	VG-22		VG-16		Total Field	
	Detections	Tot. No. of picks	Detections	Tot. No. of picks	Detections	Tot. No. of picks
1.5m	77	198	59	141	53	140
3m	56	83	38	56	24	35
5m	24	42	18	35	8	14
10m	7	47	10	56	4	8

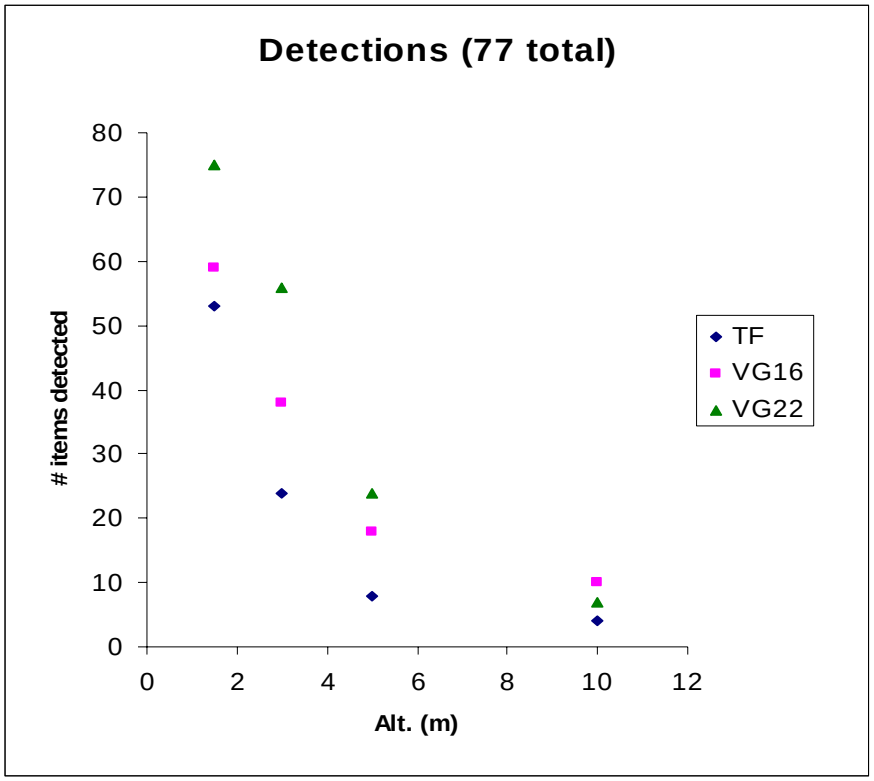

Figure 4-9. Number of test grid items detected as a function of offset for the VG-22, VG-16, and total field (TF) equivalent system configurations.

4.4.2 Detection Threshold

An assessment of optimal detection threshold for the 1.5m VG-22 data was conducted on a sub-area containing 48 items. This included all (18 each) 60mm mortars and 81mm mortars, all (3 each) BDUs and 3-lb practice bombs, the four anti-tank mines, one 155mm projectile, and the bolt blanket. Results are shown in Figures 4-10 and 4-11. In order to capture all 48 seeded items with the VG-22, a detection threshold of 1.0nT/m (or less) must be used (Figure 4-10).

The plot of detection pick ratio vs. threshold (Figure 4-11) has three distinct segments, with breaks in slope occurring at 12.5nT/m and 2.5nT/m. For these data, a picking thresholds of 12.5

nT/m or greater guarantees that every anomaly chosen is UXO-related (i.e., no unsuccessful picks). At 2.5nT/m threshold, 40 of the 48 seed items are detected, with only 57 picks, yielding an 83% success rate. The detection ratio steepens markedly below a 2.5nT/m threshold. Between 1 and 2.5nT/m threshold, the remaining seed items, require a large increase in total picks (127) yielding an overall success rate of only 38%. We anticipated that each of the three groups would be related to different types of ordnance, but inspection of the anomalies (in the southeast portion of the area shown in Figure 4-5) indicates that, apart from the 155mm and bolt blanket, large anomalies are distributed among all types of seed items, so that the groupings contain a mix of ordnance types, depths, and orientations.

It is important to note that in many, if not all, cases, the non-seed picks correspond to geologic and/or man-made background at the site, rather than system noise. The 48-anomaly area that was selected for the assessment of detection threshold was chosen, in part, because it had less background interference than other parts of the test grid. However, the study area was not void of anomalies, many having amplitudes that exceed those of some of the smallest seeded items.

4.4.3 Positioning Analysis

The location accuracy appears to have a uniform bias that may be due to the difference in GPS base station used by the airborne and ground survey teams. The VG-22 locations at 1.5m flight altitude based on the analytic signal peaks showed a mean offset of 0.6m with a standard deviation of 0.3m. The locations based on the dipole inversion improved that to a mean of 0.3m and a standard deviation of 0.2m. The distribution is shown in Figure 4-12. The outliers in the inversion locations are all small targets (60mm and BDUs) with relatively weak signals.

Figure 4-13 shows the mean errors (not RMS) in easting and northing for both system configurations as a function of reference altitude. The ‘total’ positioning error is the RMS error, calculated as the sum of the squares of the differences between measured and actual easting and northing. The VG-22 system shows smaller mean positioning errors in both northing and easting than the VG-16 system, and consistently shows a smaller overall positioning error. Overall positioning errors increase as a function of altitude in a nearly linear fashion. The small mean errors in northing at 10m indicate that deviations to the north are roughly compensated by deviations to the south, yielding almost zero mean. A similar feature is observed in the easting at 10m. The total (RMS) mean positioning error at 10m is about 2.7m and matches the pattern of total errors at other altitudes. The standard deviation of positioning errors also increases as a function of altitude in a nearly linear manner, but shows no obvious difference between VG-16 and VG-22 performance.

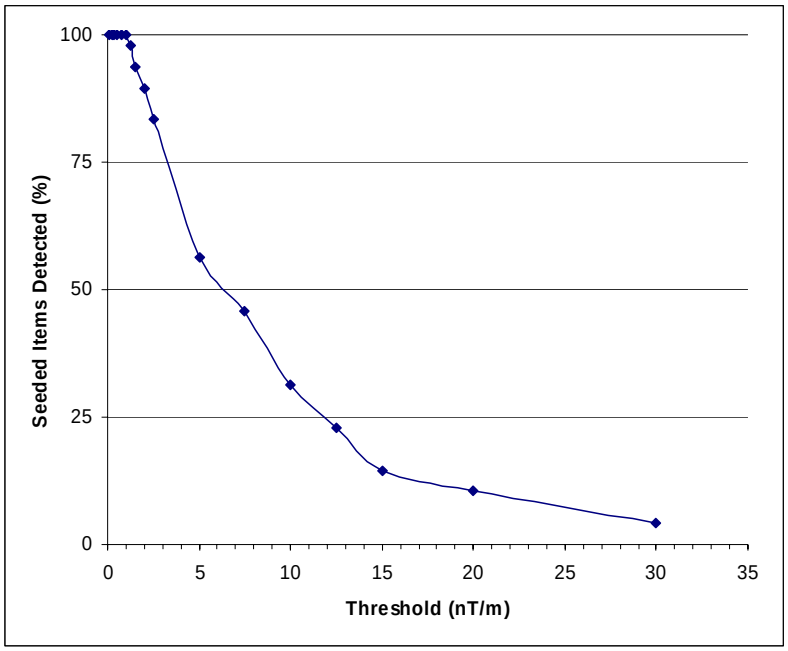

Figure 4-10. Percentage of seeded items detected as a function of threshold. A threshold of 1nT/m is required in order to detect all targets.

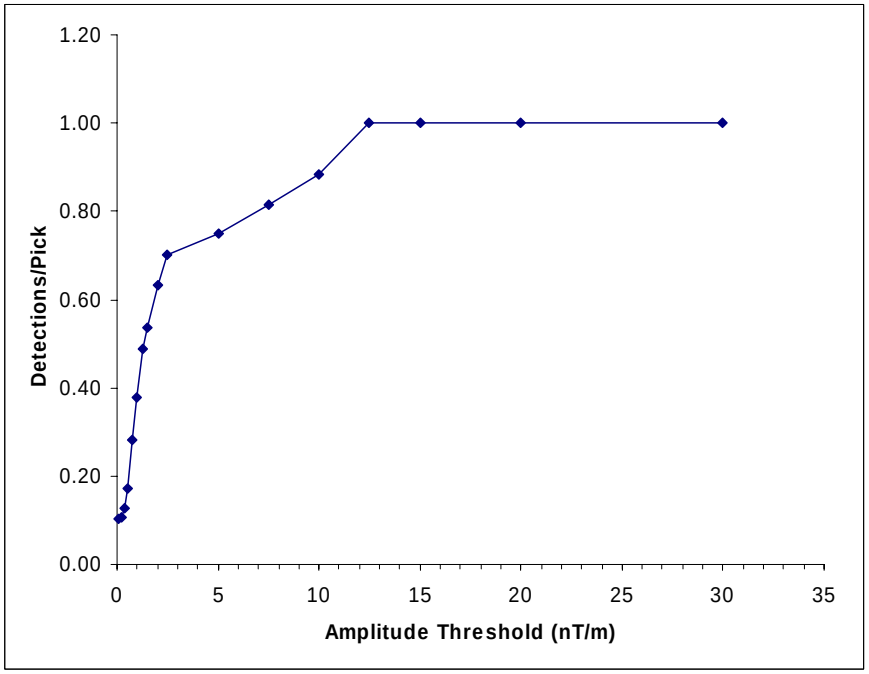

Figure 4-11. Ratio of detected seeds to total picks, as a function of amplitude threshold. In order to detect all 48 seeded items, one must accept a ratio of 0.37 for this data set.

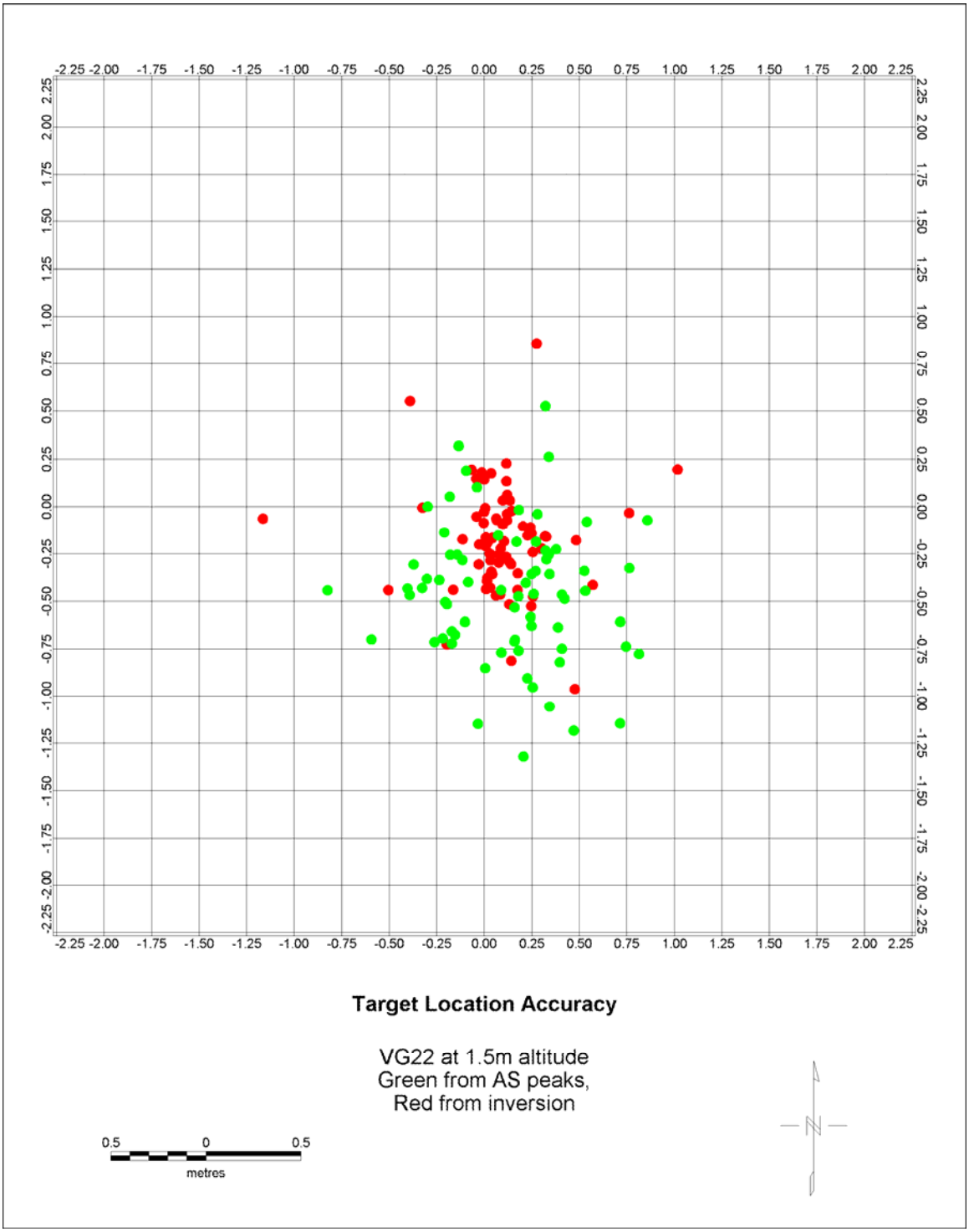

Figure 4-12. Target location accuracy plot for VG22 at 1.5m altitude. Green dots are the locations based on the analytic signal peaks. Red dots are locations based on the inversion results.

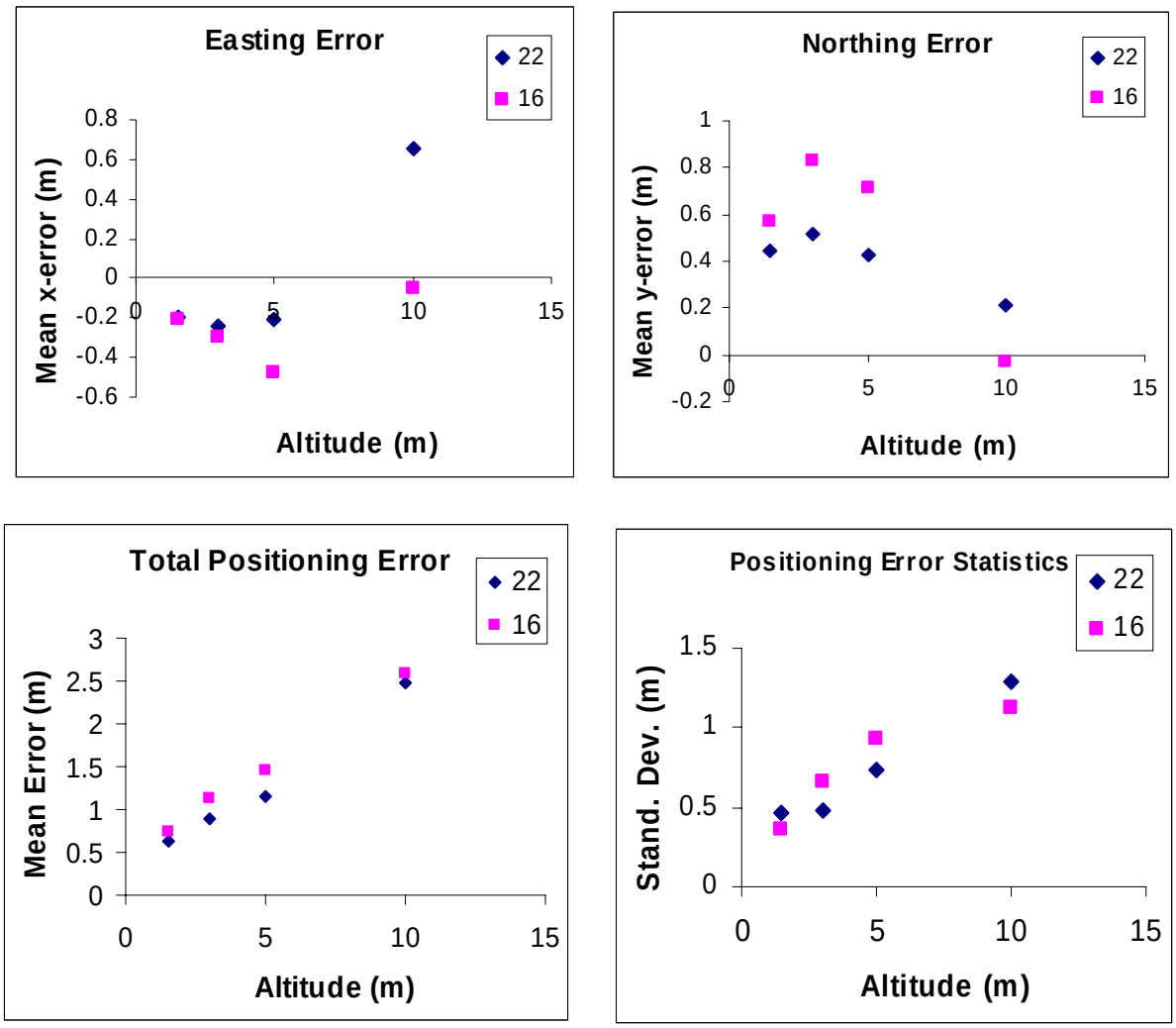

Figure 4-13. Summary of positioning errors as a function of altitude and system configuration.

4.4.4 Anomaly amplitude vs. offset from targets

Finally, anomaly amplitudes were assessed as a function of target type, orientation, and offset from the targets. We selected two representative ordnance types, 155mm and 81mm, and show the amplitudes as a function of the sum of target depth and sensor altitude above ground level. In Figures 4-14 and 4-15, these are shown in log-linear plots. Clearly there is a wide disparity in amplitude among objects of a particular type, independent of orientation. Careful review shows good agreement between the VG22 and VG-16 responses to individual items, with the VG-22 amplitudes consistently higher than the corresponding VG-16 response to the same items. On both plots, red lines are used to represent an approximate envelope for the VG-22 system, and blue lines represent approximate envelopes for the VG-16 system. The benefit of the VG22 system is more apparent with the 81mm data (Fig 4-15), but can be recognized in both.

In Figures 4-14 and 4-15, the range of amplitudes at any given depth is greater for the VG-16 than for the VG-22 system. If this relationship holds in a broader context, it could be associated with a wider range of possible lateral sensor offsets for the VG-16 system (0.0-0.85 for VG-16 vs. 0.0-0.5m for VG-22).

When similar plots are prepared for ground-based measurement, the combination of system and geologic noise can be represented as a constant, and used to evaluate likelihood of detection for items buried at a particular range of depths. With airborne data, however, the data acquisition can occur at a range of altitudes, and though system noise is expected to be independent of depth, the geologic noise will fall off with sensor altitude, as the amplitudes of anomalies associated with seeded items fall off with depth. Likewise, the "11x" anticipated detection limit (limit of detection where depth is eleven times ordnance diameter) can be drawn as a constant on a depth chart for ground-based measurements, but for airborne data, the ordinate is the sum of altitude and depth, so the 11x line becomes 11(x + h) , where h is altitude. These variations in noise and offset that vary with altitude cause the interpretation of these figures to be more complicated, but no less valuable as an interpretation tool.

At 1.5m altitude, site noise resulted in a detection threshold of 1.0 nT/m. This threshold allowed detection of all ferrous seeded items in the grid. Most of the rest of the picks used a threshold of about 0.2nT/m (independent of altitude), which may approximate the system noise threshold in the absence of geologic background anomalies.

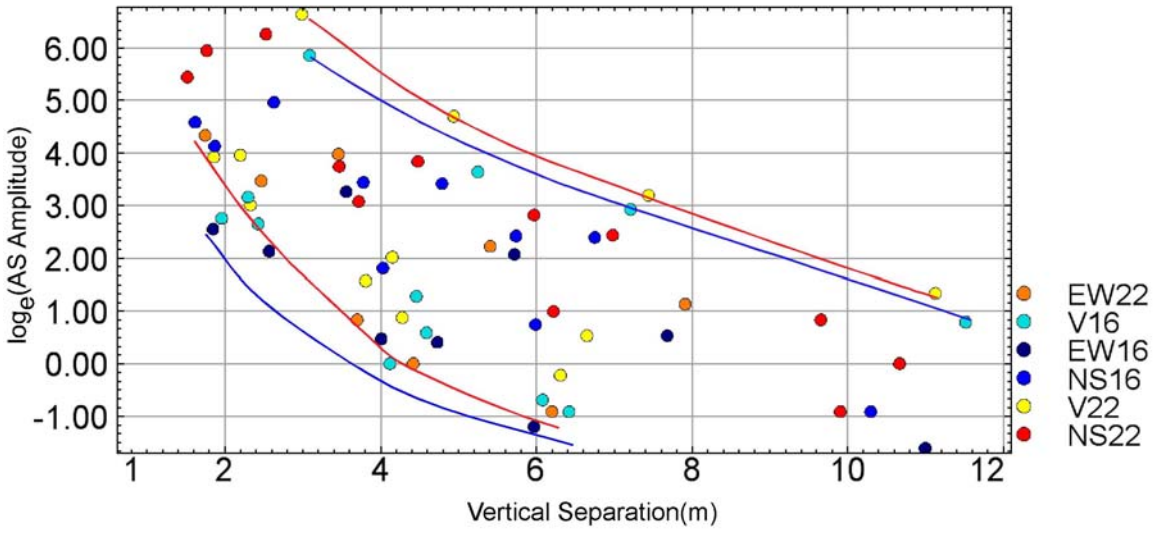

Figure 4-14. Peak anomaly amplitudes for 155mm plotted as a function of vertical offset (depth + altitude) in m. The vertical axis of the plot is the log of the amplitude in nT/m. The three orientations and two systems are distinguished by color coding. Approximate bounds for the VG-22 system are shown in red, while those for the VG-16 are shown in blue.

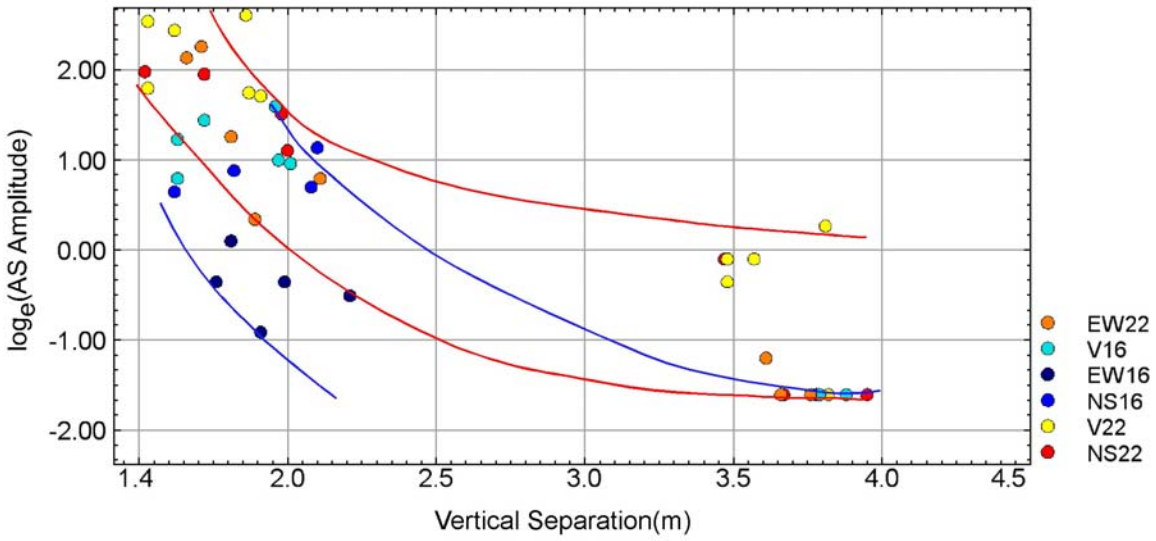

Figure 4-15. Peak anomaly amplitudes for 81mm plotted as a function of vertical offset (depth + altitude) in m. The vertical axis of the plot is log of the amplitude in nT/m. The three orientations and two systems are distinguished by color coding. Approximate bounds for the VG-22 system are shown in red, while those for the VG-16 are shown in blue.

Several important conclusions can be drawn from these results:

1) The detection results for the VG-22 system are excellent, and are better than we anticipated even for a test grid. Of note is the 100% detection of 60mm and 81mm and other small items (e.g. BDUs, 3lb practice bombs) at 1.5m altitude.
2) The sensitivity of the VG-16 system was noticeably less than that of the VG-22 system, as anticipated. It is also considerably better than the total field surrogate, even though the latter was derived from the lower sensors of each gradiometer, which would be at lower altitude than the center of each corresponding gradiometer.
3) None of the configurations, including the ground-based configuration were successful in detecting the MK-118 Rockeyes. We note that the magnetic signature of these items, as measured at the test stand, are roughly the same as that of the 20mm, which is well below the detection threshold for any known airborne system. The weak signature occurs because these items are composed predominantly of aluminum with a copper band (R. Fling, personal communication, 12/2006). It is therefore surprising that they have *any* magnetic signature, and we attribute this to impurities in the aluminum or minor ferrous components.
4) The results from 5m and 10m nominal survey altitudes were surprising, in that they indicate greater sensitivity than was anticipated. It is particularly noteworthy that many of the 81s were detectable at 5m, and there appears to be response to the ”ordnance sheets” (20mm, 40mm, 60mm) even at 10m.
5) Target location errors show a standard deviation of 0.3m for the analytic signal peaks and 0.2m for the inversion results. Additional work on the inversion code will improve the performance. A consistent offset of about 20cm has been noted in the results and is thought to be associated with the different base stations used by the surveyors and airborne team.

6) The ROC curves show that a simple univariate sorting based on normalized inversion fit produces good results. A multivariate sorting to include other parameters may improve this.

4.5 Field Results – FKPBR

4.5.1 Data Processing Parameters

The data were desampled in the signal processing stage from a raw 1200 Hz format to a 120 Hz recording rate using a finite impulse response (FIR) anti-alias filter. All other raw data were interpolated to a 120 Hz rate. This results in a down-line sample density of approximately 15cm at typical survey speeds. Data were converted to an ASCII format and imported into a Geosoft format database for processing. With the exception of the differential GPS post-processing and the calculation of compensation coefficients, all data processing was conducted using the Geosoft software suite.

4.5.1.1 Positioning

The pilot was guided during flight by an on-board navigation system. This provided sufficient accuracy for data collection (approximately 1m), but was inadequate for final data positioning. To increase the accuracy of the final data positioning, a base station GPS was established at a USGS monument. Raw data were collected in the aircraft and on the ground for differential corrections. These were applied in post-processing to provide 2cm accuracy in the antenna positioning (based on our software's quality assurance parameters). The final latitude and longitude data were projected onto an orthogonal grid using the North American Datum 1983 (NAD 83) UTM Zone 13N meters.

The locations of each magnetometer sensor and the GPS antenna were measured relative to one another by a civil surveyor while the system was in a hangar. In-flight locations are determined by using the GPS antenna location and the aircraft orientation, as measured by an inertial navigation unit. This system outputs pitch, roll and azimuth. These data are combined with the physical geometry of the array to calculate the position and relative height of each magnetometer sensor.

Vertical positioning was monitored by laser altimeter with an accuracy of 2cm.

4.5.1.2 Magnetic Data Processing

The magnetic data were processed in several stages. This included correction for time lags, removal of sensor dropouts, compensation for dynamic helicopter effects, correction for sensor heading error, and removal of helicopter rotor noise. Each of these steps is further discussed below. The magnetic analytic signal (total gradient) was derived from the measured vertical magnetic gradient data.

4.5.1.3 Quality Control

The data were examined in the field to ensure sufficient data quality for final processing. Each of the processing steps listed above were evaluated and tested. The adequacy of the compensation data, heading corrections, time lags, orientation calibration, overall performance and noise levels, and data format compatibility were all confirmed during data processing. During survey operations, flight line locations were plotted to verify full coverage of the area. Missing lines or areas where data were not captured were rejected and reacquired. Data were also examined for high noise levels, data drop outs, unacceptable diurnal activity or other unacceptable conditions. Lines deemed to be unacceptable were re-flown during the acquisition stage. Occasional lines

deviated from a straight flight path due to local topography or vegetation.

4.5.1.4 Time Lag Correction

There is a lag between the time an instrument makes a measurement and when it is time-stamped and recorded. This applies to the magnetometers, fluxgate and the GPS. Accurate positioning requires a correction for this lag. Time lags between the magnetometers, fluxgate and GPS signals were measured by a proprietary utility. This utility sends a single EM pulse that is timed to the GPS signal and visible in the data streams of the fluxgate and magnetometers. This lag was corrected in all data streams before processing.

4.5.1.5 Sensor Drop-outs

Cesium vapor magnetometers have a preferred orientation to the Earth's magnetic field. As a result of the motion of the aircraft, the sensor dead zones will occasionally align with the Earth's field. In this event, the readings oscillate between very large negative and positive numbers. This usually occurs only during turns between lines, and rarely during on-line surveying (<1 sec of data loss per day). All dropouts were removed manually during processing.

4.5.1.6 Aircraft Compensation

The presence of the helicopter in close proximity to the sensors causes considerable deviation in the readings, which requires compensation. The orientation of the aircraft with respect to the sensors and the motion of the aircraft through the earth's magnetic field are contributing factors. A calibration flight is flown to record the information necessary to remove these effects. The maneuver consists of flying a box-shaped flight path at high altitude to gain information in each of the cardinal directions. During this procedure, the pitch, roll and yaw of the aircraft are varied. This provides a complete picture of the effects of the aircraft at all headings in all orientations. The entire maneuver was conducted twice for comparison. The information was used to calculate coefficients for a 19-term polynomial for each sensor. The fluxgate data were used as the baseline reference channel for orientation. The polynomial is applied post flight to the raw data, and the results are referred to as the compensated data.

The use of vertical gradient reduces the raw compensation noise through common-mode rejection. The effectiveness of this can be seen in Figure 4-16. The raw vertical gradient noise in this sample is 6.6x lower than the total field data from the component sensors. This reduces the amount of airframe noise that the compensation routine must eliminate.

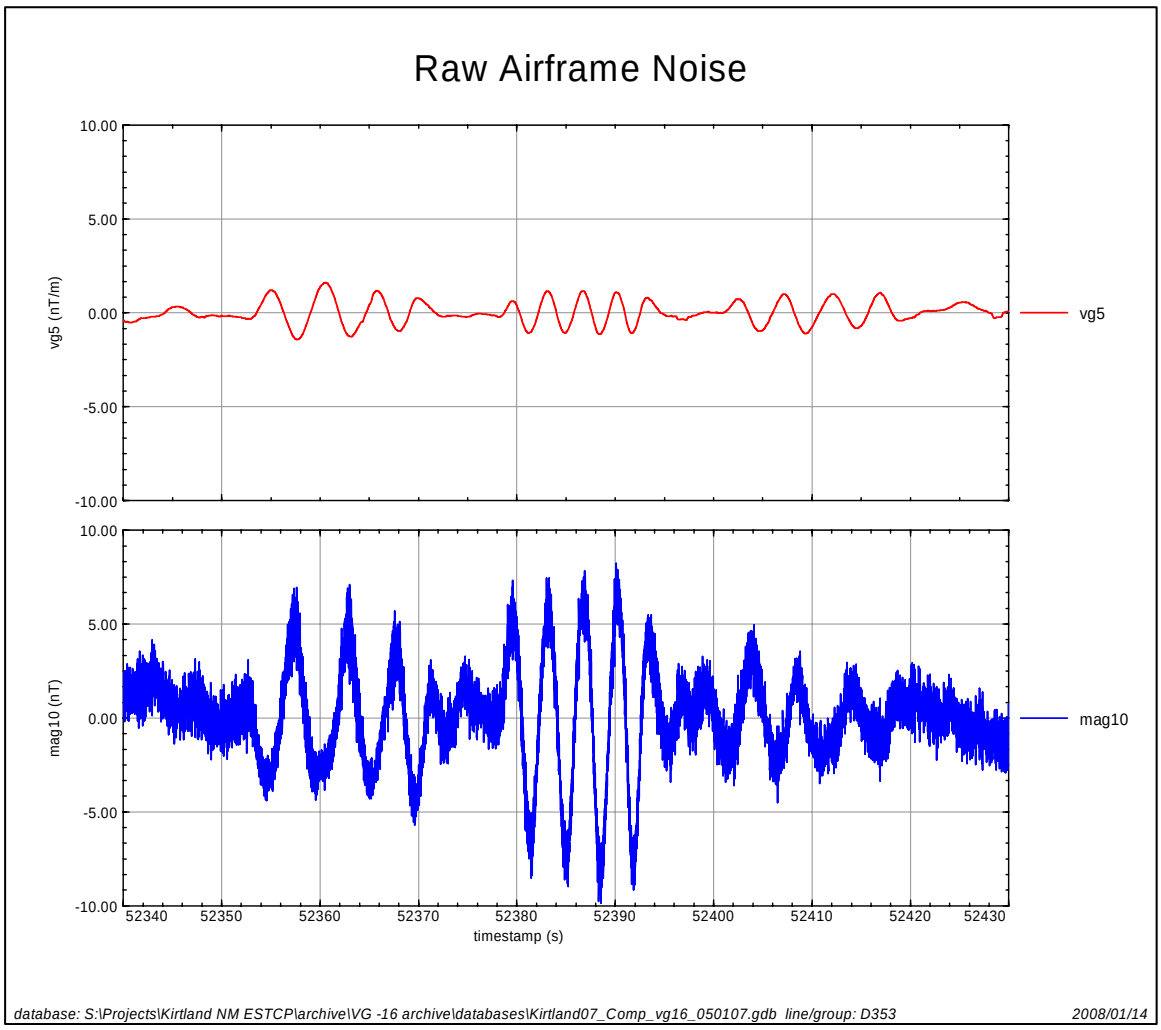

Figure 4-16. Raw airframe noise prior to compensation over a 90sec data sample. The vertical gradient demonstrates a 6.6x reduction in noise. The high frequency noise observable in the total field profile is rotor noise.

4.5.1.7 Rotor Noise

The aircraft rotor spins at a rate of about 400rpm. This introduces noise to the magnetic readings at a frequency of approximately 6.6 Hz. Harmonics at multiples of this base are also observable, but have much smaller amplitudes. This frequency is usually higher than the spatial frequency created by near-surface metallic objects and is removed with a frequency filter. The use of vertical gradient virtually eliminates this noise source as can be seen in Figure 4-17. The raw rotor noise in this sample is 4.3x lower in the vertical gradient than the associated total field.

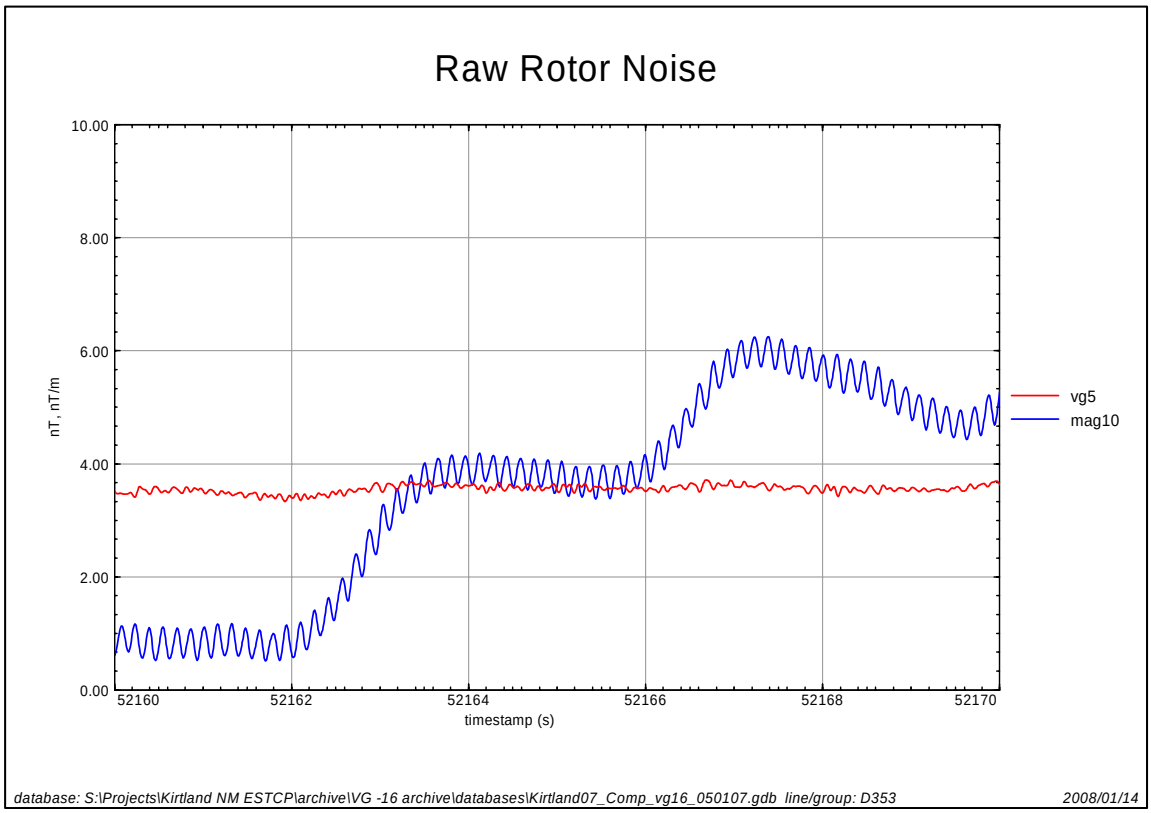

Figure 4-17. A 10s data sample comparing raw total field (blue) and vertical gradient (red) profiles. The vertical gradient demonstrates a 4.3 times reduction in raw peak-peak rotor noise. The low frequency changes in the total field data represent the magnetic signature of the moving airframe which is removed by compensation. The 4.3 times increase in signal/noise ratio is dependent upon the observation that the amplitude of a total field dipole anomaly at a given altitude is numerically equivalent, within a factor of two, to the amplitude of a vertical gradient anomaly at the same altitude, within the 1.5-7m range (e.g. an object that produces a 1nT total field anomaly would yield a vertical gradient anomaly of roughly 1nT/m; see Gamey et al., 2004).

4.5.1.8 Heading Corrections

Cesium vapor magnetometers are susceptible to heading errors. The result is that one sensor will give different readings when rotated about a stationary point. This error is usually less than 0.2 nT. Heading corrections are applied to adjust readings for this effect.

4.5.1.9 Magnetic Diurnal Variations

The earth's magnetic field can vary by hundreds of nT over the course of a day. This means that measurements made in the air include a randomly drifting background level. A base station sensor was established to monitor and record this variation every three seconds. The time stamps on the airborne and ground units were synchronized to GPS time. Diurnal removal is not necessary with a vertical gradient configuration, but it is monitored as a guide to background conditions. The diurnal activity recorded at the base station was extremely quiet.

4.5.1.10 Vertical Magnetic Gradient

The vertical magnetic gradient is measured as the difference between measured values in each gradiometer pod (bottom magnetometer minus top). This is a distinction from total magnetic field surveys in which vertical magnetic gradient is calculated, rather than measured. The VG-16 data are gridded at 0.5m intervals. The VG-22 data for this survey are gridded at 0.25m intervals.

4.5.1.11 Analytic Signal

The analytic signal is calculated from the gridded vertical magnetic gradient data as the square root of the sum of the squares of three orthogonal magnetic gradients. It represents the maximum rate of change of the magnetic field in three-dimensional space – a measure of how much the magnetic field would change by moving a small amount in the direction of maximum change.

There are several advantages to using the analytic signal. It is generally easier to interpret than total field or than vertical gradient data for small object detection because it has a simple positive response above a zero background. The amplitude of the response depends on the strength of the magnetic anomaly. In comparison, total field and vertical gradient maps typically display a dipolar response to small, compact sources (having both a positive and negative deviation from the background). The actual source location is at a point between the two peaks that is dependent upon the magnetic latitude of the site and the properties of the source itself. Analytic signal is essentially symmetric about the target, is always a positive value and is less dependent on magnetic latitude. More generally, the analytic signal highlights the corners of source objects, but for small targets at the latitude of this survey, these corners converge into a single peak almost directly over the target.

4.5.2 Calibration Lines

At the beginning and end of each day, with occasional exceptions, data were acquired along a pair of calibration lines that were established at the onset of the project for QA purposes. In all, the test line was flown 26 times by the VG-16 and 20 times by the VG-22. Ordnance items in the calibration lines included all of those that were seeded in the blind test grid, as well as a pair of M-38 simulants. Standard calibration items that had been used previously in WAA work were planned, but were unavailable at the time of the survey. This data set provided a basis for selecting thresholds for picking anomalies in the data from the blind seeded area (South Area).

A representative plot from the VG-22 is shown in Figure 4-18. It shows the analytic signal results from the west-bound fly-over on the morning of April 27. Targets are identified by text with their locations shown as circles. Crosses mark the location of analytic signal peaks that were chosen by the automated picking routine's final parameter selection. All targets were detected except for one of the two 60mm mortars. That is 94% detection overall with 50% detection of the 60mm mortars. In total, 39 picks were made, 15 of which were targets. Since no excavations were done on this test grid site we cannot calculate a false positive ratio or speculate as to the nature of the other anomalies, but this is equivalent to 15 picks/acre. These statistics are entirely consistent with the results over the grid as a whole for the VG-22 which were 90% overall Pd and 56% detection of 60mm mortars based on 12 picks/acre (see Table 4-5).

The results from the VG-16 from the afternoon east-bound fly-over of May 2 are shown in Figure 4-19. The overall Pd is 75%, detecting all targets 81mm and above, but missing all smaller targets. Given the small number of targets emplaced in the test grid (only one or two of each),

these results are consistent with performance over the main body of the grid (67% Pd overall, targets smaller than 81mm show <50% detection).

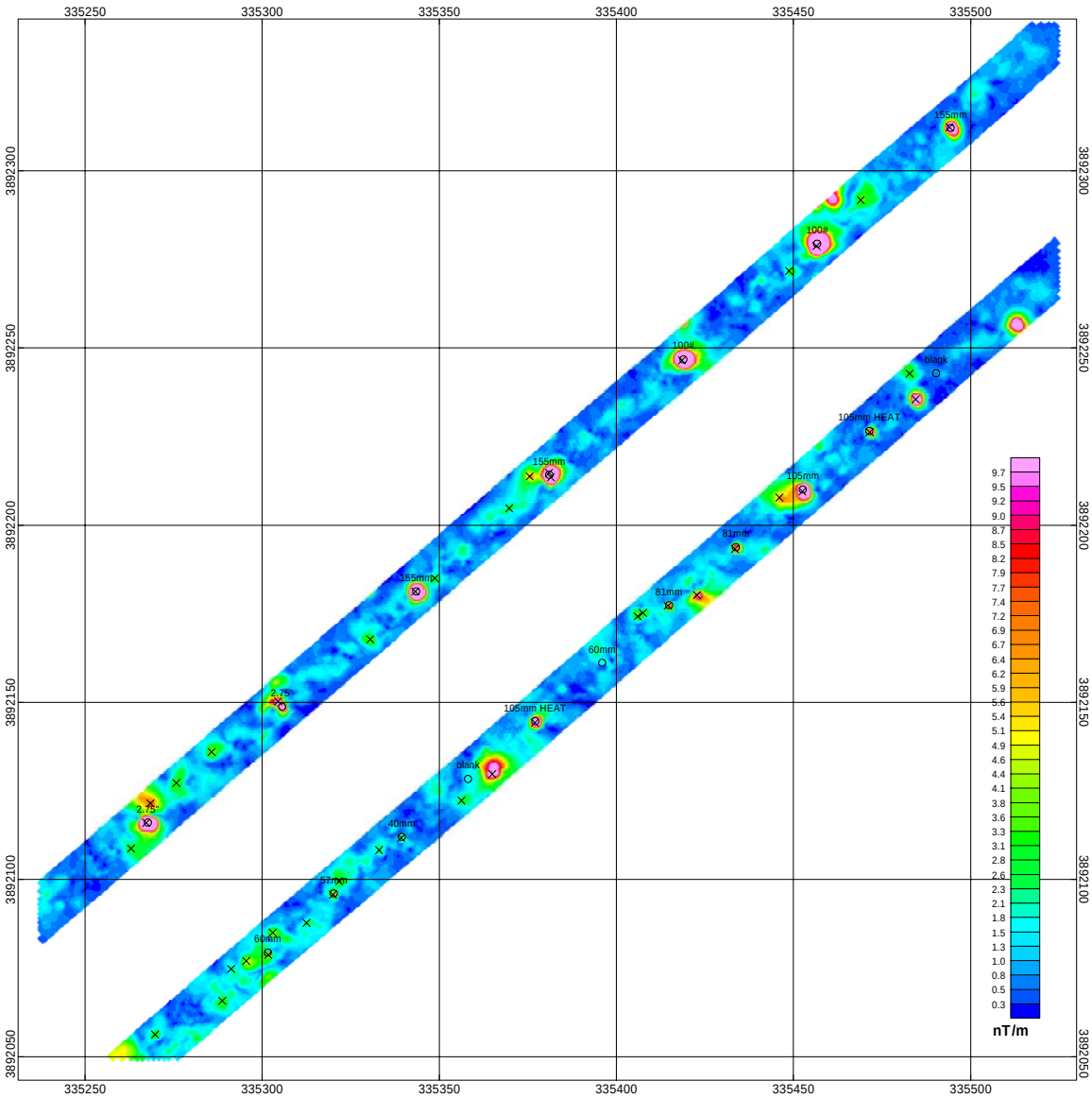

Figure 4-18. Analytic signal results from the VG-22 over the calibration grid.

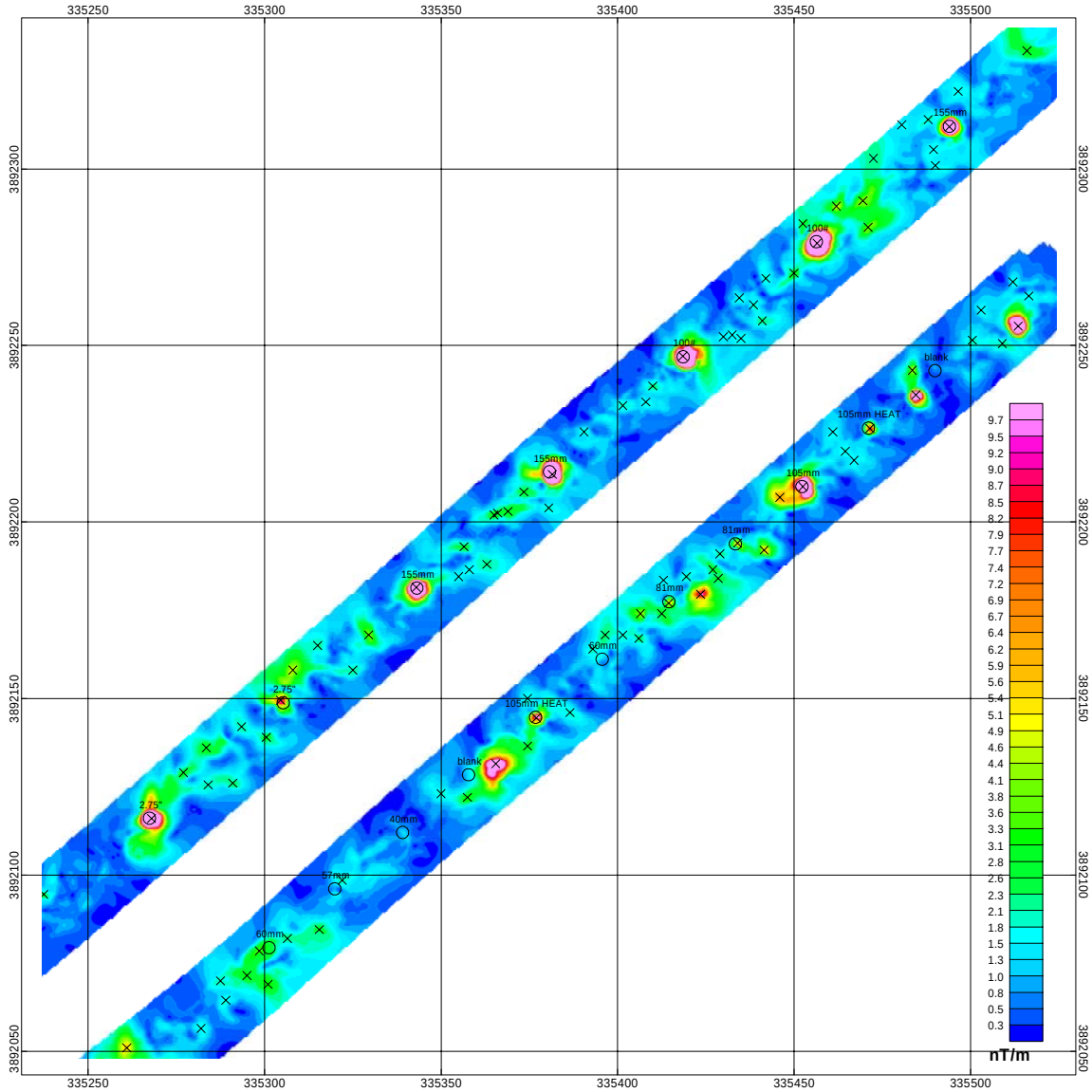

Figure 4-19. Analytic signal results from the VG-16 over the calibration grid.

4.5.3 South Area

The entire 500-acre South Area was flown with both systems. Resulting vertical gradient and analytic signal maps are shown in Figures 4-20 through 4-23.

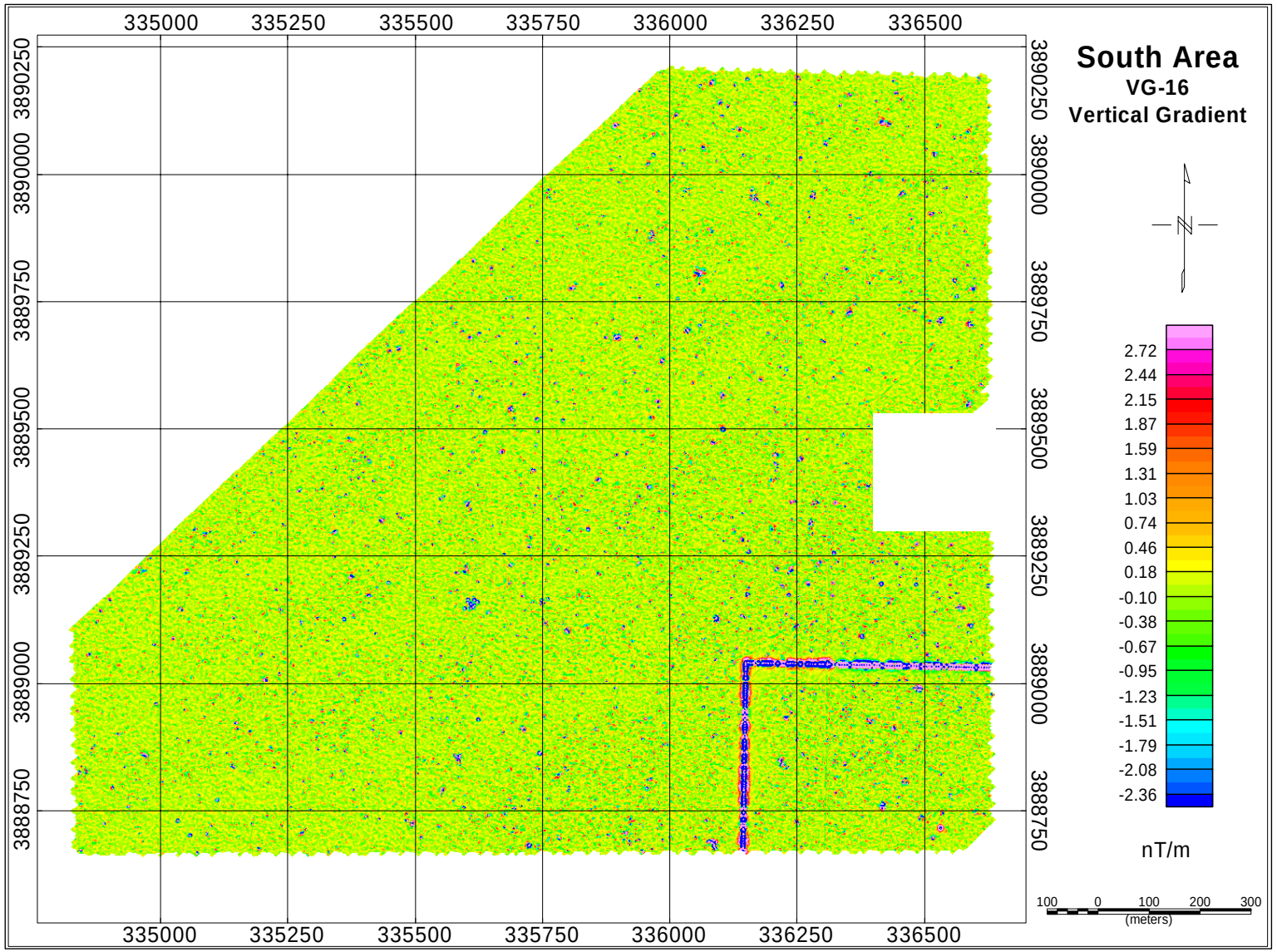

Figure 4-20. VG-16 vertical magnetic gradient map of the South Area at FKPBR.

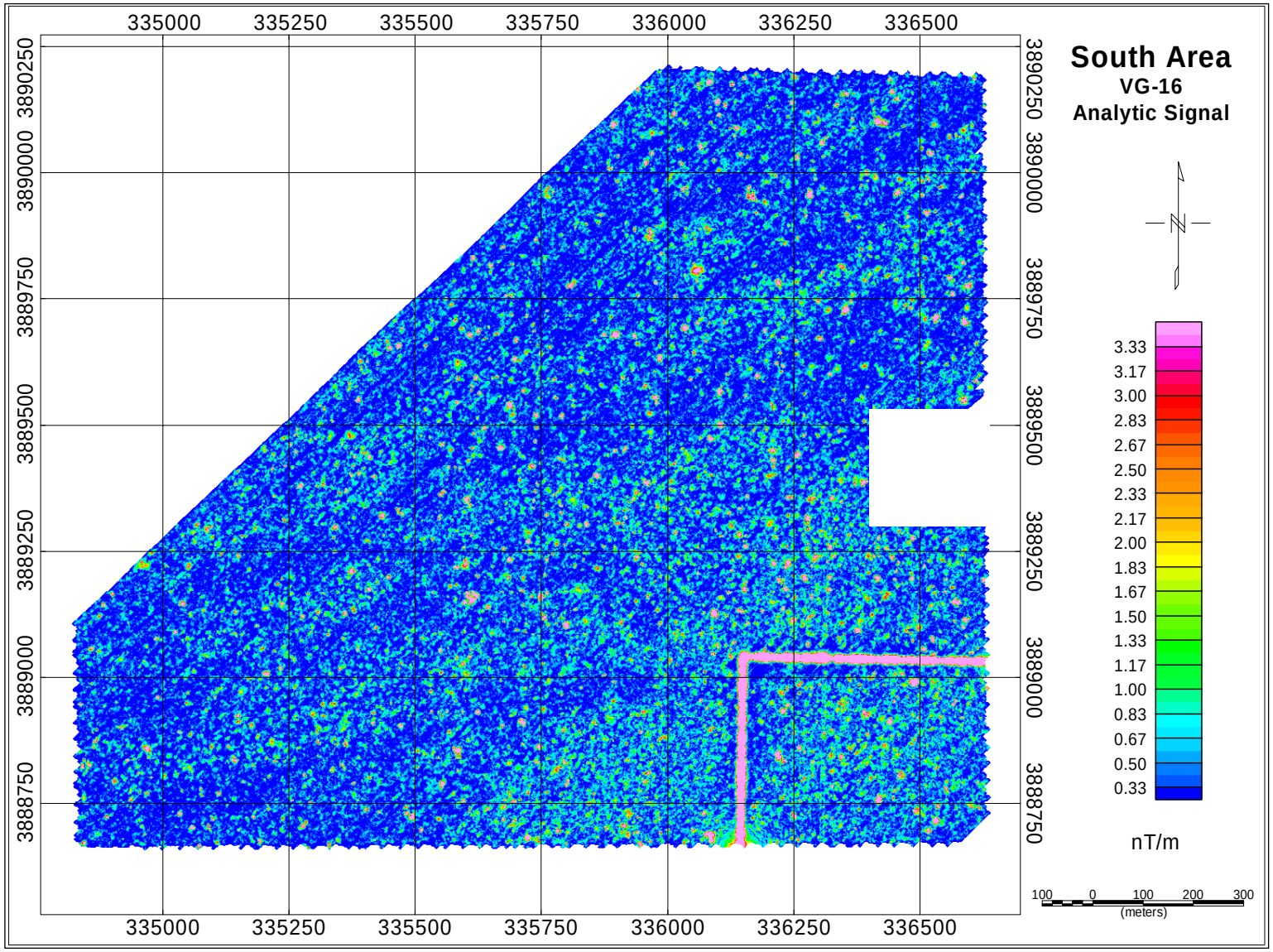

Figure 4-21. VG-16 analytic signal map of the South Area at FKPBR.

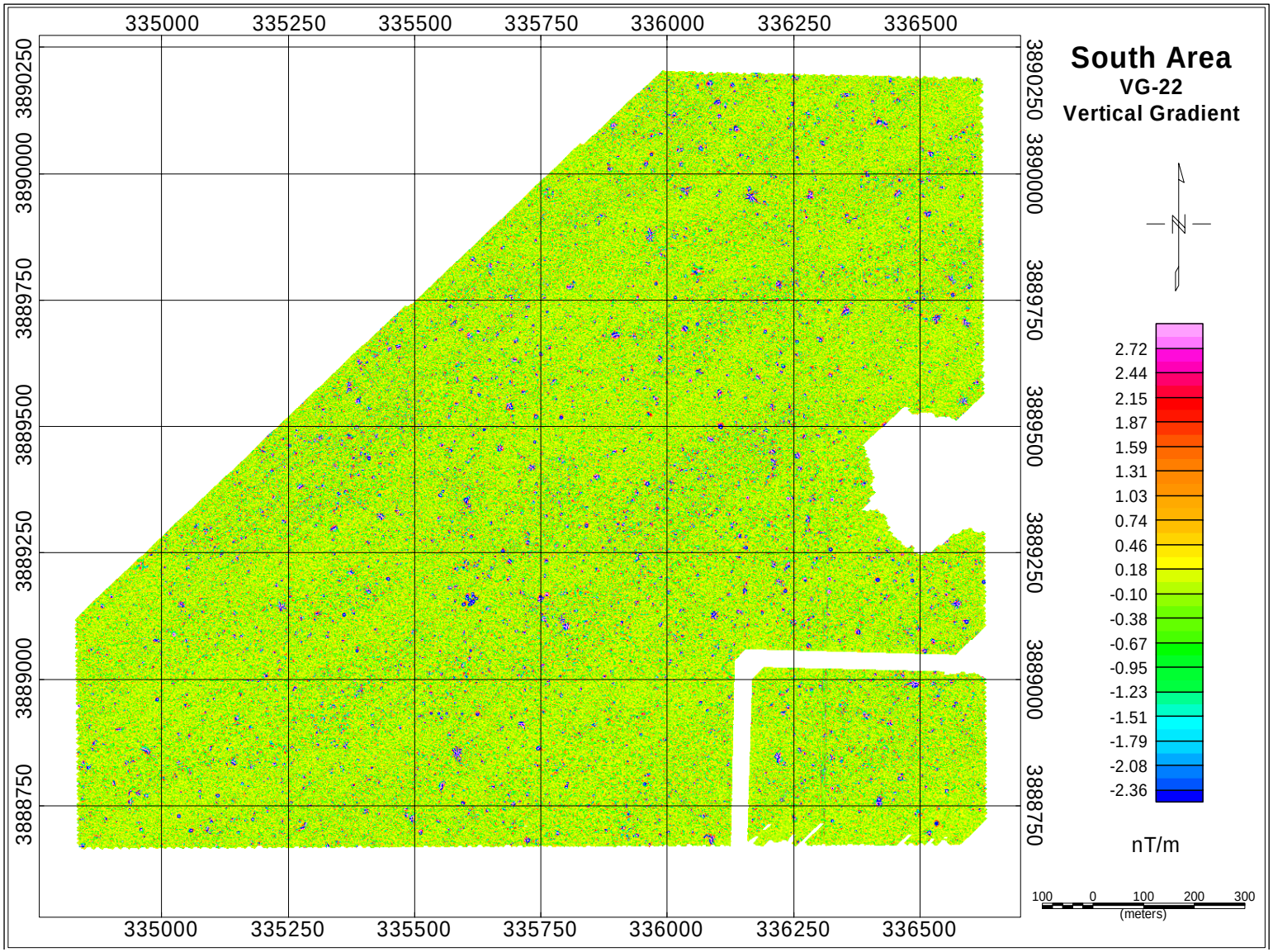

Figure 4-22. VG-22 vertical magnetic gradient map of the South area at FKPBR.

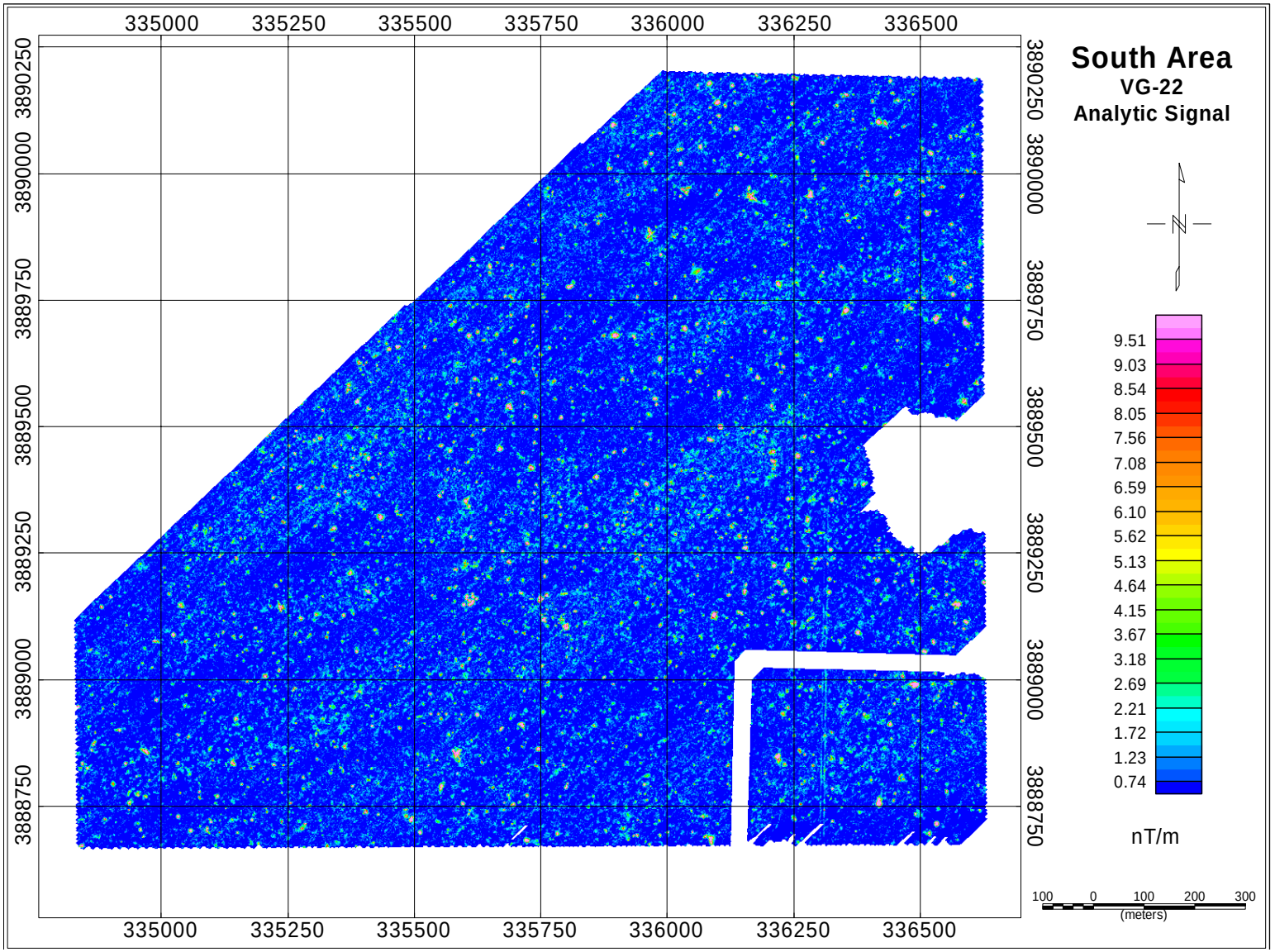

Figure 4-23. VG-22 analytic signal map of the South Area at FKPBR.

4.5.4 North Area

As indicated previously, data were acquired within two 500-acre tracts within the North Area. These are designated Areas A (west) and B (east). VG-16 data were acquired within the entire 500-acre tracts (designated Area A-16 and Area B-16), while VG-22 data were acquired within two 250-acre areas within those tracts (designated Area A-22 and Area B-22). VG-16 and VG-22 results for Area A are shown in Figures 4-24 through 4-27 while the results for Area B are shown in Figures 4-28 through 4-31. Recall that the VG-22 system flew 250-acre blocks within the 500-acre blocks flown with VG-16.

In order to conduct validation excavations, ESTCP requested data from two smaller areas within North Area A. We refer to these as Validation Area 1 and Validation Area 2. The vertical gradient and analytic signal maps for these two areas, for both VG-16 and VG-22 are shown in Figures 4-32 through 4-35.

Finally, data were acquired over North Area B-16 at 5m altitude with the VG-16 system in order to simulate relative performance over sites where vegetation or other factors inhibit operation at lower altitudes. The vertical gradient and analytic signal maps for this portion of the survey are shown in Figures 4-36 and 4-37.

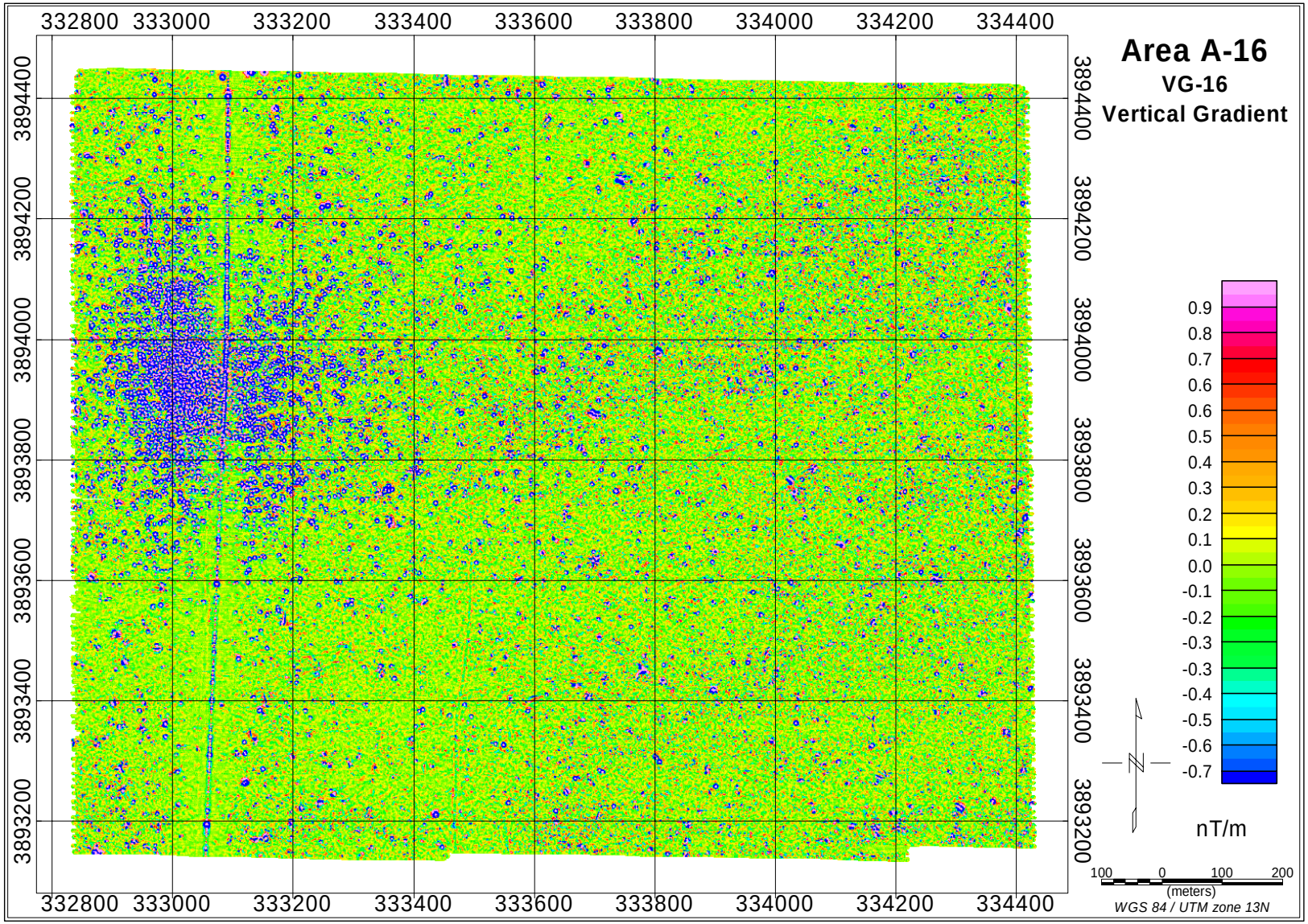

Figure 4-24. VG-16 vertical magnetic gradient of North Area A at FKPBR.

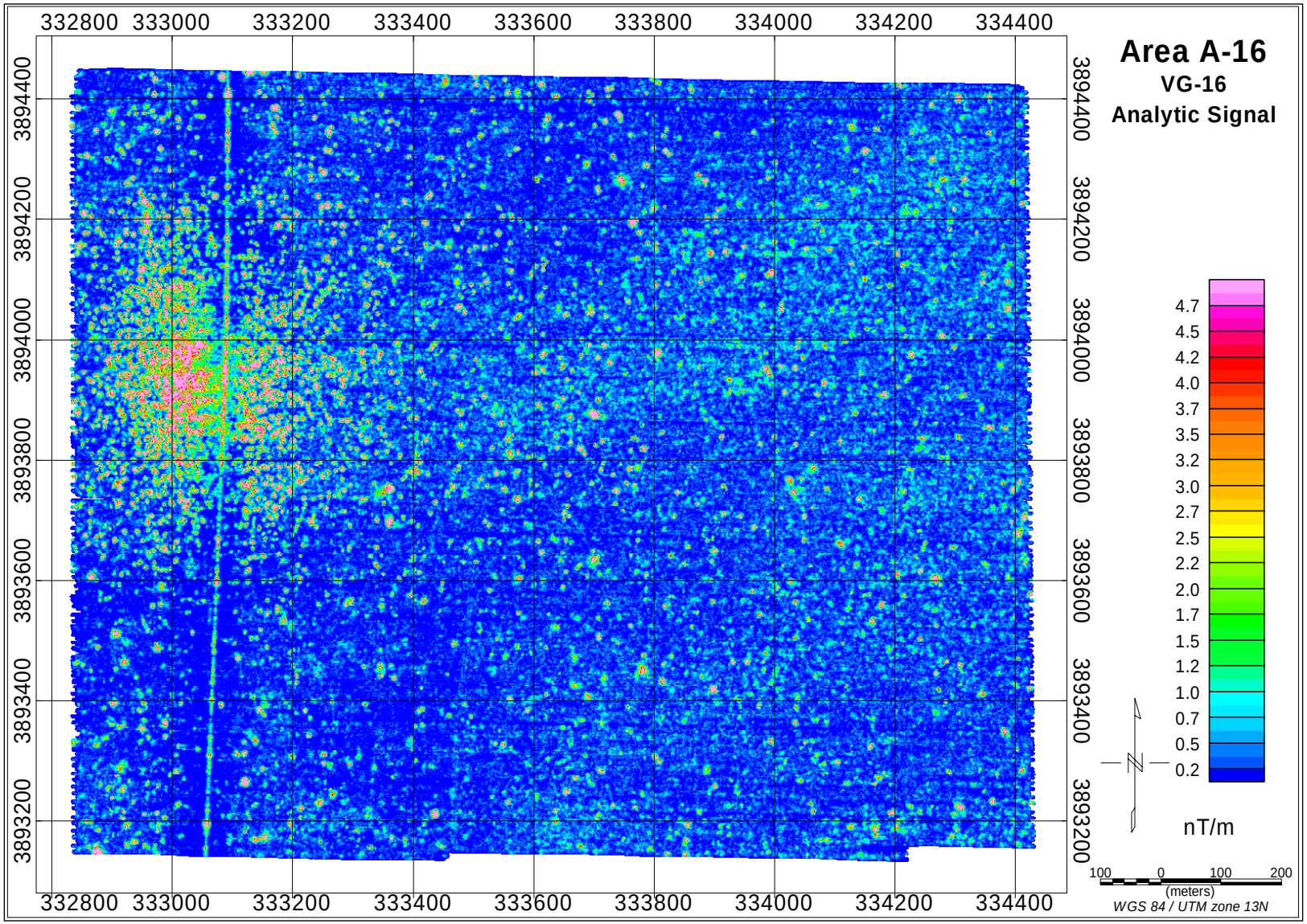

Figure 4-25. VG-16 analytic signal map of North Area A at FKPBR.

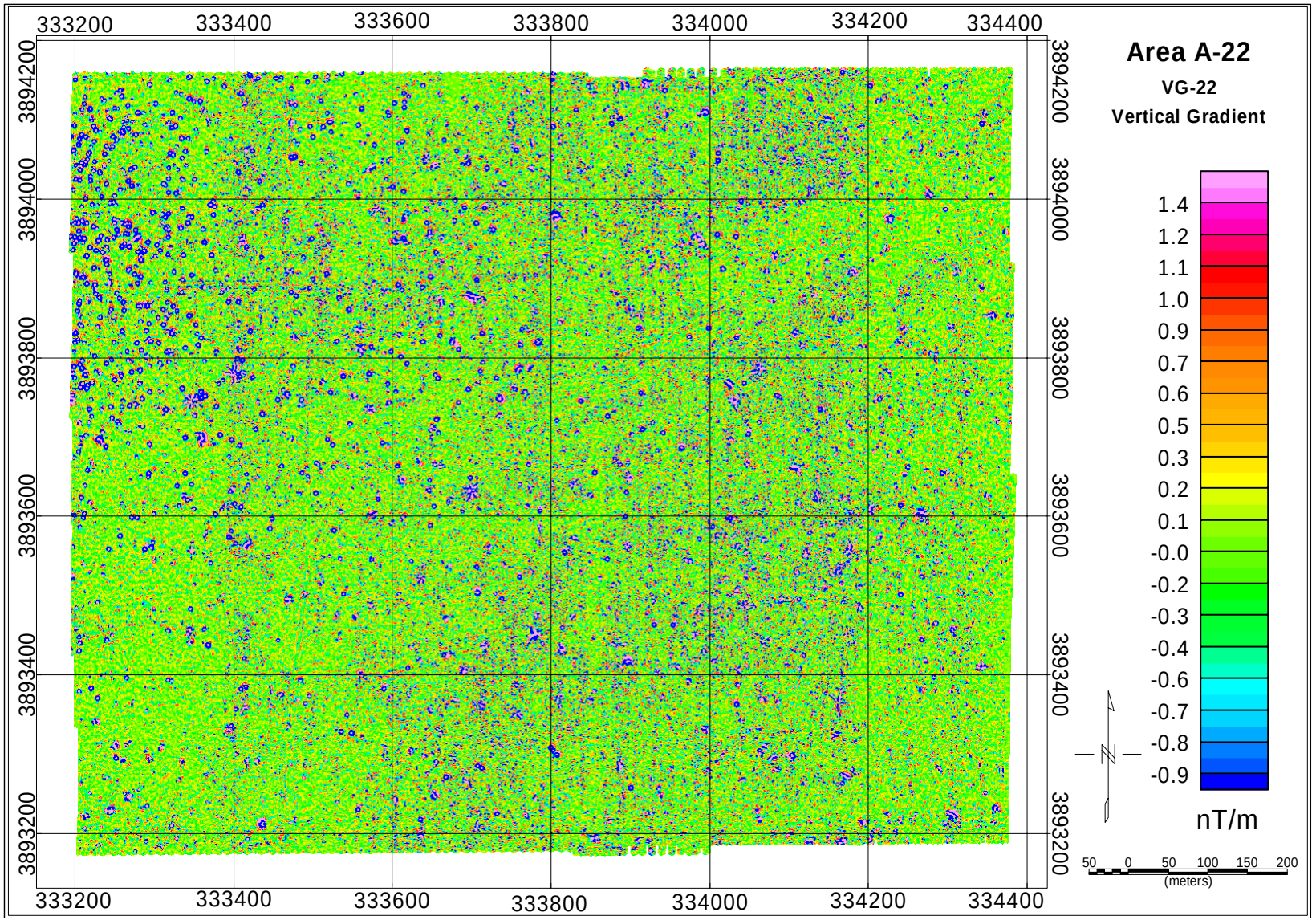

Figure 4-26. VG-22 vertical magnetic gradient map of North Area A at FKPBR.

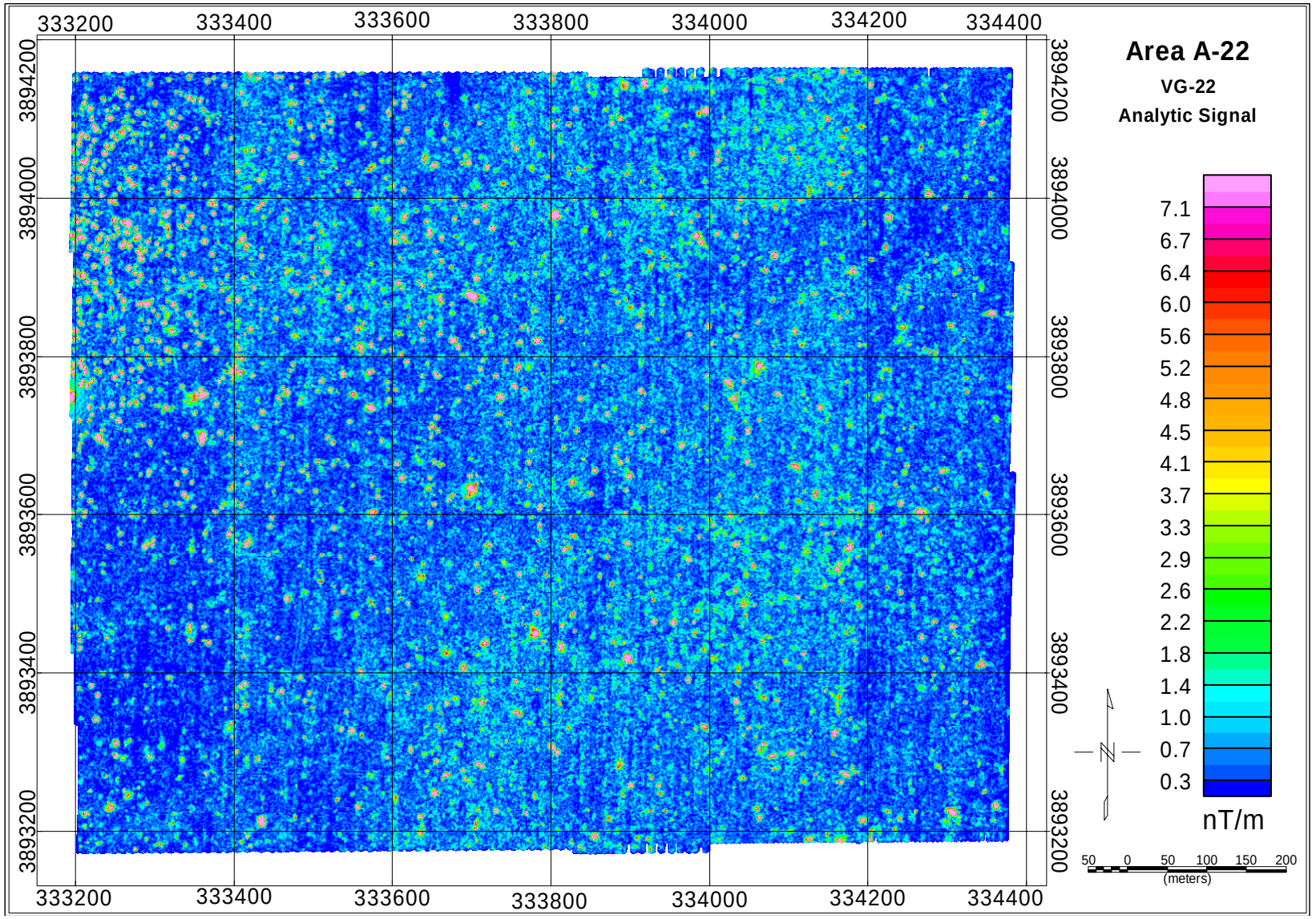

Figure 4-27. VG-22 vertical magnetic gradient map of North Area A at FKPBR.

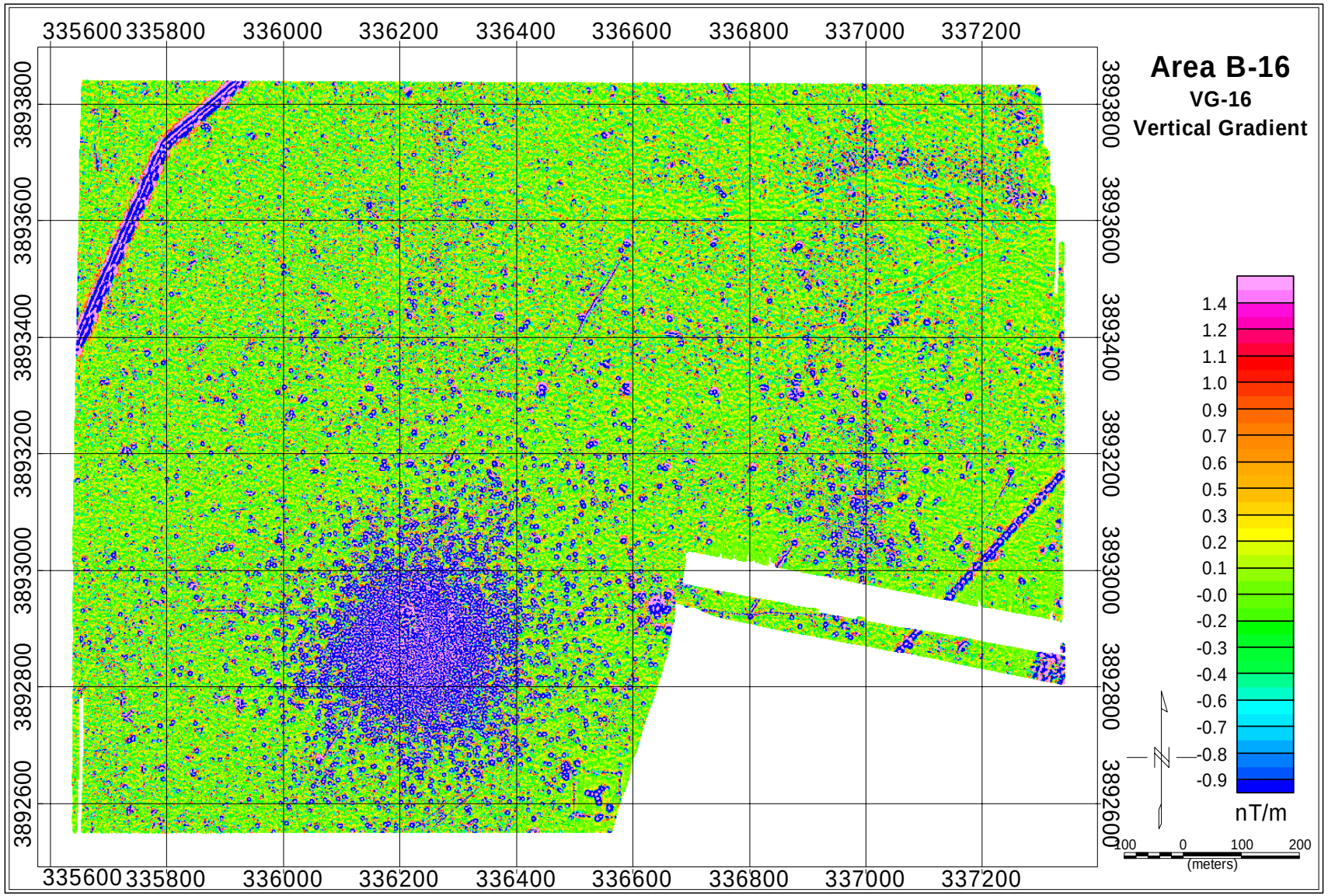

Figure 4-28. VG-16 vertical magnetic gradient map of North Area B at FKPBR.

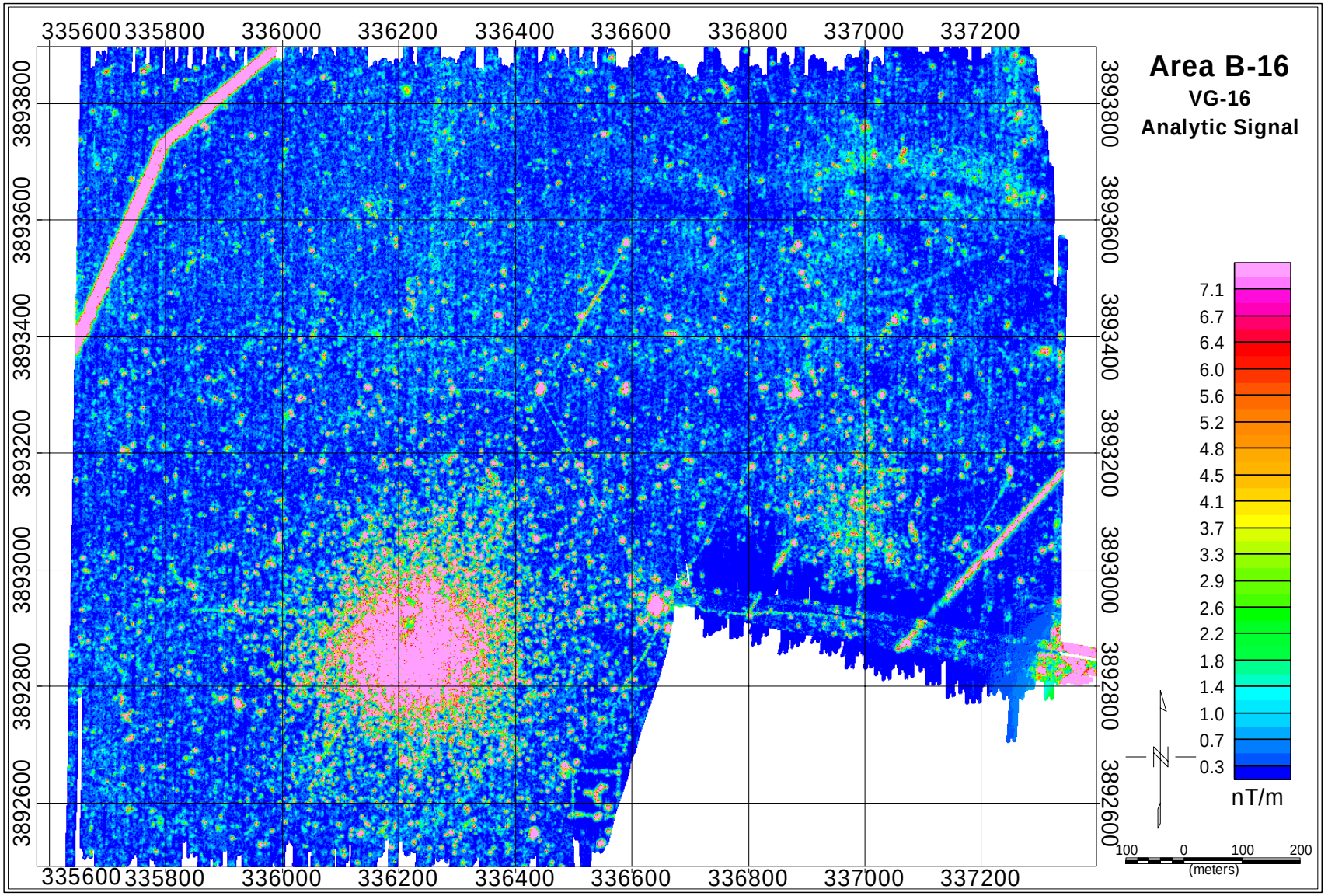

Figure 4-29. VG-16 analytic signal map of North Area B at FKPBR.

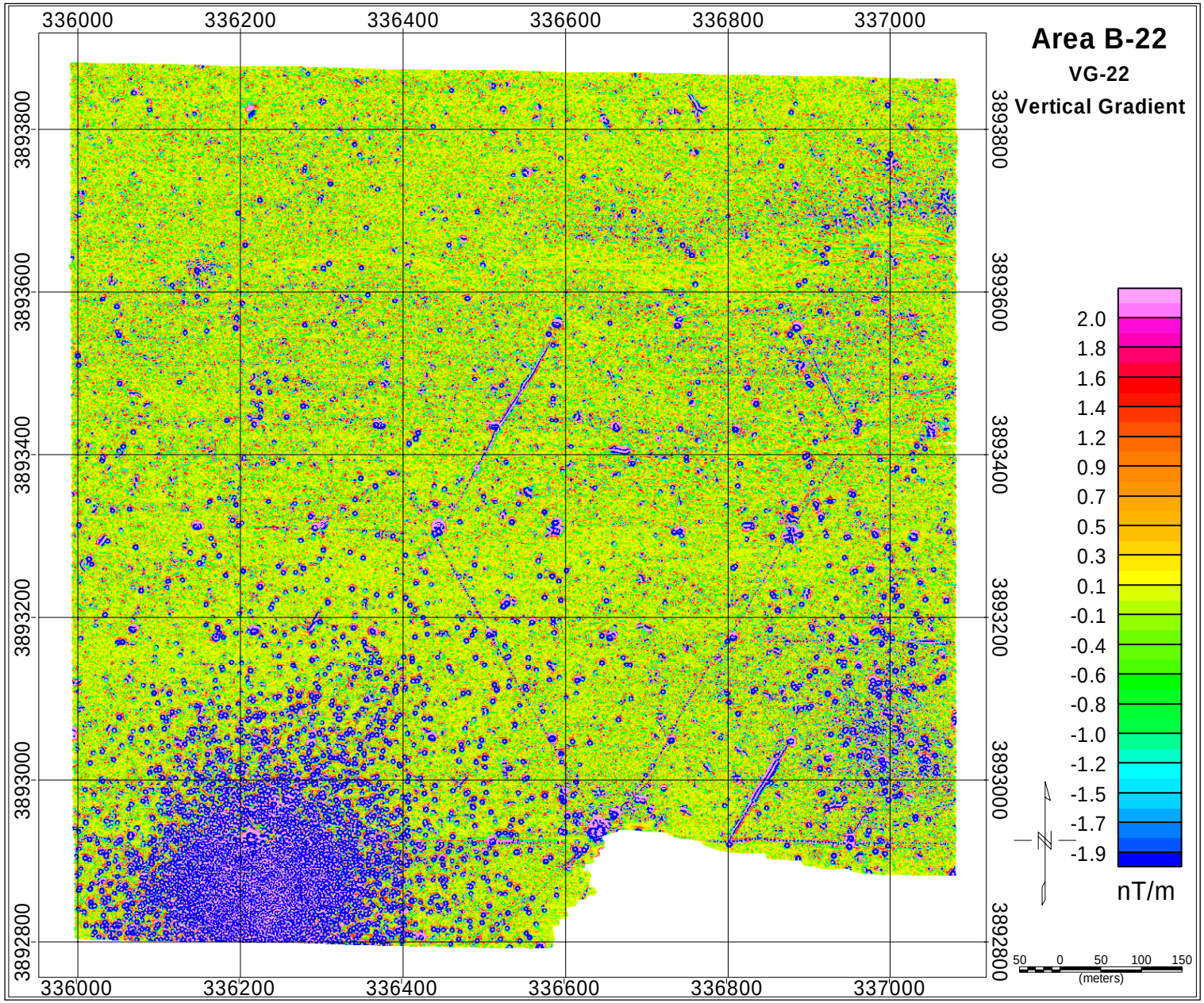

Figure 4-30. VG-22 vertical magnetic gradient map of North Area B at FKPBR.

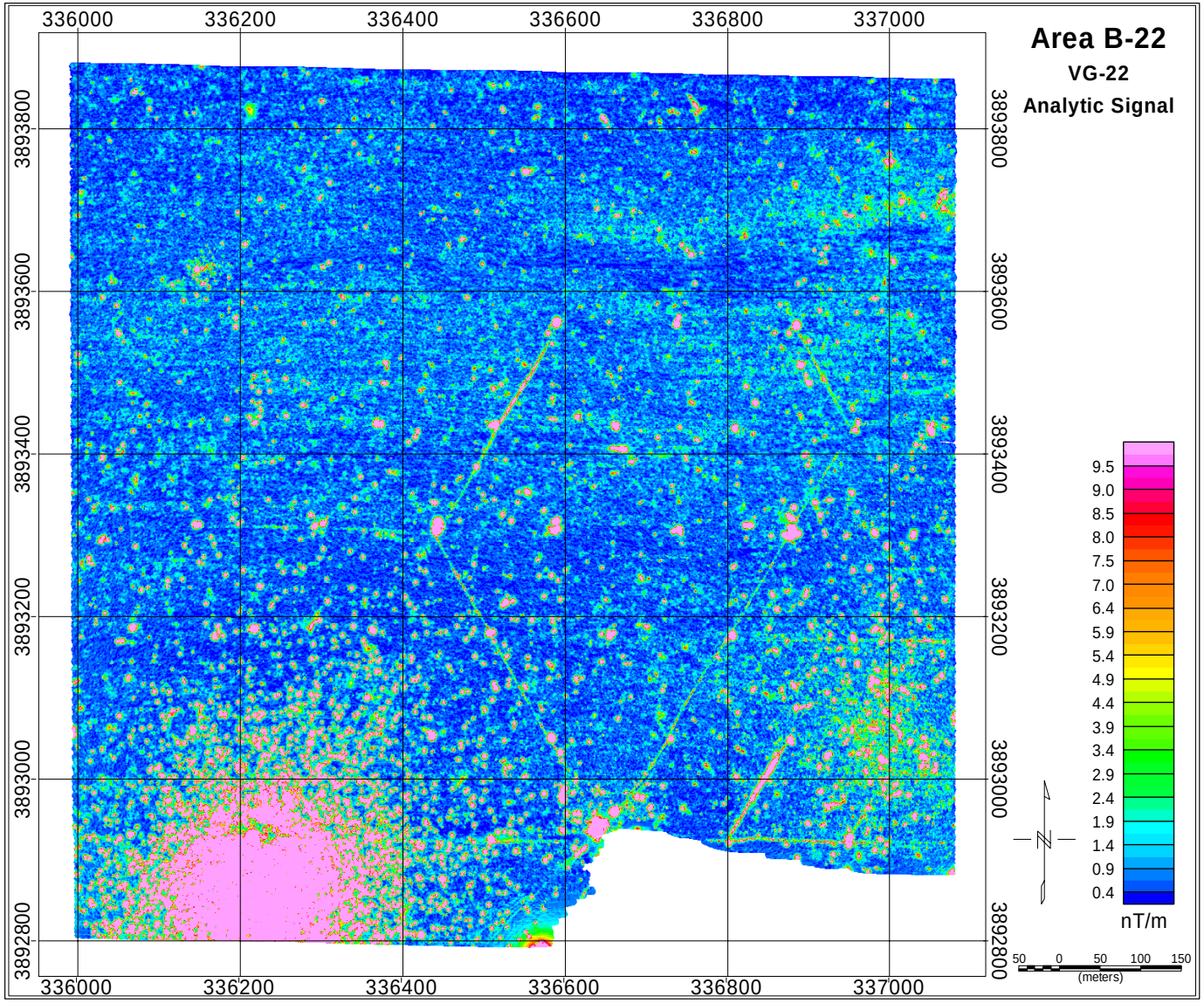

Figure 4-31. VG-22 analytic signal map of North Area B at FKPBR.

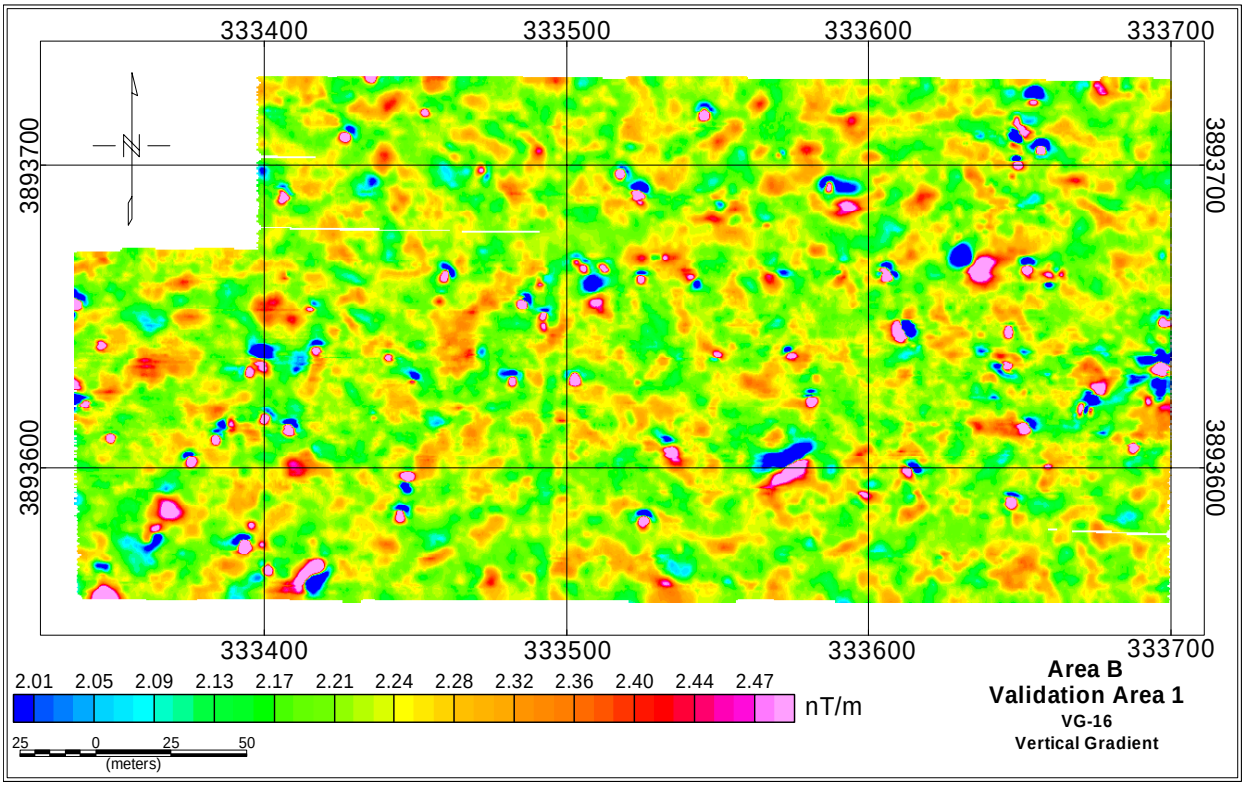

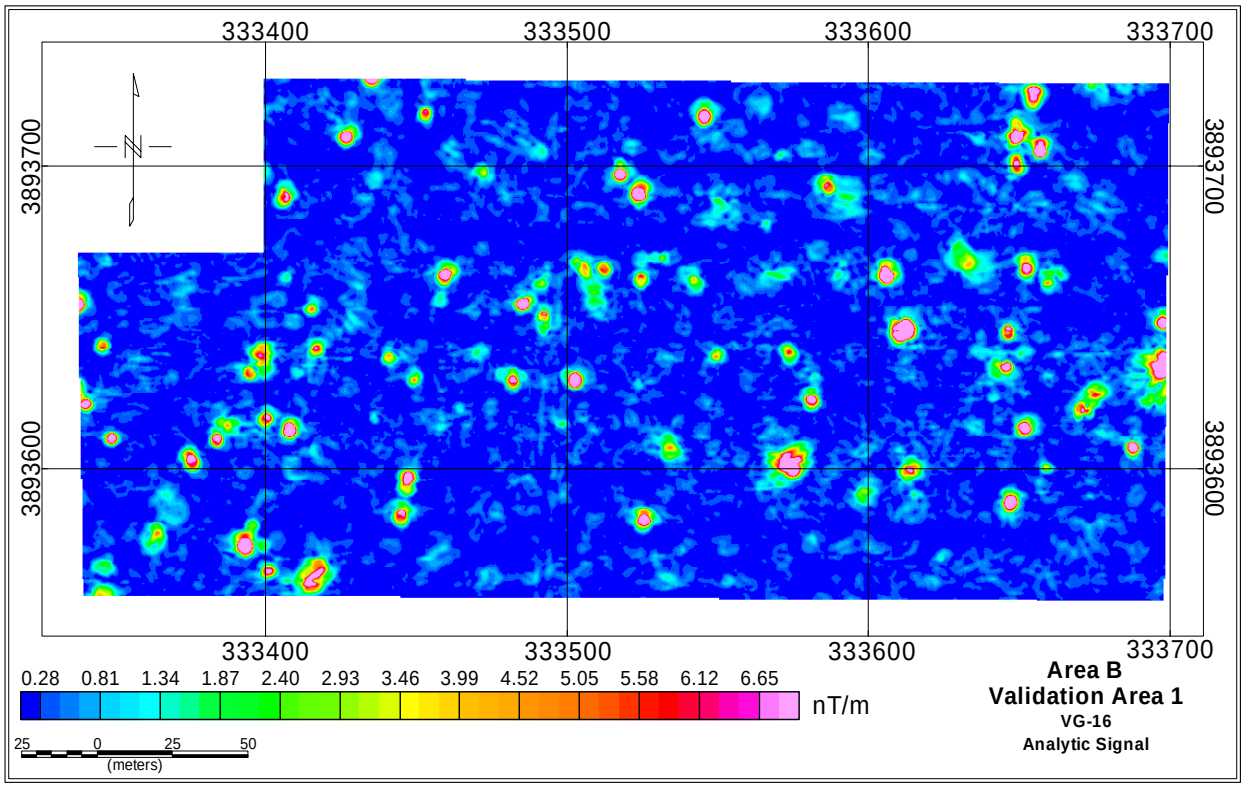

Figure 4-32. VG-16 maps for Validation Area 1, Area B, at FKPBR: a) vertical magnetic gradient map; and b) analytic signal.

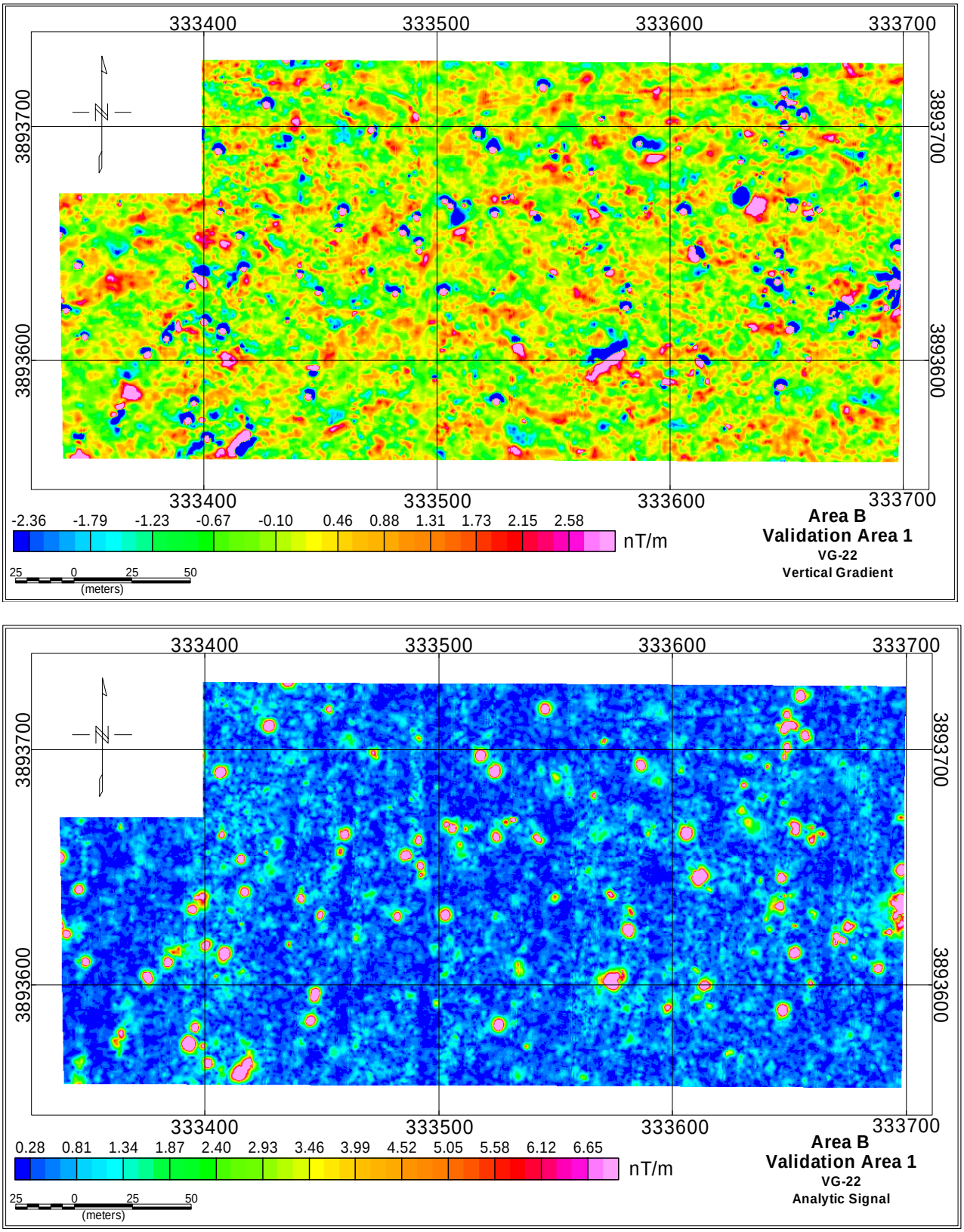

Figure 4-33. VG-22 maps for Validation Area 1, Area B, at FKPBR: a) vertical magnetic gradient map; and b) analytic signal.

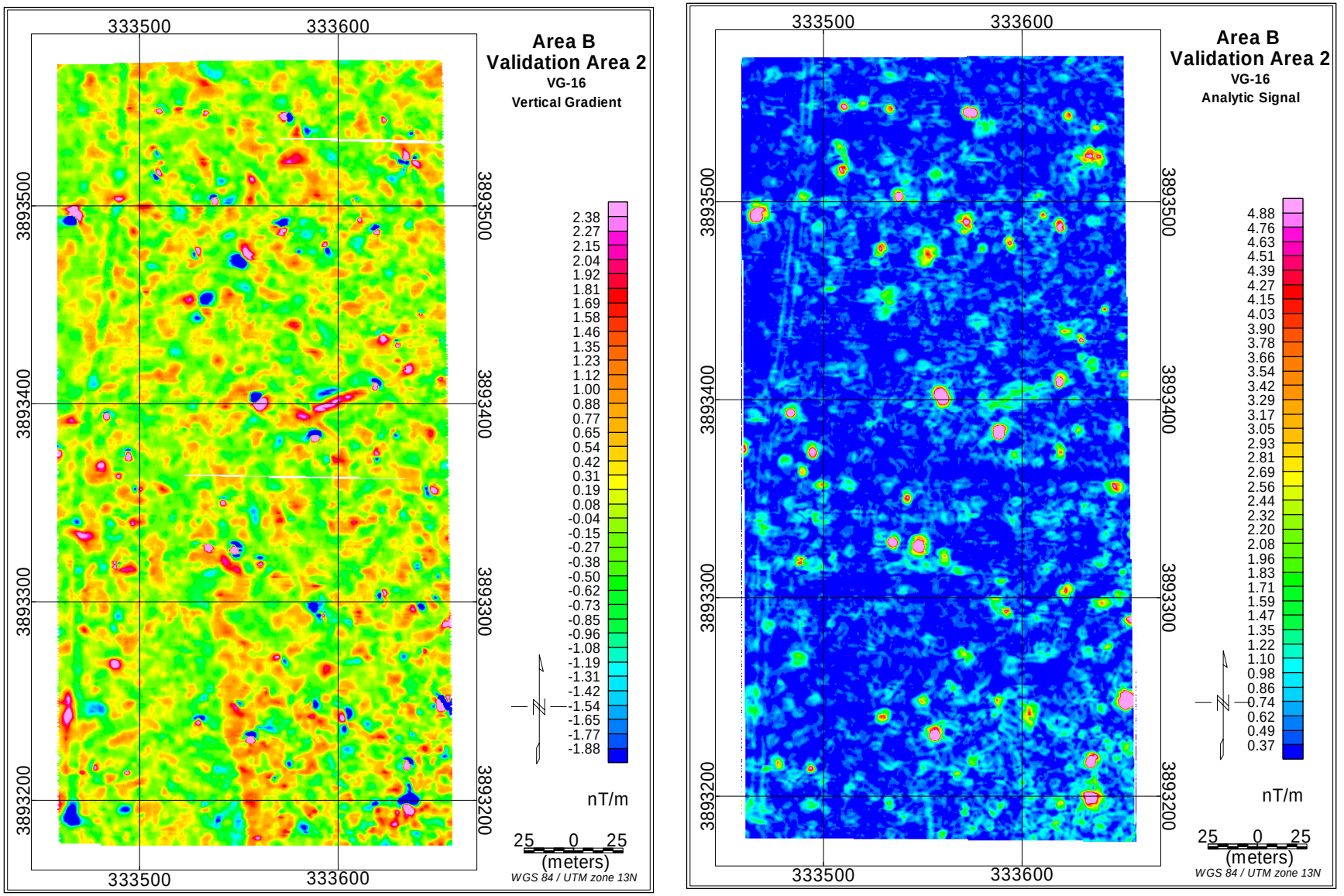

Figure 4-34. VG-16 maps for Validation Area 2, Area B, at FKPBR: a) vertical magnetic gradient map; and b) analytic signal.

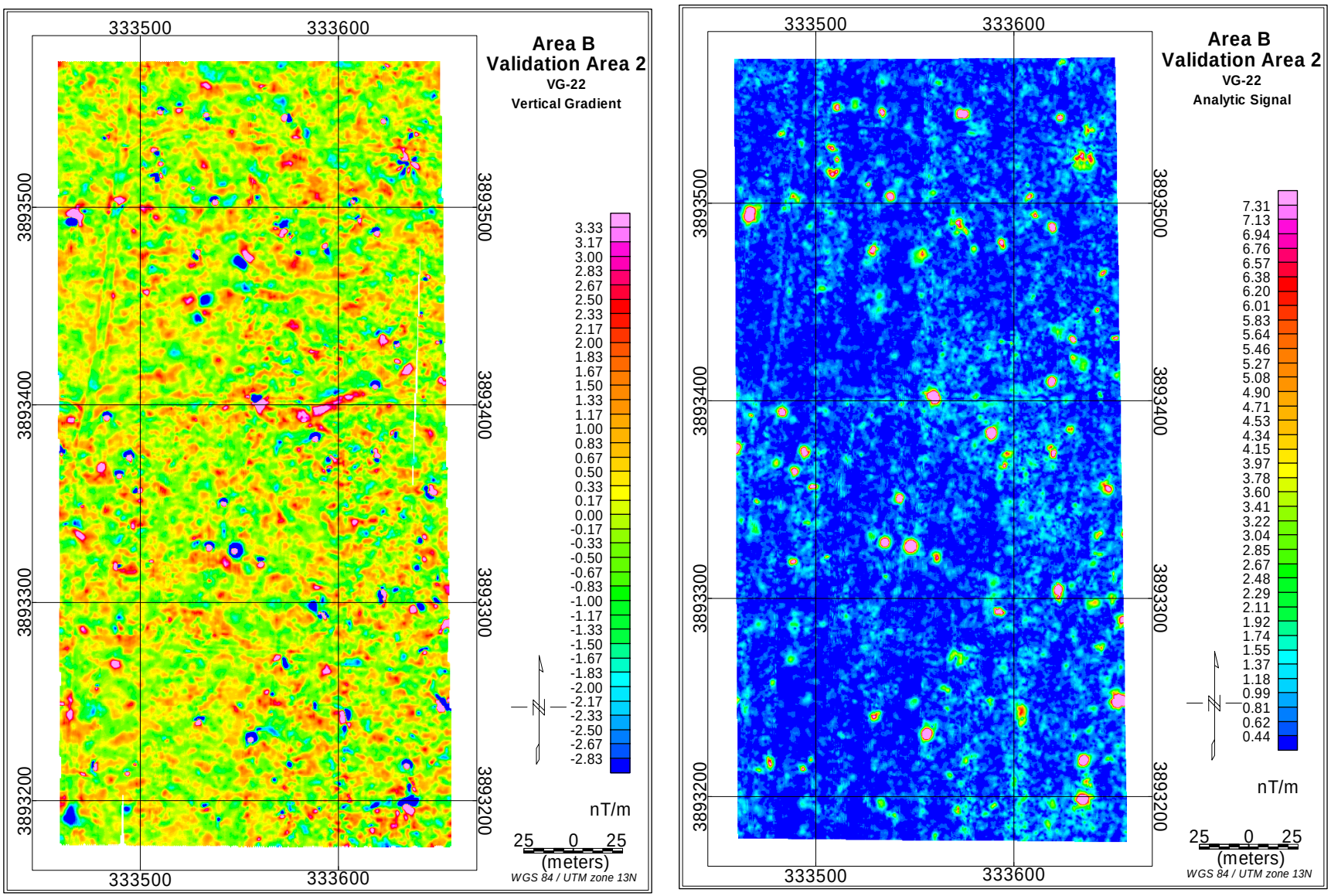

Figure 4-35. VG-22 maps for Validation Area 2, Area B, at FKPBR: a) vertical magnetic gradient map; and b) analytic signal.

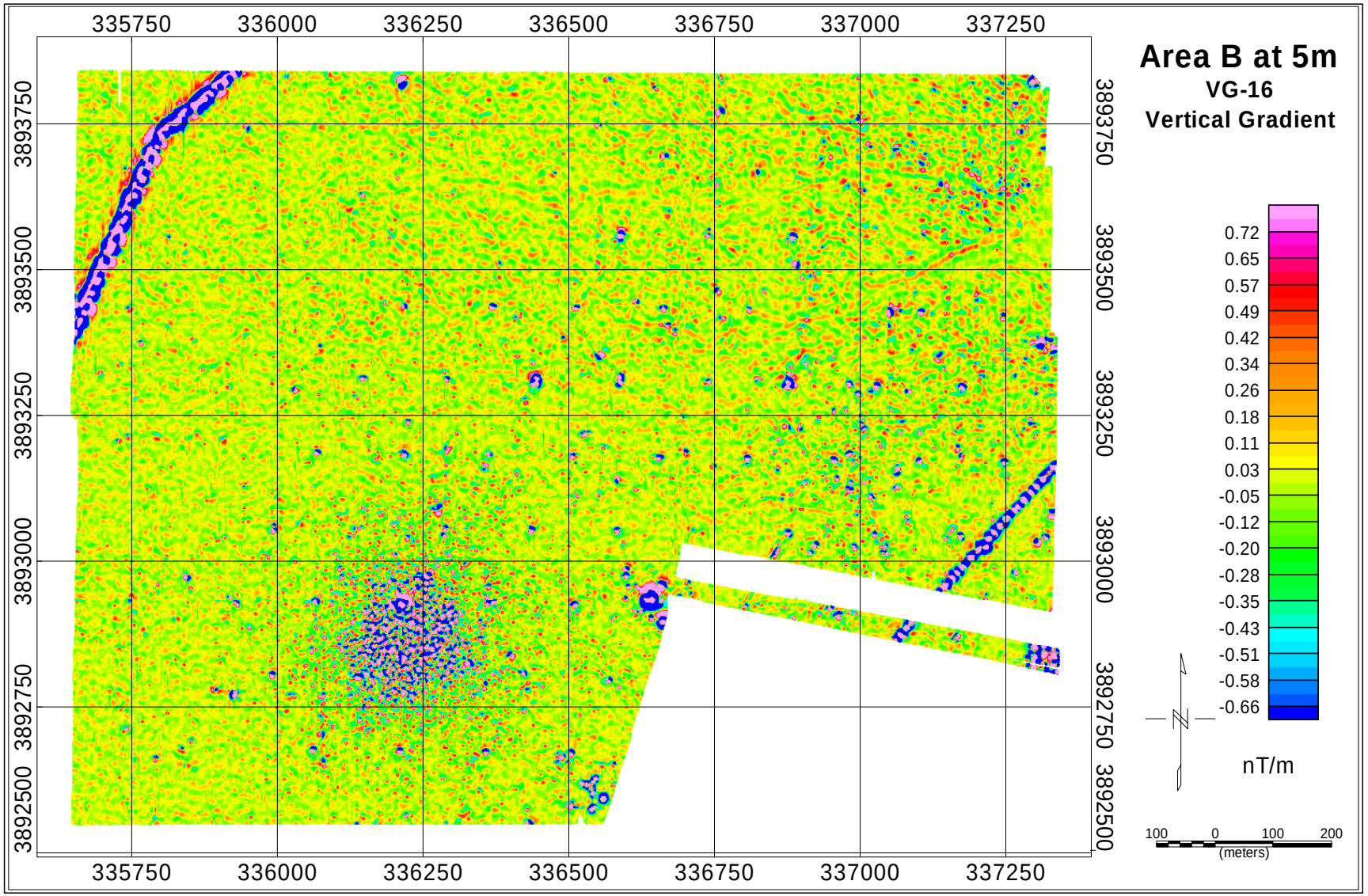

Figure 4-36. VG-16 vertical magnetic gradient map for Area B, at FKPBR, acquired at an altitude of 5m

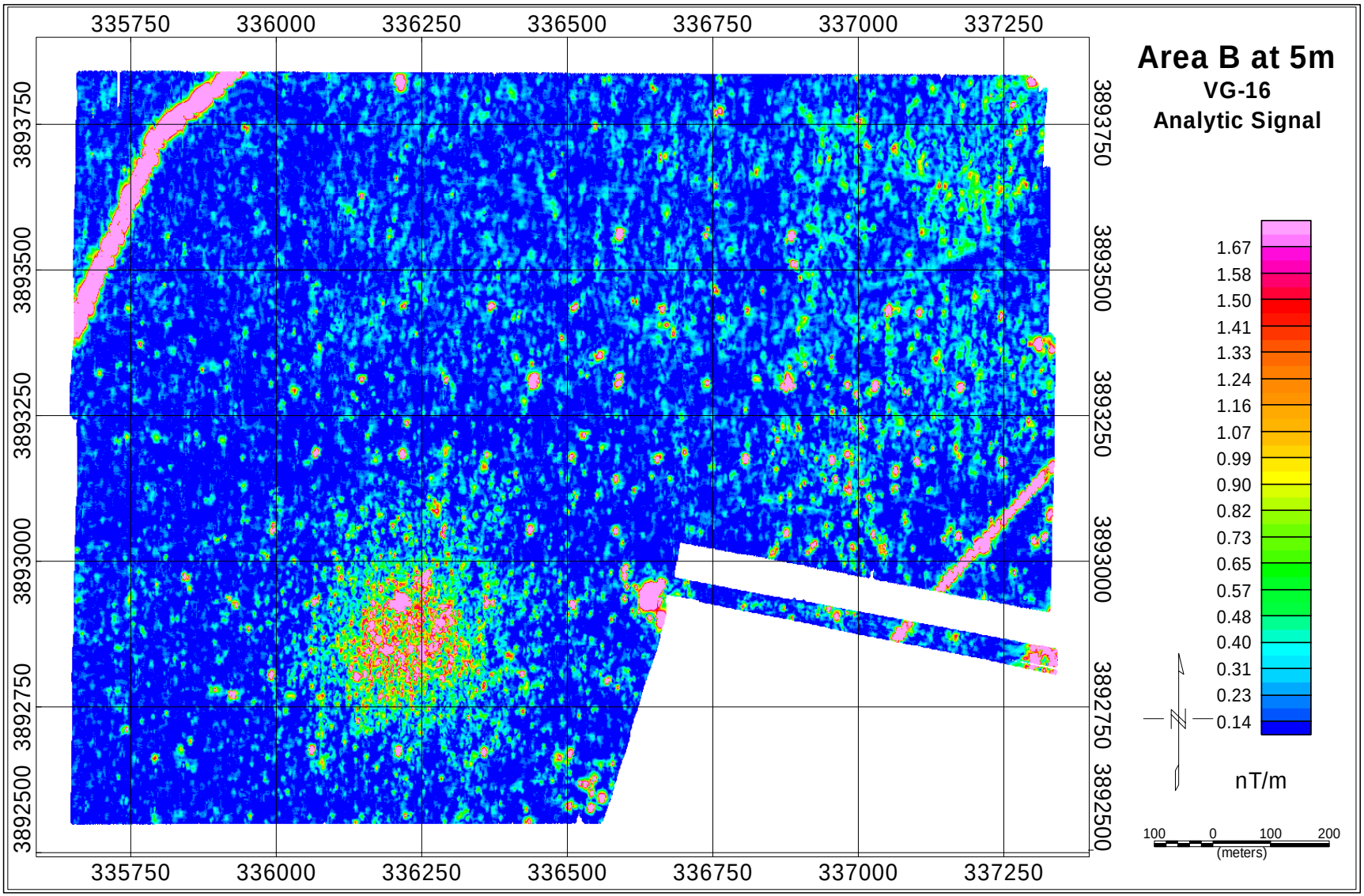

Figure 4-37. VG-16 analytic signal map for Area B, at FKPBR, acquired at an altitude of 5m

4.5.5 Anomaly Selection

All targets were picked automatically from the analytic signal peaks using a 2.5nT/m threshold against a background noise level of 1.0nT/m (mode of the gridded data). Anomalies were then inverted to fit a single magnetic dipole model. The final target locations were taken from the inversion results. Where the inversion failed to resolve a target, the original analytic signal peak location was used. This process resulted in 6391 targets from the VG-22 and 5560 targets from the VG-16. This is a relatively low number of targets for an airborne survey, amounting to 12 and 11 anomalies per acre for the VG-22 and VG-16 respectively. This is particularly remarkable since the threshold had to be set very low in order to detect the smallest of the seeded items, based on test line results.

Prior to submission for analysis, the anomaly list was divided into two categories: "probable" and "unlikely" to be UXO. The "overall" target list consisted of both "probable" and "unlikely" targets. The classification scheme was based initially on a weighted average of the inversion results (fit, size, depth, orientation). Anomalies were then examined manually to adjust their priority based on the appearance of the gridded data. Using this rudimentary discrimination model, a second set of statistics was generated using only the high priority targets.

4.5.6 Analysis of Results from Blind-Seeded Site (South Area)

The validation results of the VG-22 and VG-16 detection of seeded items are summarized in Table 4-5. As expected, the Pd for the VG-22 (90% overall) was higher than that for the VG-16 (67% overall) for all target types. The 60mm mortars displayed a surprisingly weak response with respect to their diameter resulting in a low detection probability. This is probably due to the fact that without their fins and nose cones they are actually smaller than the 57mm and 40mm projectiles (Figure 4-38).

Table 4-5: VG-16 and VG-22 seeded item detection results based on the full list of 5560 VG-16 anomalies and 6391 VG-22 anomalies.

Type	Total Seeded	VG-16 Detected	VG-16 Pd	VG-22 Detected	VG-22 Pd
155mm proj.	23	23	**100%**	23	**100%**
105mm HEAT	13	13	**100%**	13	**100%**
105mm proj.	7	6	**86%**	7	**100%**
81mm mortar	18	13	**72%**	18	**100%**
60mm mortar	18	2	**11%**	10	**56%**
57mm proj.	5	2	**40%**	4	**80%**
40mm proj.	4	0	**0%**	4	**100%**
Total	88	59	**67%**	79	**90%**

Figure 4-38. Photograph of the smaller ordnance types seeded for the demonstration. From left to right: 80mm mortar, 60mm mortar, 57mm projectile, 40mm projectile.

The source of the vast majority of the anomalies in this area remains unknown. Although they may be false positive responses, it must be allowed that they could be real ordnance on the basis of their proximity to a known bombing target.

By isolating the "probable" component of the target list from the "overall" list, we see the effect of the "unlikely" targets (Table 4.6). The "probable" target list for the VG-16 was much shorter than the VG-22 list, making direct comparison more difficult. The VG-22 results remained largely unchanged, dropping from 90% to 86% Pd with 10 anomalies per acre. One of the anomalies that was dropped from the high priority list was a 155mm projectile with an excellent signature. This was the result of a typographic error during the manual classification process. Only two other targets were lost, and these were both 60mm mortars with weak signals. All of the 40mm and 57mm projectiles were captured in the original "probable" target list.

The location accuracy of the two systems is detailed in Table 4-7 and Figure 4-39. Analysis of both systems used a maximum 1.5m search radius; although none of the positive detections were found at this maximum range. The higher standard deviation in the VG-16 target location errors was expected due to the wider sensor spacing (1.7m in VG-16 vs. 1.0m in VG-22) and coarser grid interval. The reason for the 15cm systematic shift in the VG-16 East position is unknown, since both systems used identical base station and positioning equipment.

Table 4-6: VG-16 and VG-22 seeded item detection results based on the *"probable"* list of 1682 VG-16 anomalies and 5019 VG-22 anomalies.

Type	Total Seeded	VG-16 Detected	VG-16 Pd	VG-22 Detected	VG-22 Pd
155mm proj.	23	23	**100%**	22*	**96%**
105mm HEAT	13	11	**85%**	13	**100%**
105mm proj.	7	6	**86%**	7	**100%**
81mm mortar	18	8	**44%**	18	**100%**
60mm mortar	18	0	**0%**	8	**44%**
57mm proj.	5	0	**0%**	4	**80%**
40mm proj.	4	0	**0%**	4	**100%**
Total	88	48	**55%**	76	**86%**

*missed target had an excellent signature, but a typographic error resulted in its being reduced in priority instead of increased during the classification process.

Table 4-7: Positioning errors for seeded targets

Positioning errors	VG-16	VG-22
Mean Offset	15cm	2cm
Mean East Offset	+15cm	-0.4cm
Mean North Offset	-2cm	-2cm
Mean Radial Offset	39cm	23cm
Std Dev East Offset	33cm	21cm
Std Dev North Offset	29cm	22cm
Std Dev Radial Offset	44cm	30cm

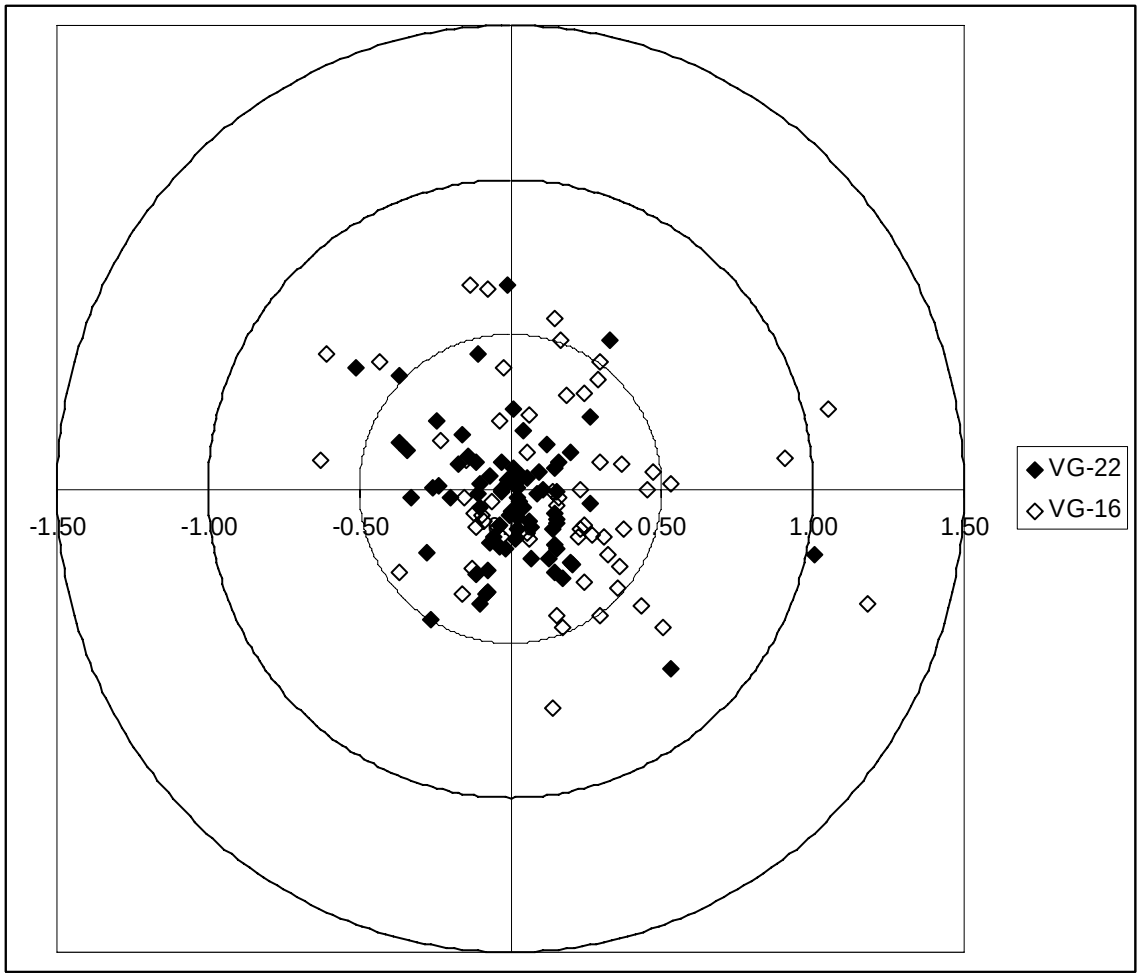

Figure 4-39. Scatter plot of target positioning errors out to the maximum 1.5m search radius.

4.5.7 Analysis of "Missed" Targets

The IDA review of seeded test site results (Table 4-6) indicates a Pd for VG-22 of 90% overall with only 56% for 60mm mortar rounds. Anomalies from the eight missed 60mm and one missed 57mm were reviewed in an effort to determine the reason they were missed. Altitude was consistent over the entire grid, and did not vary significantly for the missed targets, so this explanation was dismissed. The nine "missed" anomalies are shown in Figure 4-40. These demonstrate that nearly all of the missed targets were associated with an isolated anomaly, but upon further review, it was determined that these peaks fell below the picking threshold of 2.5nT/m.

The Pd for VG-22 at the South Area could therefore be improved by lowering the detection threshold to 2.0nT/m. This would require an increase in the number of picks from 6391 to 10,528, or from 12 picks/acre to 20 picks/acre. This results in detection of the missed 57mm and six of eight missed 60mm, for a revised Pd of 98%. Of the remaining two 60mm anomalies, one had no discernable geophysical signature and the second was moderately strong. The anomalies were picked using an automated procedure from the analytic signal which includes a shape

component to eliminate large, elongated anomalies. Presumably, this second target was rejected based on shape rather than amplitude.

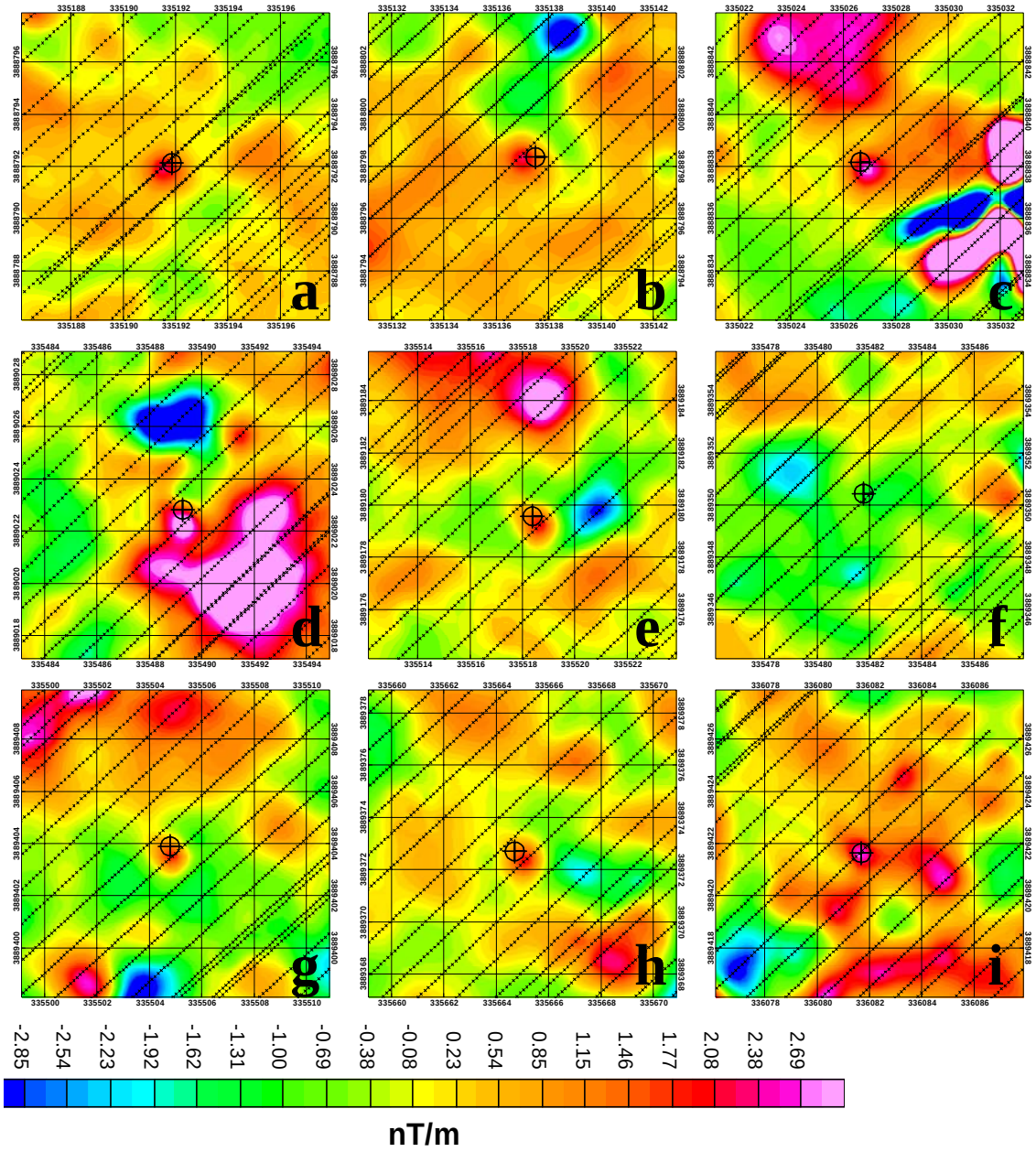

Figure 4-40. Response of the VG-22 system over the missed targets. Crosshairs are actual target locations. Small crosses are collected data points. All targets are 60mm mortars except (b) which is a 57mm projectile. Only target (f) lacks a geophysical response. Targets (c) and (f) were not picked with the lower threshold.

4.5.8 Pairs of Seeded Targets

In addition to the individual items discussed above, ESTCP also seeded pairs of 60mm targets at horizontal separations between 1m and 4m. As part of a study on the magnetic response of clustered targets (Gamey, 2007), it has been shown that when the ratio of the target separation to the sensor height (separation/height ratio, or SHR) exceeds 1.5 the targets should be treated as discrete anomalies. When the SHR is less than 0.5 then targets combine their amplitudes almost linearly into a single peak. Between these two limits targets cannot be distinguished as individual items, nor do their signatures combine to significantly increase the peak response amplitude. Within this middle range of partially overlapped signatures, the density of the collected data and the direction of target separation become extremely important for resolving peaks. For vertical gradient measurements, the signatures are narrower (higher spatial frequency) than total field anomalies and so these ratios must be adjusted by approximately 0.8 times. It should be recognized that these ratios are approximations only as they do not include effects from relative target positions (NS vs. EW) or data density.

The average sensor height (mid-point of gradient pair above the ground) over these targets was 1.3m with the targets having an average burial depth of 12cm. For two targets to combine signatures into a single unambiguous response, they must therefore be no more than 0.6m apart. For targets to be clearly defined as separate anomalies, they must be more than 1.7m apart. Targets spaced between these two limits are partially overlapped.

Max sep for fully overlapped anom	Min sep for clearly distinct anom
$Sep / Height = 0.5x0.8 = 0.4$	$Sep / Height = 1.5x0.8 = 1.2$
$Height = 1.3m + 0.1m$	$Height = 1.3m$
$Sep = 0.6m$	$Sep = 1.7m$

Seeded target pairs were arranged with two pairs at 1m separation, three pairs at 2m, three pairs at 3m and two pairs at 4m. None of these pairs are so close that they should produce a single dipole response with double the peak amplitude. The pairs which are 1m apart should present a single, possibly distorted signature with amplitude similar to a single 60mm. The pairs which are 2m, 3m and 4m apart should be treated as discrete items.

As with the overall data set, the anomalies were selected using an automated approach from analytic signal (see Section 4.5.7). The VG-16 detected a single peak over only two of the ten pairs of 60mm targets. This is comparable to the overall detection capability of the system for these targets. The VG-22 detected all ten of the pairs with different levels of resolution (Table 4-8 and Figure 4-41). Vertical gradient is presented in Figure 4-41 to demonstrate signal overlap. Two of the targets pairs were spaced 1m apart and each was detected by a single peak in the VG22 (Figure 4-42). The average radial offset between the anomaly peak and the actual individual target locations was 74cm. This reflects the inherent ambiguity in trying to locate multiple targets from a single peak. There were eight target pairs spaced 2m, 3m and 4m apart (Figure 4-43) for a total of sixteen individual items. Nine of these sixteen (56%) were detected by a single anomaly peak with an average radial offset distance of 36cm. This is directly comparable to the detection probability (56%) and radial offset distance (36cm) achieved for the individual 60mm seeded items in the rest of the grid.

Table 4-8: Positioning errors for seeded targets

Positioning errors	VG-16	VG-22
Mean Offset	15cm	2cm
Mean East Offset	+15cm	-0.4cm
Mean North Offset	-2cm	-2cm
Mean Radial Offset	39cm	23cm
Std Dev East Offset	33cm	21cm
Std Dev North Offset	29cm	22cm
Std Dev Radial Offset	44cm	30cm

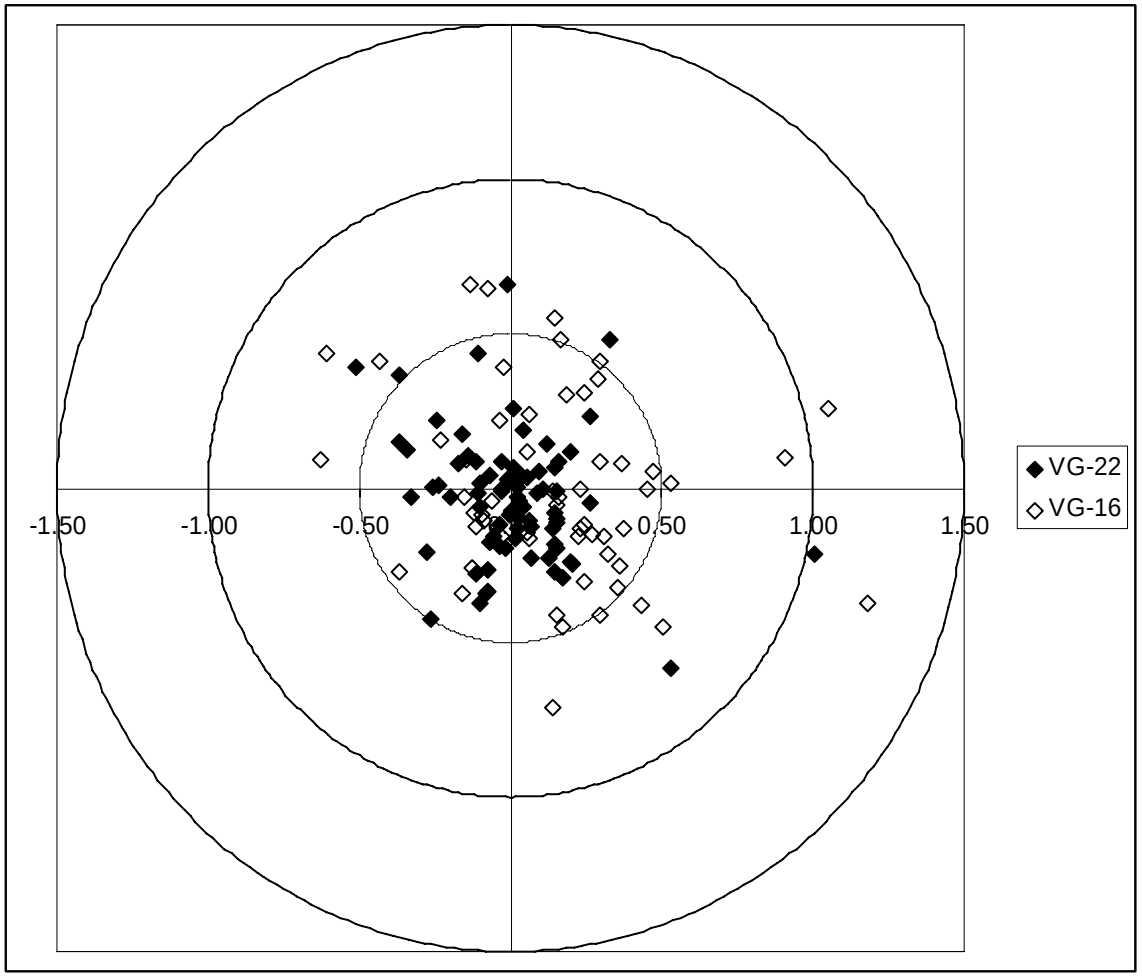

Figure 4-41. Scatter plot of target positioning errors out to the maximum 1.5m search radius.

Table 4-9: Target offset distances and detection probabilities for pairs of 60mm targets using the VG-22. Targets spaced less than 1.5 times the sensor height should be treated as a single magnetic response. Targets spaced less than 1.0 times the sensor height will have an elevated peak amplitude. The nominal sensor height over these targets is 2m.

	East Offset	North Offset	Radial Offset	Pd
60mm pairs, 1m separation, (treat pair as single target)	-5cm	+23cm	74cm	100% (2 of 2 pairs)
60mm pairs, 2-4m separation, (treat pair as two discrete targets)	-5cm	+5cm	36cm	56% (9 of 16 targets)
60mm singles from seed items, (all discrete targets)	+6cm	-13cm	36cm	56% (10 of 18 targets)

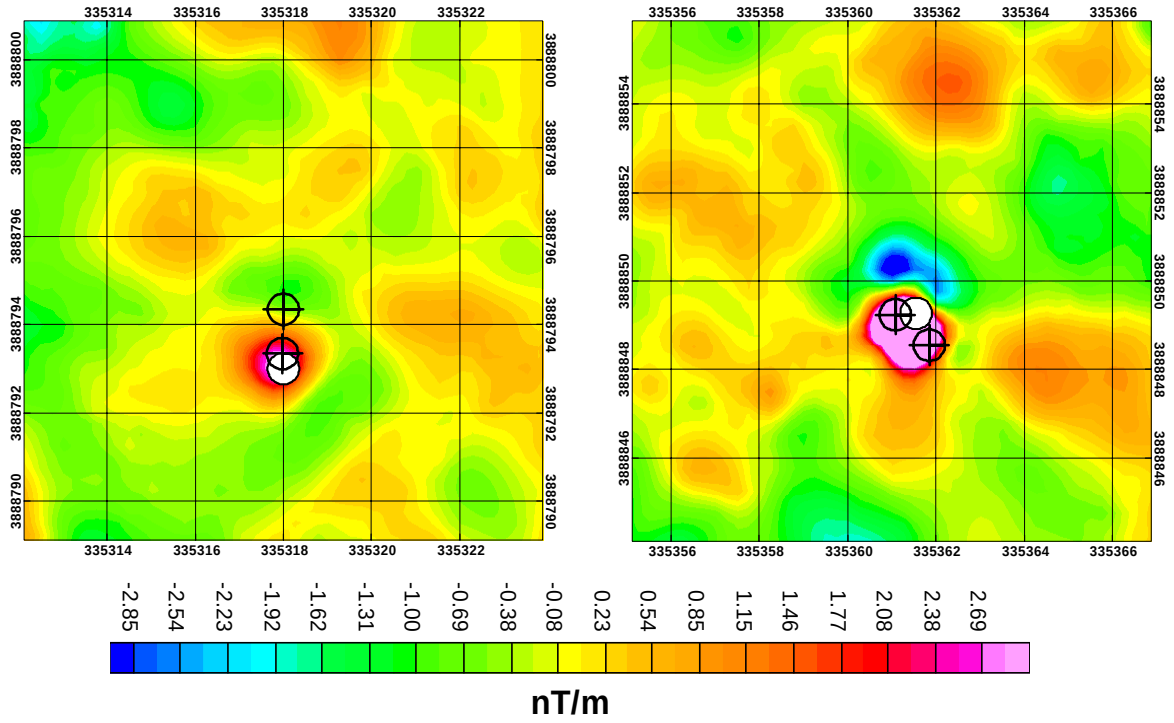

Figure 4-42. VG-22 response around 60mm seed items spaced 1m apart. These should be treated as partially overlapped anomalies. Crosshairs are actual target locations. White circles are picked target locations.

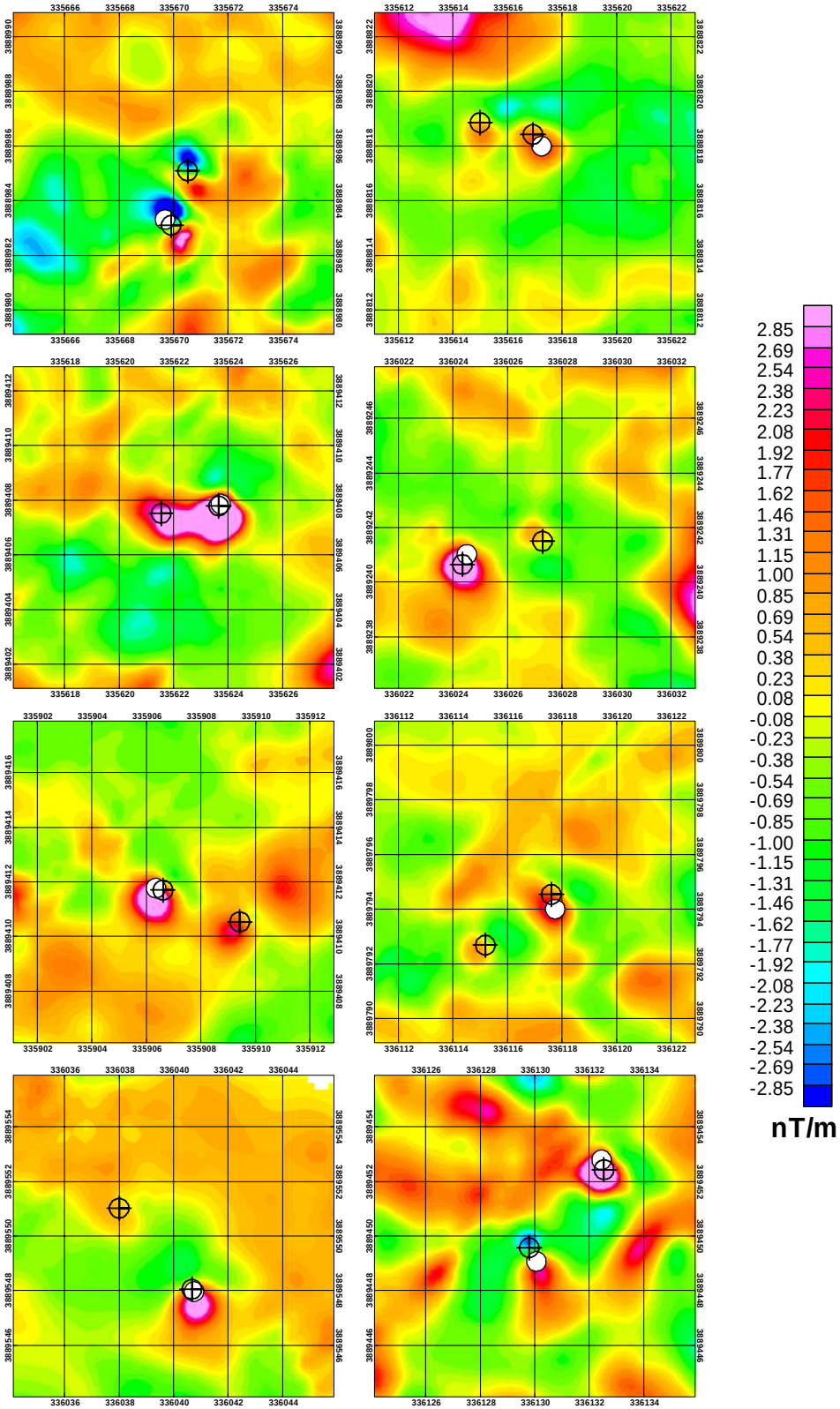

Figure 4-43. VG-22 response around 60mm seed items spaced 2m, 3m and 4m apart. These should be treated as distinct anomalies. Crosshairs are actual target locations. White circles are picked target locations.

4.5.9 Conclusions from Blind Seeded Area Analysis

The results of the blind-seeded evaluation in the South Area indicate that the VG-16 system constitutes a modest improvement over total field systems, while allowing data acquisition at higher altitudes. The sensitivity of the VG-22 system is superior to other airborne systems for UXO mapping and detection. Further assessment of the VG-22 system could be conducted to evaluate its sensitivity to small items, as there were small numbers of these items in the test grid. Evaluation with greater quantities of similar and smaller ordnance items would allow better delineation of the system limitations.

4.5.10 North Area Validation Results

As indicated earlier, validation was conducted within the northwest area (green zone in Figure 3-4). Maps for the North Area and the two validation sites are shown in Figures 4-28 through 4-39. Battelle provided prioritized dig lists for these two areas, based on the selection process described for the South Area. The dig lists are provided in the Data Archive (see Appendix B). After IDA reviewed the dig lists, Battelle was provided results from 25% of the study area, in order to develop a revised prioritization of the dig list. This was intended as a means for assessing the effectiveness of using feedback from early dig results to guide subsequent anomaly prioritization.

The two validation sites were chosen because of the availability of existing ground-based SEMS data, and because they were positioned on the edge of a target, with Area 1 being closer to the center of the target than Area 2. Anomalies within these areas were generally isolated with few overlapping anomalies. Analysis of validation results revealed that:

> "Unfortunately, the targets in the two areas yielded (arguably) few UXO-like objects (permeable body of revolution with a major polarizability axis). One target bore some semblance of a body and tail-fins. The thin walled practice bombs were mostly rusted away or pancaked. [This is not] the best set to practice discrimination on because most of the ordering is classifying various states of scrap and geology. There were a couple "intact practice bombs" found in a sample dig just north of Area 1. The hope was that by digging the whole 100% coverage patch, more would be found. This wasn't the case, and after viewing the pictures from the field, I believe our optimism came from the liberal definition of "intact practice bomb" used in the original dig reports." (Michael May, IDA, personal communication, December 13, 2007)

The dig results included considerable frag (2 oz to 2 lb), but consisted primarily of clutter and geologic sources. As a result, it was determined to conduct an analysis of the validation data by separating "point-like targets" (including clutter and 'hot rocks', but not 'hot dirt', geology, or 'no-finds' and non-point targets. These were used to formulate 'pseudo-ROC curves' as shown in Figure 4-44 through 4-47, where the first two represent 100% blind results, and the latter two represent the results after partial (25%) disclosure. All VG-22 alarms matched with a ground-based alarm. VG detected 78% of point like targets that were detected with the ground-based system and 81% of non-point targets. VG-16 detected 55% of point like targets and 81% of non-point targets. There is no consistent preference for analytic signal vs. inversion ranking for anomaly prioritization, and no significant benefit to feedback can be recognized. Further testing will be required to reliably assess the effectiveness of the inversion and feedback approaches.

The positional accuracy in the two Validation Sites was similar to that in the South Area, as shown in Figure 4-48. For VG-16, the mean miss distance was 0.36m with a standard deviation of 0.27m, while for VG-22, it was 0.26m with a standard deviation of 0.19m.

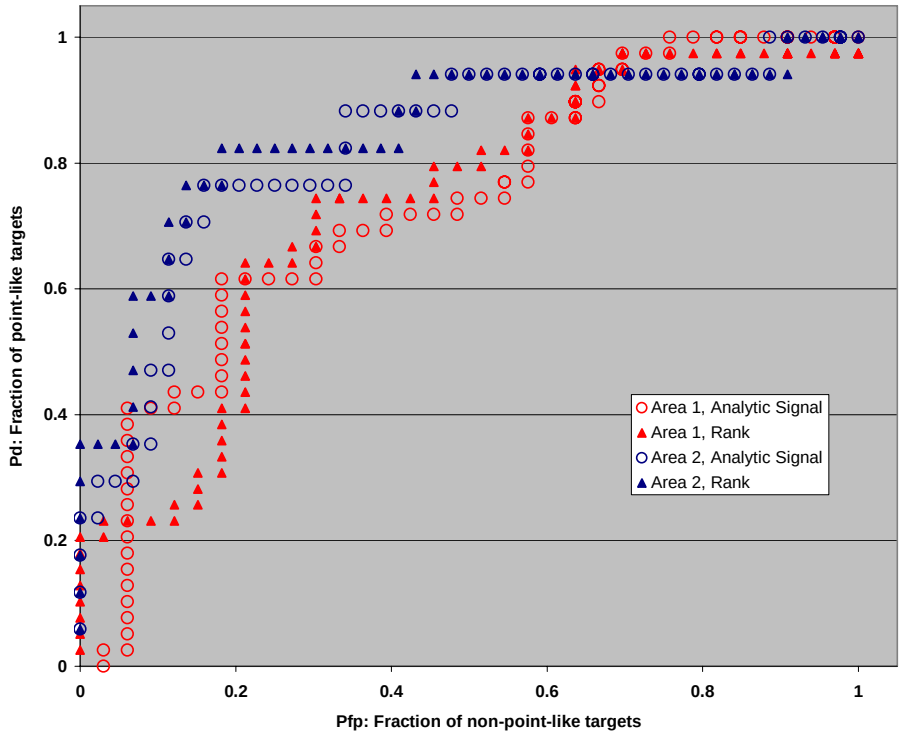

Figure 4-44. 100% Blind Pseudo-ROC curves for VG-16 at North Areas 1 and 2.

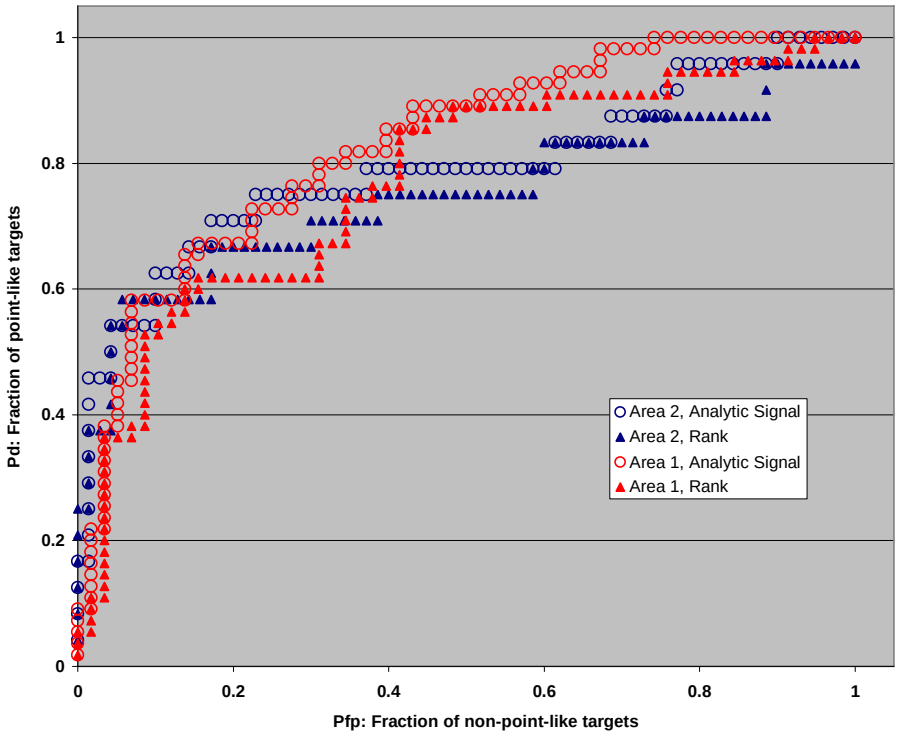

Figure 4-45. 100% Blind Pseudo-ROC curves for VG-22 at North Areas 1 and 2.

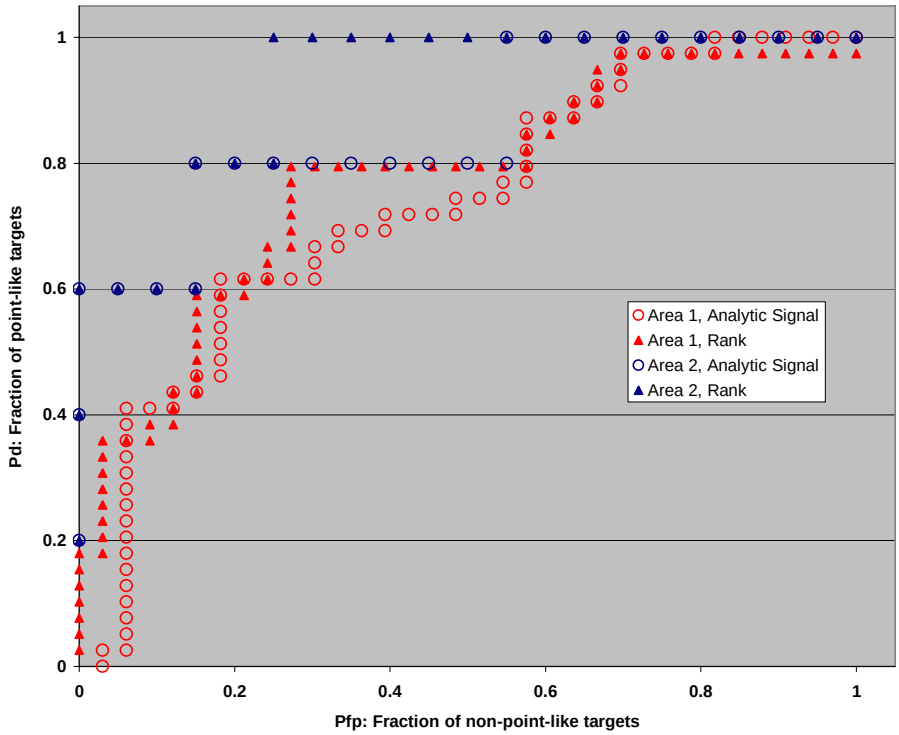

Figure 4-46. Post-disclosure Pseudo-ROC curves for VG-16 at North Areas 1 and 2.

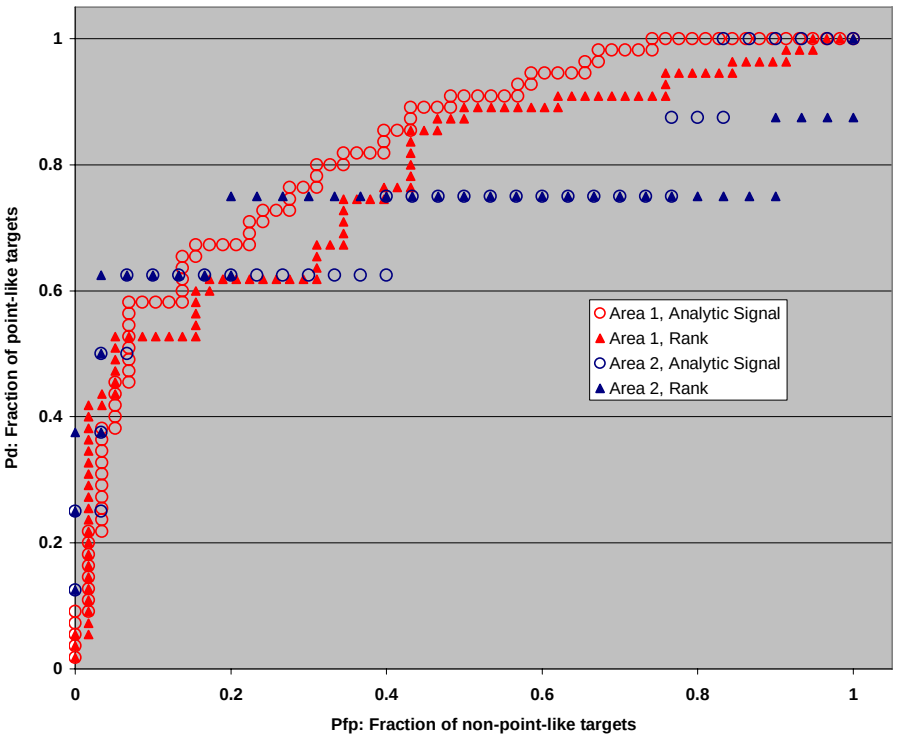

Figure 4-47. Post-disclosure Pseudo-ROC curves for VG-22 at North Areas 1 and 2.

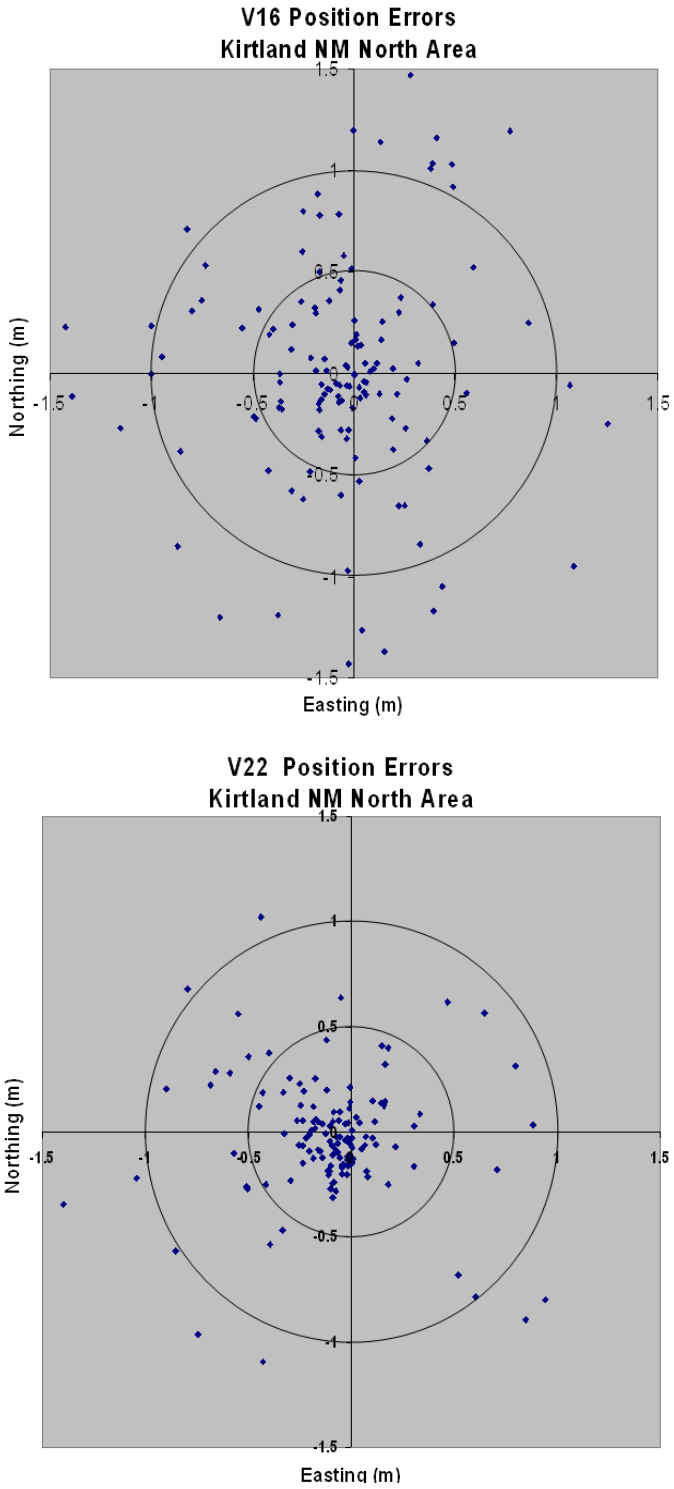

Figure 4-48. Positioning errors for VG-16 and VG-22 for the North Area at FKPBR.

4.5.11 Comparison of data from 5m altitude with low level results

Vertical magnetic gradient and analytic signal maps of Area B for nominal 5m altitude are shown in Figures 4-36 and 4-37. These may be compared with their low-altitude counterparts in Figures 4-28 and 4-29. A dig list for 5m altitude data is provided in Appendix 3. Unfortunately, both of the validation sites were selected in Area A, so that we are unable to ground-truth the detection of UXO with VG-16 at 1m to its performance at 5m. However, some insight may be gained by comparing the dig lists. There were 2001 anomalies picked for 5m altitude at a threshold of 0.14nT/m. The low altitude dig list had 10,022 picks. 1,234 picks on the 5m list correspond to picks on the low altitude list, and 767 picks on the 5m list had no corresponding low altitude picks, where they are assumed to match when within 2m of one another.

To assess the relationship between the 5m and low-altitude picks, we prepared a list of anomalies selected from the low altitude data, ranked by decreasing analytic signal amplitude. Those anomalies which had a corresponding 5m pick were assigned a value of 1, while those not having a corresponding 5m pick were assigned a value of 0. A cumulative sum of anomalies was determined for the 5m data. These are plotted against low altitude anomaly amplitude in Figure 4.49. Corresponding equivalent dipole moments (in A-m2) can be estimated by dividing the anomaly amplitudes by 100. Note that Figure 4-49 is a log-lin plot. It shows that about 50% of anomalies having amplitudes greater than about 25nT/m are also detected at 5m. This is represented in alternative (log-log) form in Figure 4-50 which shows the cumulative ratio of high altitude to low altitude detects with decreasing anomaly amplitude. Recall that a cut off of 2.5nT/m was used in preparing dig lists at Kirtland. Although some of the low-altitude anomalies are detected at 5m, the proportion is much smaller for those with amplitudes less than 25nT/m.

The plot for low altitude (nominally 1.5m) in Figure 4-50 levels off at about 1nT/m. The corresponding plot for 5m altitude levels off at about 50 nT/m. This is roughly in agreement with a fourth power reduction in amplitude with altitude that is expected from a gradient configuration. The consistent 50% detection for anomalies of higher amplitude at 5m is unexplained. One would intuitively expect that an increasing number of anomalies would be detected as amplitude increases, but this is not supported by these observations.

It is obvious that fewer anomalies are detected at 5m, and that the dominant features encountered at 1.5m are retained in the 5m map. This would be of significance when considering the applicability of the system for WAA purposes at sites where vegetation, topography, or other conditions restrict operation to higher altitudes.

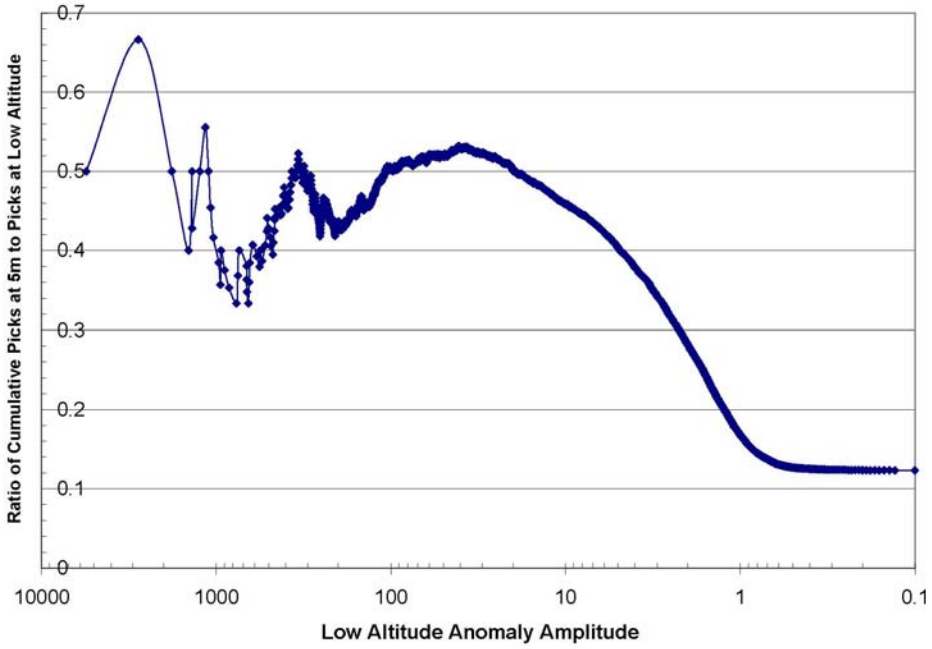

Figure 4-49. Cumulative number of picks at low altitude compared to matching picks at 5m altitude. Approximately 50% of picks having low amplitude anomalies of 25nT/m or greater have corresponding picks at 5m. Smaller anomalies are more frequently missed at 5m altitude.

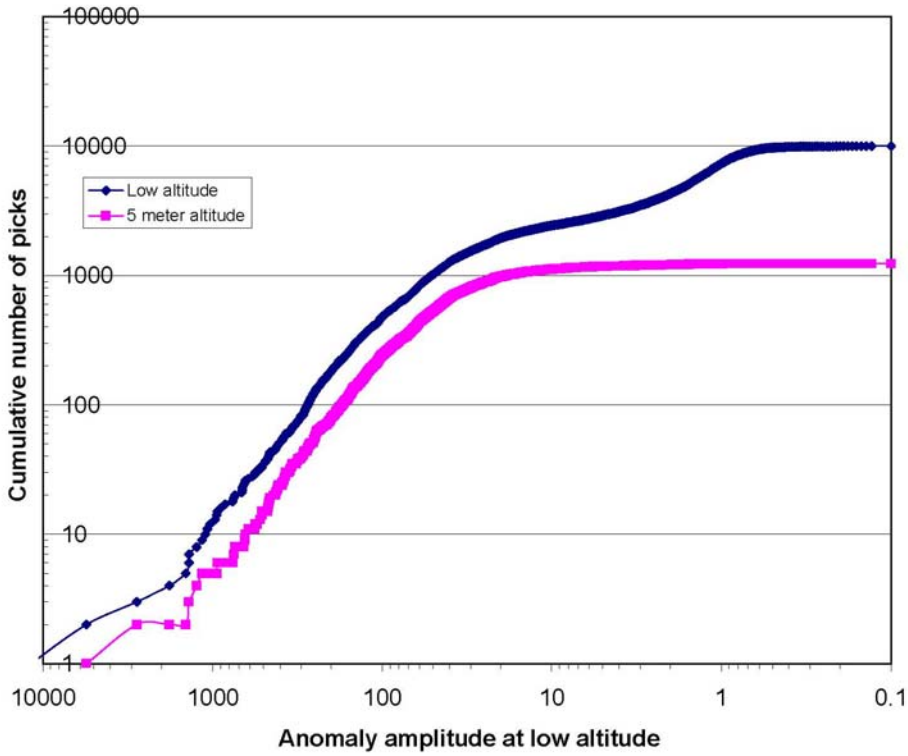

Figure 4-50. Ratio of cumulative number of picks at 5m to corresponding picks at low altitude.

4.5.12 Conclusions from North Area

Due to the paucity of ordnance in the North Area validation sites, few meaningful conclusions may be drawn from those measurements. The separation into point-like and non-point-like provides an indicator of performance, but does not provide a basis for comparing the VG systems to predecessors, or to compare attributes of this site to other sites. The ROC curves would indicate poor discrimination performance if they represented ordnance vs. non-ordnance, but the separation of point-like targets is somewhat subjective, and the anomaly amplitudes are lower than for typical M-38s, the ordnance found at the site. It is noteworthy that the pseudo-ROC curves prioritized by inversion were generally no better than those prioritized by analytic signal amplitude. Similarly, the 100% blind results were not significantly different from the partially disclosed results. It is unknown whether these results would have been different if there had been more ordnance in the validation sites.

Comparison of anomalies picked from two different acquisition altitudes show that approximately 50% of the low altitude anomalies are detected at 5m when low altitude amplitudes are greater than about 50nT/m. Detection of smaller anomalies levels off as amplitude falls below about 20nT/m for 5m altitude, and below about 1nT/m for low altitude.

4.6 Conclusions Regarding Overall System Performance

The detection capability of the VG-22 system, based on blind-seeded items in the South Area, surpassed our expectations, and showed a higher level of sensitivity than any airborne system that has been documented to date. Probability of detection (P_d) for seeded items in the 500-acre site was 90% with 12 anomaly picks per acre. Subsequent review of the data indicated that a P_d of 98% would have been achieved if we had chosen a detection threshold of 2.0 nT/m, at a cost of an additional eight picks per acre (total of 20 picks per acre). The VG-16 system showed better performance than total field systems (overall P_d of 67%), but with a smaller margin of difference than the VG-22. The validation of discrimination, based on digs peripheral to a target in the North Area, was unsuccessful in providing data that could be used to quantify the system performance, due to the paucity of UXO or even UXO-like items.

5. Cost Assessment

5.1 Cost Reporting

Cost information associated with the demonstration of the vertical magnetic gradient airborne technology was closely tracked and documented before, during, and after the demonstration to provide a basis for determination of the operational costs associated with this technology. It is important to note that the costs for airborne demonstrations and surveys are very much dependent on the character, size, and conditions at each site; ordnance objectives of the survey (e.g. flight altitude); type of survey conducted (e.g. high-density or transects); and technology employed for the survey (e.g. total field magnetic, vertical magnetic gradient, time domain electromagnetic induction) so that a universal formula cannot be fully developed. For this demonstration, Table 5-1 contains the cost elements that were tracked and documented for this demonstration. These costs include both operational and equipment costs associated with system application; mobilization and demobilization of equipment and personnel; salary and travel costs for project staff; subcontract costs associated with helicopter services, support personnel, and leased equipment; and costs associated with the processing, analysis, comparison, and interpretation of airborne results generated by this demonstration.

Table 5-1: Cost elements for vertical magnetic gradient survey demonstration at Kirtland AFB

Cost Category	Sub Category	Details	Quantity	Cost[1] (in dollars)
Pre-Survey (Start-up)	Site Characterization	Site inspection	0 days	$0
	Mobilization	Mission Plan preparation & logistics	18 days	$31,434
		Calibration Site preparation	2 days	$8,555
		Equipment/personnel transport (includes travel):	3 days	$9,641
		Helicopter/personnel transport[3] (includes travel)	4 days	$24,331
		Unpacking and system installation:	1 day	$7,073
		System testing & calibration	1 day	$2,796
Pre-survey subtotal				$83,830
Capital Equipment	System Use Rate ($700/day)		25 days	$17,500
Capital subtotal				$17,500

Operating Costs	Data acquisition	Helicopter time, including pilot and engineer labor	18 days (74 hours airtime)	$100,664
	Operator labor		18 days	$8,100
	Field Data processing	Geophysicist	25 days	$39,442
	Field support/management	Geophysicist	14 days	$24,256
	Maintenance	Geosoft software maintenance[3]	1 each	$0
	Hotel, air fares, and per diem	Survey team	18 days	$7,267
	Fuel Truck	Remote re-fueling[3]	NA	NA
	Airport Landing Fees and FBO Fees		18 days	$1170
	Project management		4 days	$6,930
Operating cost subtotal				$187,829

Post-Survey	Demobilization	Disassembly from helicopter, packing, and loading for transport: Equipment/personnel transport[3] (includes travel): Helicopter/personnel transport[3] (includes travel):	1 day 3 days 3 days	$6391 $9821 $18,364
	Additional data processing, analysis, interpretation, (at Oak Ridge offices) and Reporting			$119,703
Post-survey subtotal				$154,279
Total costs				$443,438

[1]**Includes all overhead and organization burden, fees, and associated taxes**

5.2 Cost Analysis

5.2.1 Cost Drivers

The major cost drivers for an airborne survey are the cost of helicopter services and the data processing and analysis associated with the acquired data. In terms of tasks, these constitute the majority of the field-related costs (i.e. mobilization, data acquisition, and demobilization costs) which represent the single largest cost item for an airborne survey project.

As mentioned, helicopter services are a significant component of the costs associated with the airborne survey project. This cost element is included in the mobilization, data acquisition, and demobilization tasks. The costs include helicopter airtime, fuel, pilot, aircraft engineer (mechanic), airport landing/hanger fees (if applicable), and per diem for the flight crew. Depending on survey location (distance from home base), mobilization and demobilization costs can be significant when compared to the overall data acquisition cost. Additionally, the type of survey, weather conditions, length of survey day, terrain, vegetation, and cultural features will greatly influence this cost element.

Data processing and analysis functions constitute the majority of the remaining costs associated with the field-related costs for a survey. As with helicopter services, mobilization and demobilization of the airborne survey equipment and the geophysical survey team is also a major task in terms of cost. This is typically a function of distance from the home base or previous survey location (i.e. if shared mobilization/demobilization is involved) to the intended survey project site. Peripheral costs associated with this demonstration-validation project, such as ground truth and excavations, are not part of the cost analysis.

The sensitivity of the overall cost to these drivers can be modeled under several different scenarios. Helicopter time on site is a factor of several variables. The first is the number and dimensions of the survey blocks. The greatest amount of non-survey time is spent in turns at the end of each line in preparation and alignment for the next line. As such, fewer and longer survey lines are more efficient than numerous shorter ones. Typically, lines longer than approximately 3-5 km do not gain additional efficiencies. One mitigating factor to this limit is a pilot performance issue. Longer lines typically require more frequent re-flights, since it is more difficult to maintain precision flying over such long lines. In practice, a maximum line length of 5 km is recommended.

As discussed above, other major cost drivers are mobilization, data processing, and demobilization. These costs are a function of project size and transportation distance, respectively. Processing costs and data delivery times typically decrease with experience at multiple sites. Mobilization costs are unlikely to decrease with time. The use of a local (to the survey project site) helicopter and pilot may offer decreased mobilization costs, but risks significantly increased acquisition costs if the aircraft engineer/mechanic responsible for system installation is unfamiliar with the equipment/installation process, or if the pilot is uncomfortable with the level of precision flying and height above the ground surface that is required. Moreover, this approach will likely increase the risk of accidents, and for this reason, is deemed unacceptable.

5.2.2 Cost Comparisons

5.2.2.1 VG-16 Cost Comparison

This section compares costs of three different survey technologies. These include man-portable, the ground-based MTADS system, and the VG-16 vertical magnetic gradient airborne system. Operational costs for the VG-16 system are equivalent to those of the ORAGS-Arrowhead and comparable airborne total magnetic field systems.

Based on several sources of information regarding the deployment of ground-based towed array systems on a UXO contaminated site, five scenarios are presented for the purpose of comparing airborne surveys to ground-based surveys. These sources of information are generally informal and include discussions both with industry and USAESCH staff experienced in the application of ground-based towed array surveying equipment and projects.

Following Harbaugh et al., 2007, we assume that the two ground-based technologies might survey only 2% of the total area of concern, while the airborne systems would survey between 2% and 100%. This level of ground surveying has been used in ESTCP's Wide Area Assessment Pilot Program. We also include higher proportions of ground surveying for comparison purposes. Harbaugh et al have proposed fixed costs of $75k (mobilization, demobilization, reporting) and acreage costs of $500/acre for use of MTADS at two sites. Similarly, they submit fixed costs of $45k plus acreage rates of $1540/acre for man portable electromagnetic surveys at these sites. We assume that the cost of a ground-based magnetometer survey would be roughly equal to that of a ground based electromagnetic survey.

Comparisons between airborne, vehicle, and man-portable magnetometer surveys are summarized in Table 5.2. These scenarios address sites of 1,000 to 50,000 acres of geographic extent, with varying rates of coverage from 100% to 2%. Airborne costs range from $71 to $181 per acre for a 100% coverage survey using the VG-16 WAA system. These costs include a nominal $50,000 mobilization cost from our bases of operation in Tennessee and Ontario, Canada. Airborne costs are corroborated by recent work for non-ESTCP sponsors, e.g. the surveys at Kirtland AFB, Fort McCoy, Camp Lejeune, Pinecastle Range Complex, and Fort Ord.

Man-portable systems generally have significantly higher acquisition costs than airborne systems (ranging from $500 to $3,000 per acre, depending on site conditions), are extremely time-consuming, and may present risks to personnel, equipment, and the environment. Neither the airborne nor the ground based survey costs include the cost of excavation

Comparison of the airborne array to a ground-based towed array of magnetometers similar to MTADS may be more representative for several reasons:

- MTADS was deployed at several of the same sites as the airborne technology (as reflected in several IDA reports), which enables an easy comparison for broad-area search technology.
- USAESCH performed an assessment of costs associated with contractors that employ ground-based towed arrays for geophysical surveying at UXO sites.

The extent of coverage possible with an airborne system renders comparisons to hand-held man-portable systems somewhat inappropriate.

Table 5-2. Costs for airborne, ground vehicle and man-portable survey platforms for varying WAA survey densities. Shaded cells are minimum cost. Man-portable are most cost effective for 0-30ac actual coverage, vehicular systems from 30-150ac and airborne over 150ac. All costs in thousands of dollars and include fixed mobilization costs.

$k VG-16	Coverage				
Acres	100%	50%	25%	10%	2%
1000	$ 231	$ 186	$ 150	$ 146	$ 143
2000	$ 292	$ 215	$ 163	$ 148	$ 144
5000	$ 495	$ 308	$ 226	$ 170	$ 153
20000	$ 1,510	$ 789	$ 462	$ 293	$ 198
50000	$ 3,600	$ 1,790	$ 997	$ 524	$ 269

$k vehicle	Coverage				
Acres	100%	50%	25%	10%	2%
1000	$ 575	$ 325	$ 200	$ 125	$ 85
2000	$ 1,075	$ 575	$ 325	$ 175	$ 95
5000	$ 2,575	$ 1,325	$ 700	$ 325	$ 125
20000	$ 10,075	$ 5,075	$ 2,575	$ 1,075	$ 275
50000	$ 25,075	$ 12,575	$ 6,325	$ 2,575	$ 575

$kman	Coverage				
Acres	100%	50%	25%	10%	2%
1000	$ 1,585	$ 815	$ 430	$ 199	$ 76
2000	$ 3,125	$ 1,585	$ 815	$ 353	$ 107
5000	$ 7,745	$ 3,895	$ 1,970	$ 815	$ 199
20000	$ 30,845	$ 15,445	$ 7,745	$ 3,125	$ 661
50000	$ 77,045	$ 38,545	$ 19,295	$ 7,745	$ 1,585

# covered ac	Coverage				
Acres	100%	50%	25%	10%	2%
1000	1000	500	250	100	20
2000	2000	1000	500	200	40
5000	5000	2500	1250	500	100
20000	20000	10000	5000	2000	400
50000	50000	25000	12500	5000	1000

Although somewhat simplistic and generalized in nature, it is readily apparent that the advantage of airborne surveys over ground-based surveys becomes greater as the area of concern becomes larger. These figures illustrate that man-portable platforms are most cost effective for sites requiring less than 30ac of actual coverage. Vehicular systems are most effective for 30-150ac, and airborne systems are most effective for sites larger than 150ac.

Costs for MTADS surveys may vary from those estimated in Table 5-2. The following was extracted from a relevant IDA report (Andrews et al., 2001): "For this demonstration, the MTADS total cost was $377,296. If the excavation costs of $169,096 and the reporting costs of $24,000 are removed, the MTADS costs for the deployment, survey, and analysis parts of this demonstration were $184,200. Note that this does not separate out the costs of the EMI work. The MTADS surveyed a total of more than 150 acres for a cost of $1,222 per acre". For the

ORAGS-Arrowhead (which compare favorably with the costs for the vertical magnetic gradient system), the total costs for the demonstrations and surveys ranged from $159,096 to $348,080k, for a cost of $86 to $704 per acre, including mobilization. According to the IDA report conclusions, "cost estimates prepared by the performers indicate that the per acre cost of the MTADS is about 2–3 times higher that those of airborne systems. These figures are very rough estimates and may not accurately reflect the cost differences seen in operational surveys." The MTADS costs are summarized in Table 5.3.

As mentioned previously, an even closer comparison of the Battelle VG-16 array costs are the costs associated with the previous ORAGS-Arrowhead and ORAGS-Hammerhead ESTCP demonstrations and DoD surveys. The cost factors involved in the Battelle VG-16, ORAGS-Hammerhead, and ORAGS-Arrowhead surveys are very similar. Apart from the learning curve associated with field experience, only the rate of survey coverage has changed significantly between the two generations of the technology. The ORAGS-Arrowhead and ORAGS-Hammerhead survey coverages were based on 12m flight line spacing, which is virtually the same as the Battelle VG-16 system.

In Table 5-2, we provided costs for airborne surveys covering between 2% and 100% of the area of interest with ground-based surveys covering 2% of the area of interest. An unresolved question is where the equivalency would lie between airborne and ground-based technologies – Which is more valuable - a 10% airborne survey, or a 2% ground-based survey? The answer would clearly lie in the detectability of the ordnance of interest at the site for both systems, and the uncertainty about ordnance contamination in areas that are not surveyed. The greater sensitivity of ground-based systems must be balanced against the probability of ordnance contamination within areas that are not surveyed. The choice will likely vary from site-to-site. Ground-based systems have more cost constraints that are site-dependent than airborne systems (e.g. unnavigable terrain, vegetation that must be cleared, vibration-sensitive ordnance, etc.), and this may also affect the selection of approaches.

5.2.2.2 VG-22 Cost Comparison

VG-22 was designed as a more sensitive system for detecting individual ordnance items, and as such it is appropriate to compare costing for VG-22 surveys to 100% ground-based surveys (Table 5-4). The costs for VG-22 are higher than those for VG-16 due to the 6m swath width for VG-22 compared to a 12m swath width for VG-16. Ground-based survey costs are based on Harbaugh et al. 2007, as with Table 5-2. Mobilizations are estimated in the same manner as in Table 5-2.

In Table 5-4, we have treated VG-22 as a surrogate for ground surveys. This may be appropriate where target ordnance items are large (e.g. 81mm and larger) for which VG-22 Pd values are high, as indicated by the Kirtland tests. Alternatively, VG-22 might be used where a larger proportion of small ordnance must be detected in order to justify use of the airborne survey for WAA applications. In some cases, this might involve partial coverage of a site with VG-22, a scenario with costs which would be different from those estimated in Tables 5-2 and 5-4.

Table 5-3: Representative cost for MTADS ground-based survey

Cost Category	Sub Category	Costs ($)
Fixed Costs		
1. Capital Costs	**Mobilization/Demobilization**	6,614
	Planning/Preparation/Health and Safety Plan (Mission Plan)	1,746
	Equipment	Included in Survey Cost
	Management Support	Included in Survey Cost
		Subtotal 8,360
Variable Costs		
2. Operation And Maintenance	**Ground-Based Survey**	129,650
	Labor for Data Processing, Analysis, and Interpretation	37,800
	Instrument Rental or Lease	Included in Survey Cost
	Travel and Miscellaneous Materials	26,060
	Reporting	4,230
		Subtotal 197,740
3. Other Technology-Specific Costs	**Excavation for Ground-Truthing and Verification**	Not Included
	Geophysical Prove-out	5,616
		Subtotal 5,616
4. Miscellaneous Costs	**None Noted**	0
Total Costs		
		Total Technology Cost 211,716
		Throughput Achievable (acres per hour) 3
		Unit Cost per acre 735

Table 5-4: Costs for 100% coverage with VG-22 airborne and ground-based surveys.

Area (acres)	Airborne Cost ($/acre)	Airborne Total ($)	Vehicular Towed ($)	Man Portable ($)
1,000	291	$291 k	$575k	$1,585k
2,000	217	$ 433k	$1,075k	$3,125k
5,000	167	$833k	$2,575k	$7,745k
20,000	139	$2,786k	$10,075k	$30,845k
50,000	137	$ 6,835k	$25,075k	$72,545k

5.2.3 Cost Basis

The basis of cost for this analysis consists of the tasks and work elements necessary to provide a complete turn-key airborne geophysical survey of a current or former military site with the intended survey objective being UXO. The UXO survey objective includes detection and mapping of individual ordnance and ordnance-related artifacts, as well as clustered UXO represented by targets, impact areas, and firing fans. The operational survey criteria are assumed to be acceptable for low-altitude geophysical surveying, including relatively flat to gently-sloping terrain, little to no vegetation exceeding 1 meter in height, few if any cultural artifacts or impediments (e.g. overhead power transmission lines). Additional survey criteria included in the cost basis are favorable weather conditions requiring no downtime (e.g. low wind, excellent visibility, high cloud ceiling, no precipitation).

The tasks and work elements included in the basis of cost include development of the survey Mission Plan (includes the Work Plan and Aviation Safety Plan); helicopter, survey equipment, and personnel mobilization and demobilization to the project site; geophysical prove-out (GPO) set-up and mapping; data acquisition, quality control (QC), analysis, processing, analysis, and interpretation; project management; and reporting. Within these tasks and work elements, all labor, materials, travel, and other miscellaneous costs are fully addressed and accounted for.

5.2.4 Life Cycle Costs

Life cycle costs for airborne technology are somewhat difficult to predict. This is based, in part, on how these costs are predicated on the usage and duty cycle of the boom structure which is exposed to considerable stress during each survey application (including installation and de-installation). Our experience with the ORAGS-Arrowhead suggests that the replacement cycle for the boom components and mounting hardware is approximately 3 years based on 6 moderately-sized surveys per year. In addition, the cesium-vapor magnetometers require periodic recalibration (typically annually) and sensor refurbishment. Other components of the airborne system require little or no maintenance, including the GPS, navigation, laser altimeter, and data management system. These components have little cost associated with their life cycle beyond the investment of the original purchase.

Capital costs associated with this demonstration project were borne by Battelle, and are in the range of $750,000. These capital costs include design, development, construction, testing, and flight certification costs. This last element, flight certification, is the single aspect within the life cycle framework that requires regulatory approval (i.e. Federal Aviation Administration). This certification cost involves a determination of air worthiness, as well as the detailed weights and balances required for system operation. This is a single investment which is incurred before application of the survey technology as a survey project site. Aside from this initial regulatory involvement, no other regulatory or institutional oversight costs apply.

Operational costs as a part of the life cycle cost assessment include the same elements addressed in the cost basis described in Section 5.2.3. These costs include development of the survey Mission Plan; helicopter, survey equipment, and personnel mobilization and demobilization to the project site; geophysical prove-out (GPO) set-up and mapping; data acquisition, quality control (QC), analysis, processing, analysis, and interpretation; project management; and reporting. Within these tasks and work elements, all labor, materials, travel, and other miscellaneous costs are fully addressed and accounted for.

No liability costs are associated with the application of the airborne technology for a survey

project site as far as life cycle costs are concerned. The issue of liability for a survey project is associated with the liability of helicopter operation, which is a routine cost for which the helicopter services provider procures insurance. All other liability associated with the survey for UXO is typically indemnified by the U.S. Government.

5.3 Cost Conclusions

As demonstrated above, comparing costs of fundamentally different technology approaches is both difficult and inconclusive. The previously discussed cost comparison provided a range of answers to the same question, namely, what are the costs of deploying each technology over the same size area under the same conditions?

For consideration of DoD-wide application of the airborne technology, a number of factors must be considered when evaluating the appropriateness of the airborne technology and potential for substantial cost savings. While initially impressive, it is not possible to simply apply these types of cost savings across the entire DoD UXO program. Sites must be of sufficient geographic extent to warrant a deployment given the high costs associated with mobilization and demobilization. In addition, survey objectives, terrain, geology, vegetation, and cultural artifacts must also be considered for such a deployment. Extremely variable terrain and/or the presence of tall vegetation can greatly limit or impede the use of the airborne technology for the UXO objectives of interest. Finally, the project objective must be consistent with the detection limits and capabilities of the airborne system to make such a deployment feasible.

6. Implementation Issues

6.1 Environmental Checklist

In order to operate, each system must have Federal Aviation Administration approval (STC certificate). The required testing and evaluation was completed before mobilization. In addition, ground crews are required to complete the 40-hour HAZWOPR course and to maintain their annual 8-hour refreshers for operation at most UXO sites.

6.2 Other Regulatory Issues

We are aware of no additional regulatory requirements for operation at the FKPBR site.

6.3 End-User Issues

The primary stakeholders for UXO issues at the FKPBR site have not been specified.

7. References

Beard, L.P., D.A. Wolf, B. Spurgeon, T.J. Gamey, W.E. Doll, 2003, Rapid screening of large-area magnetic data for unexploded ordnance, Proceedings of SAGEEP 2003, pp1097-1102.

Billings, S.D., L.R. Pasion, D.W. Oldenburg, 2002, Inversion of magnetics for UXO discrimination and identification, Proceedings of UXO/Countermine Forum 2002, 10p.

Breiner, S., 1973, Applications manual for portable magnetometers, Geometrics, 58p.

Doll, W.E., T.J. Gamey, L.P. Beard, A.M. Emond, D.T. Bell, 2004, Comparison of airborne vertical magnetic gradient and total field products for mapping and detection of UXO and ferrous wastes, 74th Ann. International. Meeting: Society. of Exploration Geophysics.

Doll, W.E., T.J. Gamey, L.P. Beard, D.T. Bell, and J.S. Holladay, 2003, Recent advances in airborne survey technology yield performance approaching ground-based surveys, *The Leading Edge*, v. 22, n. 5, p. 420-425.

Gamey, T.J. and R. Mahler, 1999, A comparison of towed and mounted helicopter magnetometer systems for UXO Detection, Extended Abstract in *Proceedings of the 1999 SAGEEP Symposium*, p. 783-792.

Gamey, T. J., W. E. Doll, L. P. Beard, and D. T. Bell, 2004, Analysis of correlated noise in airborne magnetic gradients for UXO detection, , *Jour. Env. and Eng. Geophysics*, v. 9, n. 3, p. 115-125.

Gamey, T.J., 2007, UXO clusters and sheet-like anomalies in wide-area assessment surveys, Proceedings of SAGEEP-07, p980-992.

Harbaugh, G. R., Steinhurst, D. A., and Khadr, N., 2007, Wide area UXO contamination evaluation by transect magnetometer surveys, Pueblo Precision Bombing and Pattern Gunnery range #2, Victorville Precision Bombing Ranges Y and 15, Final Report, 100 pp., available at http://www.estcp.org/viewfile.cfm?Doc=MM%2D0533%2DTR%2DPueblo%2DVictorville%2Epdf.

Oak Ridge National Laboratory, 2005. Final Report on 2002 Testing of an Airborne Vertical Magnetic Gradiometer System, August 2005, 92pp, available at http://www.estcp.org/viewfile.cfm?Doc=MM%2D0037%2DIR%2Epdf.

PRC Inc, 1994, Unexploded ordnance advanced technology demonstration program at Jefferson Proving Ground (phase I), US Army Environmental Center Report no. SFIM-AEC-ET-CR-94120.

Salem, A., T.J. Gamey, D. Ravat, K. Ushijima, 2001, Automatic detection of UXO from airborne magnetic data using a neural network, Proceedings of SAGEEP 2001, 9p.

Tuley, M. and Dieguez, E, Analysis of Airborne Magnetometer Data from Tests at Isleta Pueblo, new Mexico, February 2003, IDA Document D-3035, May 2005.

8. Points of Contact

Points of contact are given below in Table 8-1.

Table 8-1: Points of Contact

Point Of Contact	Organization Name and Address	Phone/Fax/Email	Role in Project
William E. Doll	Battelle 105 Mitchell Rd. Suite 103 Oak Ridge TN 37830	865-483-2548 865-599-6165 dollw@battelle.org	Principal Investigator and Project Manager
David T. Bell	Battelle 105 Mitchell Rd. Suite 103 Oak Ridge TN 37830	865-483-2547 865-250-0578 belldt@battelle.org	Battelle-Oak Ridge Office Manager
D. Scott Millhouse	U.S. Army Engineering and Support Center, Huntsville 4820 University Square Huntsville, AL	256-895-1607 256-895-1602 Scott.D.Millhouse@HND01.usace.army.mil	ESTCP Project COR

Appendix A: Analytical Methods Supporting the Experimental Design

None

Appendix B: Data Storage and Archiving Procedures

Data Format

All data are recorded by automated collection systems. All raw data are write protected and all intermediate data are retained in the root database. Selection and ranking of anomalies for investigation are made by a combination of automated routines and manual refinement. Down-selection of the original list was made to exclude such obvious features as fences and roads.

All data are handled in SI units, and all positioning data are compiled in the NAD83 UTM projection. Alternate units and/or projections may be accommodated after the final data processing.

Data files included:
The archive files that are provided to ESTCP as a supplement to the Final Report are listed in Table B-1.

Table B-1. Archive files provided to ESTCP

		Dig Lists	XYZ grids	GeoTiffs	Data
North Area A	500 VG16		AVG16.dat	AVG16.tif	AVG16.asc
	250 VG22		AVG22.dat	AVG22.tif	AVG22.asc
	Sub 1 VG16	VG16a1.xyz	VG16a1.dat	VG16a1.tif	
	Sub 2 VG16	VG16a2.xyz	VG16a2.dat	VG16a2.tif	
	Sub 1 VG22	VG22a1.xyz	VG22a1.dat	VG22a1.tif	
	Sub 2 VG22	VG22a2.xyz	VG22a2.dat	VG22a2.tif	
North Area B	500 VG16 – 5m	BVG16-5m.xyz	BVG16-5m.dat	BVG16-5m.tif	BVG16-5m.asc
	500 VG16	BVG16.xyz	BVG16.dat	BVG16.tif	BVG16.asc
	250 VG22		BVG22.dat	BVG22.tif	BVG22.asc
South Area	VG16	SVG16.xyz	SVG16.dat	SVG16.tif	SVG16.asc
	VG22	SVG22.xyz	SVG22.dat	SVG22.tif	SVG22.asc

Dig lists: Lists of anomalies that might represent UXO related targets
XYZ grid files: Grid files for all data represented in map form
GeoTiff Image files
Final Databases: All data that has been used to generate grids and maps above

Pick lists have the following format:

Target_ID	x (utm-m)	y (utm-m)	AS
1937	336641.0	3892937.0	137.030
1902	336216.0	3892930.0	82.849
1717	336660.0	3892900.0	45.252
6462	336589.0	3893562.0	19.019

Target ID: ID given to each target

x (utm-m): Universal Transverse Mercator x coordinate in meters
y (utm-m): Universal Transverse Mercator y coordinate in meters
AS: Analytic signal value of anomaly

XYZ grid Files Format:

x (utm-m)	y (utm-m)	Value
336641.0	3892937.0	137.030

x (utm-m): Universal Transverse Mercator x coordinate in meters
y (utm-m): Universal Transverse Mercator y coordinate in meters
Value: The value of the parameter that has been gridded (i.e. Vertical gradient, Altitude)

Tiff Image files:
Georeferenced image files of all gridded data.

Database Format:

X	Y	hae	Alt	VG	Line

x: Universal Transverse Mercator x coordinate in meters
y: Universal Transverse Mercator y coordinate in meters
hae: Height above ellipsoid
Alt: Sensor height above ground
VG: vertical gradient
Line: Line #